Omaha Public Power District
444 South 16th Street Mall
Omaha, Nebraska 68102-2247

August 3, 2000
LIC-00-0064

U.S. Nuclear Regulatory Commission
Attn: Document Control Desk
Mail Station P1-137
Washington, D.C. 20555

References:
1. Docket No. 50-285
2. Operating License DPR-40 Amendment No. 158
3. Letter from OPPD (W. G. Gates) to NRC (Document Control Desk) dated June 23, 1993 (LIC-93-0119)
4. Letter from OPPD (W. G. Gates) to NRC (Document Control Desk) dated August 12, 1993 (LIC-93-0200)
5. Letter from OPPD (S. K. Gambhir) to NRC (Document Control Desk) dated January 30, 1998 (LIC-98-0009)
6. Letter from OPPD (S. K. Gambhir) to NRC (Document Control Desk) dated November 15, 1999 (LIC-99-0107)
7. Letter from NRC (L. R. Wharton) to OPPD (S. K. Gambhir) dated November 30, 1999
8. Letter from OPPD (S. K. Gambhir) to NRC (Document Control Desk) dated January 24, 2000 (LIC-00-0005)

SUJECT: Application for Amendment of Operating License

In this letter, Omaha Public Power District (OPPD) submits an *Application for Amendment of Operating License* which seeks to delete Section 3.D, *License Term* from the Fort Calhoun Station (FCS) Unit No. 1 Operating License No. DPR-40. OPPD previously submitted a similar *Application for Amendment of Operating License* via Reference 5. That application included an updated fluence analysis report (Westinghouse calculation/report SE-REA-95-003, *Fast Neutron Fluence Evaluations for the Fort Calhoun Unit 1 Reactor Pressure Vessel*, dated November 1995). The Reference 6 letter provided an alternate method for calculating RT_{PTS}, as documented in report CEN-636, Rev. 0, from ABB Combustion Engineering Nuclear Power, *Evaluation of Reactor Vessel Surveillance Data Pertinent to the Fort Calhoun Reactor Vessel Beltline Materials – Basis for Prediction of RT_{PTS} for the Fort Calhoun RPV.*

A001

In the Reference 7 letter, the NRC transmitted staff concerns related to the alternate method for prediction of RT_{PTS} at the expiration of the FCS license. The primary concern was the lack of surveillance data for the limiting weld combination for FCS. A meeting of NRC, OPPD, and ABB Combustion Engineering Nuclear Power representatives was held at NRC Headquarters on January 6, 2000, to discuss the staff concerns and OPPD plans for resolving the issue. These plans included acquisition of data from Kansai Electric Power Company's Mihama 1 plant, whose surveillance program included the limiting FCS weld material. The participants at this meeting agreed that: (1) OPPD should withdraw the Reference 5 license amendment application, and (2) OPPD should subsequently resubmit the application with a revised version of report CEN-636.

The Reference 8 letter from OPPD withdrew the Reference 5 license amendment application and the supplemental information submitted via Reference 6. On March 13, 2000, an additional meeting was held at NRC Headquarters to discuss the expected analysis results using the Mihama data and OPPD's proposed approach for addressing the NRC staff concerns.

OPPD has revised the *Application for Amendment of Operating License* as agreed to at the January 6, 2000 meeting. The end of license fluence has been reevaluated to eliminate credit for FCS surveillance program fluence adjustments, consistent with Draft Regulatory Guide, DG-1053, *Calculational and Dosimetry Methods for Determining Pressure Vessel Neutron Fluence.* This application includes an updated fluence analysis (Westinghouse Electric Company WCAP-15443, *Fast Neutron Fluence Evaluations for the Fort Calhoun Unit 1 Reactor Pressure Vessel,* dated July 2000). The methodology for calculating RT_{PTS} is documented in report CEN-636, Rev. 2, from Westinghouse - CE Nuclear Power, *Evaluation of Reactor Vessel Surveillance Data Pertinent to the Fort Calhoun Reactor Vessel Beltline Materials – Basis for Prediction of RT_{PTS} for the Fort Calhoun RPV,* dated July 2000. Using the methodology based on Regulatory Guide 1.99, Rev. 2, Position 2.1 in this report, the revised projected RT_{PTS} at the end of the current license term (August 9, 2013) is 250°F, and the projected RT_{PTS} at the end of a renewed license term (August 9, 2033) is 268°F. Both of these values are within the current 10 CFR 50.61 pressurized thermal shock screening criterion value of 270°F for axial welds.

In the above evaluations, plant operation with a 0.85 long term load factor was utilized for projecting fluence. An increase in the long term load factor from 0.77 to 0.85 does not cause the critical weld material to exceed the RT_{PTS} screening criteria of 10 CFR 50.61. All reactor vessel beltline plates and welds will remain below the PTS screening criteria for a period exceeding 20 years beyond the current 40 year license term. Based on these results, and because 10 CFR 50.61 requires updating the assessment whenever there is a significant change in projected values of RT_{PTS}, Section 3.D is redundant to present regulations and can be deleted from Operating License No. DPR-40.

Attachment A contains a mark-up reflecting the requested change in the operating license. Attachment B provides the *Discussion, Justification, and No Significant Hazards Considerations*. Attachment C is Westinghouse Electric Company WCAP-15443, *Fast Neutron Fluence Evaluations for the Fort Calhoun Unit 1 Reactor Pressure Vessel*, dated July 2000. Attachment D is Report CEN-636, Rev. 2, from Westinghouse - CE Nuclear Power, *Evaluation of Reactor Vessel Surveillance Data Pertinent to the Fort Calhoun Reactor Vessel Beltline Materials – Basis for Prediction of RT_{PTS} for the Fort Calhoun RPV,* dated July 2000.

OPPD requests NRC approval of this proposed amendment by December 31, 2000. OPPD plans to implement the proposed amendment within 30 days of NRC approval.

Please contact me if you have any questions.

Sincerely,

W. G. Gates
Vice President

WGG/TCM/tcm

c: E. W. Merschoff, NRC Regional Administrator, Region IV
L. R. Wharton, NRC Project Manager
W. C. Walker, NRC Senior Resident Inspector
B. E. Casari, Director - Environmental Health Division, State of Nebraska
Winston & Strawn

UNITED STATES OF AMERICA
NUCLEAR REGULATORY COMMISSION

In the Matter of	)	
	)	
Omaha Public Power District	)	Docket No. 50-285
(Fort Calhoun Station	)	
Unit No. 1)	)	

AFFIDAVIT

W. G. Gates, being duly sworn, hereby deposes and says that he is the Vice President in charge of all nuclear activities of the Omaha Public Power District; that as such he is duly authorized to sign and file with the Nuclear Regulatory Commission the Application for Amendment dated July 31, 2000 concerning deletion of Section 3.D, *LICENSE TERM* of Facility Operating License No. DPR-40; that he is familiar with the content thereof; and that the matters set forth therein are true and correct to the best of his knowledge, information, and belief.

W. G. Gates
Vice President

STATE OF NEBRASKA)
) ss
COUNTY OF DOUGLAS)

Subscribed and sworn to before me, a Notary Public in and for the State of Nebraska on this 3 day of August 2000.

Notary Public Carol J. Kelley

GENERAL NOTARY-State of Nebraska
CAROL J. KELLEY
My Comm. Exp. May 3, 2002

BEFORE THE UNITED STATES

NUCLEAR REGULATORY COMMISSION

In the Matter of	)	
	)	
Omaha Public Power District	)	Docket No. 50-285
(Fort Calhoun Station	)	
Unit No. 1)	)	

APPLICATION FOR AMENDMENT
OF
OPERATING LICENSE

Pursuant to Section 50.90 of the regulations of the U. S. Nuclear Regulatory Commission ("the Commission"), Omaha Public Power District, holder of Facility Operating License No. DPR-40, herewith requests that this License be amended to delete Section 3.D, *License Term.*

The proposed changes are provided in Attachment A to this Application. A Discussion, Justification and No Significant Hazards Consideration Analysis, which demonstrates that the proposed changes do not involve significant hazards considerations, is contained in Attachment B. Attachment C is Westinghouse Electric Company WCAP-15443, *Fast Neutron Fluence Evaluations for the Fort Calhoun Unit 1 Reactor Pressure Vessel*, dated July 2000. Attachment D is CEN-636, Rev. 2, from Westinghouse - CE Nuclear Power, *Evaluation of Reactor Vessel Surveillance Data Pertinent to the Fort Calhoun Reactor Vessel Beltline Materials – Basis for Prediction of RT_{PTS} for the Fort Calhoun RPV,* dated July 2000. The proposed changes would not authorize any change in the types or any increase in the amounts of effluents that will be released, or a change in the authorized power level of the facility.

WHEREFORE, Applicant respectfully requests that Section 3.D of Facility Operating License No. DPR-40 be deleted in the form attached hereto as Attachment A.

A copy of this Application, including its attachments, has been submitted to the Director - Environmental Health Division, Nebraska State Department of Health, as required by 10 CFR 50.91.

OMAHA PUBLIC POWER DISTRICT

By W. G. Gates
W. G. Gates
Vice President

Subscribed and sworn to before me this 13 day of August 2000.

Notary Public Carol J. Kelley

GENERAL NOTARY-State of Nebraska
CAROL J. KELLEY
My Comm. Exp. May 3, 2002

LIC-00-0064
ATTACHMENT A
Proposed Revision to Operating License DPR-40

A. Maximum Power Level

Omaha Public Power District is authorized to operate the Fort Calhoun Station, Unit 1, at steady state reactor core power levels not to exceed 1500 megawatts thermal (rated power).

B. Technical Specifications

The Technical Specifications contained in Appendix A, as revised through Amendment No. 193, are hereby incorporated in the license. The licensee shall operate the facility in accordance with the Technical Specifications.

C. Security and Safeguards Contingency Plans

The licensee shall fully implement and maintain in effect all provisions of the Commission-approved physical security, guard training and qualification, and safeguards contingency plans including amendments made pursuant to provisions of the Miscellaneous Amendments and Search Requirements revisions to 10 CFR 73.55 (51 FR 27817 and 27822) and to the authority of 10 CFR 50.90 and 10 CFR 50.54(p). The plans, which contain Safeguards Information protected under 10 CFR 73.21, are entitled: "Fort Calhoun Station Physical Security Plan," with revisions submitted through September 30, 1988; "Fort Calhoun Station Guard Training and Qualification Plan," with revisions submitted through August 17, 1979; and "Fort Calhoun Station Safeguards Contingency Plan," with revisions submitted through March 20, 1979. If certain security modifications are delayed beyond expectations of the schedule, approved compensatory measures must be implemented during the transition period.

~~D. License Term~~

~~The license amendment is contingent on the limitations of monitoring of the long-term load factor to assure that it does not exceed the assumed value of 0.77, and that a reevaluation of the end of license fluence with ENDF/B-VI cross sections and updated uncertainties will be performed to assure that the value of RT_{PTS} will not exceed the screening criterion being in place.~~

D~~E~~. Fire Protection Program

Omaha Public Power District shall implement and maintain in effect all provisions of the approved Fire Protection Program as described in the Updated Safety Analysis Report for the facility and as approved in the SERs dated February 14, and August 23, 1978, November 17, 1980, April 8, and August 12, 1982, July 3, and November 5, 1985, July 1, 1986, December 20, 1988, November 14, 1990, March 17, 1993 and January 14, 1994, subject to the following provision:

Omaha Public Power District may make changes to the approved Fire Protection Program without prior approval of the Commission only if those changes would not adversely affect the ability to achieve and maintain safe shutdown in the event of a fire.

E~~F~~. Additional Conditions

The Additional Conditions contained in Appendix B, as revised through Amendment No. ___, are hereby incorporated into this license. Omaha Public Power District shall operate the facility in accordance with the Additional Conditions.

4. This amended license is effective as of the date of issuance and shall expire at midnight on August 9, 2013

FOR THE ATOMIC ENERGY COMMISSION

Original signed by:
A. Giambusso

A. Giambusso, Deputy Director
for Reactor Projects
Directorate of Licensing

Enclosures:
1. Appendix A - Technical Specifications
2. Appendix B - Additional Conditions

Date of Issuance: August 9, 1973

LIC-00-0064
ATTACHMENT B
DISCUSSION, JUSTIFICATION, AND NO SIGNIFICANT HAZARDS ANALYSIS

DISCUSSION AND JUSTIFICATION:

The Omaha Public Power District (OPPD) proposes to delete Section 3.D, *License Term*, from Fort Calhoun Station (FCS) Unit 1 Operating License No. DPR-40.

The long-term load factor described in Section 3.D is used in the projection of reactor vessel fast neutron fluence and consequently for calculation of the RT_{PTS} value to ensure that the 10 CFR 50.61 screening criteria for reactor vessel integrity are not exceeded. The previous fluence analysis performed by Combustion Engineering (ABB/CE) used a 0.77 load factor in conjunction with the ENDF/B-IV cross section library. As shown in Attachment C, Westinghouse Electric Company has completed an analysis (Westinghouse WCAP-15443, "Fast Neutron Fluence Evaluations for the Fort Calhoun Unit 1 Reactor Pressure Vessel," dated July 2000) to update the ABB/CE calculation.

In the updated analysis, the long-term load factor was increased from 0.77 to 0.85 to reflect improvement in both the present and the long-term projected FCS Unit 1 operating efficiency. The updated analysis also used the ENDF/B-VI cross section library. The neutron fluence calculations are carried out using forward and adjoint formulations in r,θ geometry of the two dimensional Discrete Ordinates Transport (DOT) code. The anisotropic scattering is treated with a P_3 expansion of the scattering cross section and the angular discretization is modeled with a S_8 order of quadrature. The actual core power distribution and neutron source distributions from 14 cycles of operation (13.6 Effective Full Power Years) were utilized, which included the spectral changes due to plutonium accumulation. The BUGLE-93 cross section library which is based on the data set of the Evaluated Nuclear Data File/B-VI (ENDF/B-VI) was used. The Westinghouse DOT code was benchmarked to the ENDF/B-VI cross sections using the Poolside Critical Assembly (PCA) simulator experiment at the Oak Ridge National Laboratory (ORNL), surveillance capsule and cavity dosimetry measurements.

The results of these fluence evaluations demonstrate that the best estimate fast neutron exposure of the pressure vessel can be determined with a 1σ uncertainty of ±13% for Φ (E>1.0MeV), ±19% for Φ (E>0.1MeV) and ±14% for dpa. These uncertainties are within the ±20% guidelines contained in Draft Regulatory Guide, DG-1053, *Calculational and Dosimetry Methods for Determining Pressure Vessel Neutron Fluence.*

The methodology used, as summarized above, is the same as the neutron fluence calculation section of WCAP-14040, Revision 1, *Methodology Used to Develop Cold Overpressure Mitigating System Setpoints and RCS Heatup and Cooldown Curves* (TAC# M91749). Application of the exposure methodology to the FCS reactor vessel indicates that, at the conclusion of Cycle 14, the critical weld material (i.e., weld 3-410 for the 12008/13253 weld wire heat combination) had accumulated a maximum unbiased fast neutron fluence (E>1.0MeV)

DISCUSSION AND JUSTIFICATION: (Continued)

of 1.057E19 n/cm^2 and had reached a corresponding RT_{PTS} value of 221.4°F, based on the correlations provided in Regulatory Guide 1.99, Revision 2 and 10 CFR 50.61.

Based on the use of extreme low radial leakage fuel management as embodied in the design of FCS Operating Cycle 15 to date, and projections through the last operating cycle in which Operating License DPR-40 expires, the critical weld material will have accrued a maximum fast neutron fluence of 1.728E19 n/cm^2. This number represents the unbiased fluence value used in the Westinghouse fluence anlysis (WCAP-15443, July 2000, *Fast Neutron Fluence Evaluations for the Fort Calhoun Unit 1 Reactor Pressure Vessel*), and was derived by dividing the EOL (30 EFPY) fluence number in Table 6.3-1 of SE-REA-95-003 (1.51E19) by 0.874, which was the bias used to create the table. This unbiased value does not credit FCS-specific surveillance data or a derived "fleet bias." A Westinghouse - CE Nuclear Power Report, *CEN-636, Rev. 2, Evaluation of Reactor Vessel Surveillance Data Pertinent to the Fort Calhoun Reactor Vessel Beltline Materials – Basis for Prediction of RT_{PTS} for the Fort Calhoun RPV,* dated July 2000, outlines the evaluation of surveillance data and justifies reduction of the 10CFR 50.61 margin term to 44°F for the most limiting weld wire heats (see Attachment D). Using a chemistry factor of 208.68°F for the limiting 3-410 axial weld, the 1.728E19 n/cm^2 unbiased fluence value, the 65.5°F margin term, an $RT_{NDT}(0)$ value of –56°F, and a long term load factor of 0.85 results in an RT_{PTS} value of 250°F at the end of the current license term (August 9, 2013). The projected RT_{PTS} at the end of a renewed license term (August 9, 2033) is 268°F. These values are within the PTS screening criteria of 270°F.

In accordance with 10 CFR 50.61, this assessment must be updated whenever there is a significant change in projected values of RT_{PTS} or upon request for a change in the expiration date of the facility. Thus, Section 3.D can be deleted from Operating License No. DPR-40 based upon the analysis contained in Attachment C and the fact that Section 3.D is redundant to 10 CFR 50.61 requirements.

BASIS FOR NO SIGNIFICANT HAZARDS CONSIDERATION:

The proposed change does not involve a significant hazards consideration because operation of Fort Calhoun Station (FCS) Unit 1 in accordance with this change would not:

(1) Involve a significant increase in the probability or consequences of an accident previously evaluated.

The previously evaluated accidents affected by this change are limited to the pressurized thermal shock (PTS) events. Vessel embrittlement due to fast neutron associated damage to the limiting beltline region reactor vessel material (which for Fort Calhoun Station is included in the lower course axial welds) is a component in the PTS analysis. The fast neutron, thermal neutron and dpa values of the FCS reactor vessel were recalculated using actual power history values for Cycles 1 through 14 rather than conservative estimates, along with the revised BUGLE-93 cross sections from the ENDF/B-VI cross section library to appropriately account for the iron atoms in the thermal shield and a methodology that the NRC has previously approved for neutron fluence calculations performed by Westinghouse. The fluence evaluation included data from the three surveillance capsules (W-225, W-265, and W-275) previously removed and analyzed. The RT_{PTS} evaluation applied Position 2.1 of Regulatory Guide 1.99, Revision 2 in conjunction with surveillance data from other plants containing the limiting FCS weld materials. The evaluation results indicate that the FCS reactor vessel is able to reach more than 20 years beyond current licensed life without exceeding the 10 CFR 50.61 screening criterion for RT_{PTS} of 270°F for axial welds.

In accordance with 10 CFR 50.61, this assessment must be updated whenever there is a significant change in projected values of RT_{PTS} or upon request for a change in the expiration date of the facility. Since these requirements are contained in 10 CFR 50.61, Section 3.D can be deleted from Operating License No. DPR-40 without resulting in a significant increase in the probability or consequences of any accident previously evaluated.

(2) Create the possibility of a new or different kind of accident from any previously analyzed.

The proposed change does not physically alter the configuration of the plant and no new or different mode of operation is proposed. Increasing the long term load factor from 0.77 to 0.85 more accurately projects RT_{PTS} by accounting for improvement in FCS operating cycle efficiency. Requirements for assessing and reporting RT_{PTS} are contained in 10 CFR 50.61 and therefore, the proposed change does not create the possibility of a new or different kind of accident from any previously analyzed.

(3) Involve a significant reduction in a margin of safety.

The margin of safety is defined by both the screening criteria of 10 CFR 50.61 and draft regulatory guide DG-1053 for neutron fluence calculations, which requires the methodology to be capable of providing best estimate fluence evaluations within 20 percent (1σ). The analysis for FCS shows that when the applicable regulatory criteria are applied, the screening criteria of 10 CFR 50.61 are not exceeded; therefore, the proposed change does not involve a significant reduction in a margin of safety.

Therefore, based on the above, OPPD's position is that this proposed amendment does not involve a significant hazards consideration as defined by 10 CFR 50.92, and the proposed change will not result in a condition which significantly alters the impact of FCS on the environment. Thus, the proposed change meets the eligibility criteria for categorical exclusion set forth in 10 CFR 51.22(c)(9), and pursuant to 10 CFR 51.22(b) no environmental assessment need be prepared.

LIC-00-0064
Attachment C

Westinghouse Electric Company WCAP-15443
Fast Neutron Fluence Evaluations for the
Fort Calhoun Unit 1 Reactor Pressure Vessel
July 2000

Westinghouse Non-Proprietary Class 3

WCAP-15443
Revision 0

Fast Neutron Fluence Evaluations for the Fort Calhoun Unit 1 Reactor Pressure Vessel

Westinghouse Electric Company LLC

WESTINGHOUSE NON-PROPRIETARY CLASS 3

WCAP-15443, Revision 0

Fast Neutron Fluence Evaluations For The Fort Calhoun Unit 1 Reactor Pressure Vessel

S. L. Anderson
Radiation Engineering and Analysis

July 2000

Approved:
M. C. Rood, Manager
Radiation Engineering and Analysis

Work Performed Under Shop Order 450
Purchase Order No. 27811 000
Prepared by Westinghouse for the Omaha Public Power District

WESTINGHOUSE ELECTRIC COMPANY LLC
P.O. Box 355
Pittsburgh, Pennsylvania 15230-0355

EXECUTIVE SUMMARY

This report describes a calculation of the fast neutron exposure of the Fort Calhoun Unit 1 reactor pressure vessel. The overall exposure evaluation methodology is based on guidance provided in Draft Regulatory Guide DG-1053, "Calculational and Dosimetry Methods for Determining Pressure Vessel Neutron Fluence" and makes use of the latest ENDF/B-VI neutron transport and dosimetry cross-sections included in the BUGLE-93 library.

In addition to the general description of the methodology, the qualification of the overall approach and the uncertainties associated with the use of the methodology are also provided based on:

1) Comparison of absolute calculations with measurements obtained at the Pool Critical assembly (PCA) at the Oak Ridge National Laboratory (ORNL).
2) Comparison of absolute calculations and measurements for two pressurized water reactors similar in design to Fort Calhoun, including five sets of internal surveillance capsule measurements and eight cycles of ex-vessel reactor cavity measurements (four at each reactor).
3) Comparison of absolute calculations with three sets of internal surveillance capsule measurements from the Fort Calhoun reactor.
4) An analytical sensitivity study of important input parameters applicable to the Fort Calhoun transport calculations.

The results of these fluence evaluations demonstrate that the fast neutron exposure of the pressure vessel can be calculated with a 1σ uncertainty of 15.5% for $\Phi(E \geq 1.0$ MeV. This uncertainty is well within the ±20% guideline specified in DG-1053.

Application of the exposure methodology to the Fort Calhoun reactor pressure vessel indicates that at the conclusion of Cycle 14 (13.6 Effective Full Power Years) the critical weld material 3-410 had accrued a maximum fast neutron fluence ($E \geq 1.0$ MeV) of 1.0572e+19 n/cm^2.

Based on the use of extreme low radial leakage fuel management as embodied in the design of Fuel Cycle 15 to the present, projections of future fast neutron exposure to the limiting 3-410 weld indicate that at the license expiration date August 9, 2013 the maximum fast neutron fluence ($E > 1.0$ MeV) will be 1.7280e+19 n/cm^2. For a projected operating period with a Renewed License to August 9, 2033 the maximum fast neutron fluence is projected to be 2.4108e+19 n/cm^2. This is expected to occur prior to 48 Effective Full Power Years; where the corresponding maximum exposure is calculated to be 2.48e+19 n/cm^2.

TABLE OF CONTENTS

LIST OF TABLES

LIST OF TABLES (Continued)

LIST OF TABLES (Continued)

LIST OF FIGURES

SECTION 1.0

INTRODUCTION

In the assessment of the state of embrittlement of light water reactor pressure vessels, an accurate evaluation of the neutron exposure of the materials comprising the beltline region of the vessel is required. This exposure evaluation must, in general, include assessments not only at locations of maximum exposure at the inner diameter of the vessel, but, also, as a function of axial, azimuthal, and radial location throughout the vessel wall.

A schematic of the beltline region of the Fort Calhoun reactor pressure vessel is provided in Figure 1.0-1. In this case, the beltline region is constructed of six (6) shell plates, six (6) longitudinal welds, and one (1) circumferential weld. Each of these thirteen materials must be considered in the overall embrittlement assessments of the beltline region.

In order to satisfy the requirements of 10CFR50 Appendix G for the calculation of pressure/temperature limit curves for normal heatup and cooldown of the reactor coolant system, fast neutron exposure levels must be defined at depths within the vessel wall equal to 25 and 75 percent of the wall thickness for each of the materials comprising the beltline region. These locations are commonly referred to as the 1/4T and 3/4T positions in the vessel wall. The 1/4T exposure levels are also used in the determination of upper shelf fracture toughness as specified in 10CFR50 Appendix G. In the determination of values of RT_{PTS} for comparison with the applicable pressurized thermal shock screening criterion, maximum neutron exposure levels experienced by each of the beltline materials are required. These maximum levels will, of course, occur at the vessel inner radius. Furthermore, in the event that a probabalistic fracture mechanics evaluation of the pressure vessel is performed or if an evaluation of thermal annealing and subsequent material re-embrittlement is undertaken, a complete embrittlement profile is required for the entire volume of the pressure vessel beltline. The determination of this embrittlement profile, in turn, necessitates the evaluation of neutron exposure gradients throughout the entire beltline.

The purpose of this report is to describe the approach used to determine the fast neutron exposure to the Fort Calhoun reactor pressure vessel; and to establish the uncertainties associated with those projections. The overall methodology used in this report is derived from the guidance provided in ASTM Standard E853 "Analysis and Interpretation of Light Water Reactor Surveillance Results"[1] and Draft Regulatory Guide DG-1053 "Calculational and Dosimetry Methods for Determining Pressure Vessel Neutron Fluence"[2], and is dependent on

plant-specific neutron transport calculations verified by available measured data to produce an accurate assessment of the pressure vessel exposure. The methodology is based on the underlying philosophy that, in order to reduce the uncertainties in vessel exposure projections, plant specific neutron transport calculations must be supported by

1) Benchmarking of the analytical approach.

2) Comparison with power reactor data bases.

3) Comparison with plant specific measurements.

In subsequent sections of this report, the methodologies used to perform calculations of the neutron environment within the Fort Calhoun reactor geometry are described. The methods utilized in the evaluation of neutron dosimetry are also described, and the comparisons of calculation with measurements obtained from Fort Calhoun in-vessel surveillance capsule irradiations are provided.

In addition to the general description of the methodology, the qualification of the overall approach and the uncertainties associated with the use of the methodology are also provided. The methods qualification and uncertainty assessments are based on:

1) Comparison of calculations with measurements obtained from the Oak Ridge National Laboratory (ORNL) Pool Critical Assembly (PCA) simulator benchmark.

2) Comparison of calculations with measurements obtained from the H. B. Robinson power reactor benchmark irradiation.

3) Comparison of calculations with measurements from a database of in-vessel surveillance capsule irradiations for pressurized water power reactors similar in design to Fort Calhoun.

4) Comparison of calculations with three sets of in-vessel surveillance capsule measurements from the Fort Calhoun reactor.

5) An analytical sensitivity study of important input parameters applicable to the Fort Calhoun transport calculations.

This report also provides an evaluation of the end of Cycle 14 neutron exposure of the Fort Calhoun pressure vessel in terms of fast neutron fluence, $\Phi(E \geq 1.0)$; fast neutron fluence, $\Phi(E \geq 0.1$ MeV); and iron atom displacements, dpa. In addition, based on the continued use of the Cycles 15 and 16 fuel loading patterns, projections of the future exposure of the vessel are provided. Also, uncertainties associated with the current and projected exposure of the pressure vessel are discussed.

Figure 1.0-1

Schematic of the Fort Calhoun Reactor Vessel Beltline

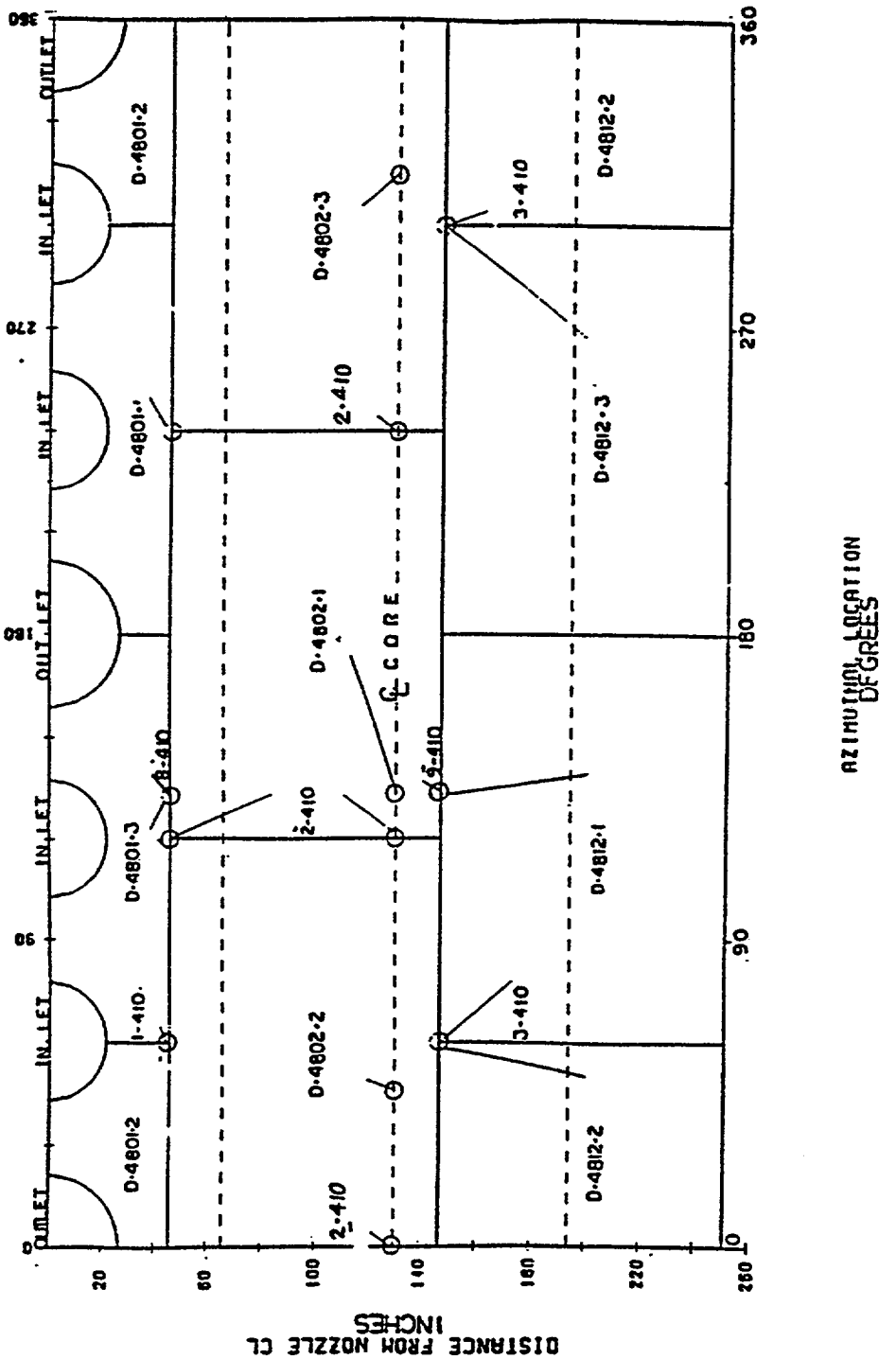

SECTION 2.0

NEUTRON TRANSPORT AND DOSIMETRY EVALUATION METHODOLOGIES

As noted in Section 1.0 of this report, the exposure of the reactor pressure vessel was developed based on a series of plant specific neutron transport calculations verified by comparison with plant specific measurements obtained from the reactor vessel materials surveillance program. In this section, the neutron transport and dosimetry evaluation methodologies are discussed in some detail, and the approach used to compare the calculations and measurements is presented.

2.1 - Neutron Transport Analysis Methods

A plan view of the Fort Calhoun Station Unit No. 1 reactor geometry at the core midplane is shown in Figure 2.1-1. Six surveillance capsules attached to the pressure vessel wall which are removed on an individual basis at frequencies defined in the Fort Calhoun Station Updated Safety Analysis Report Section 4.5 are included in the reactor design to constitute the reactor vessel surveillance program. The capsules are located at azimuthal angles of 45°, 85°, 95°, 225°, 265°, and 275° relative to the core cardinal axis as shown in Figure 2.1-1. A plan view of a surveillance capsule holder attached to the pressure vessel wall is shown in Figure 2.1-2.

From a neutronic standpoint, the surveillance capsule structures are significant. The presence of these materials has a marked effect on both the spatial distribution of neutron flux and the neutron energy spectrum in the water annulus between the thermal shield and the reactor vessel. In order to determine the neutron environment at the test specimen location, the capsules themselves must be included in the analytical model.

In performing the fast neutron exposure evaluations for the Fort Calhoun surveillance capsules and reactor vessel, two distinct sets of transport calculations were carried out. The first, a single computation in the conventional forward mode, was used primarily to obtain relative neutron energy distributions throughout the reactor geometry as well as to establish relative radial distributions of exposure parameters {$\phi(E \geq 1.0$ MeV), $\phi(E \geq 0.1$ MeV), and dpa/sec} through the vessel wall. The neutron spectral information was required for the interpretation of neutron dosimetry withdrawn from the surveillance capsules as well as for the determination of exposure parameter ratios; i.e., [dpa/sec]/[$\phi(E \geq 1.0$ MeV)], within the pressure vessel geometry. The relative radial gradient information was required to permit the projection of

exposure parameters to locations interior to the pressure vessel wall; i.e., the 1/4T, 1/2T, and 3/4T locations.

The second set of calculations consisted of a series of adjoint analyses relating the fast neutron flux, $\phi(E \geq 1.0$ MeV), at surveillance capsule positions and at several azimuthal locations on the pressure vessel inner radius to neutron source distributions within the reactor core. The source importance functions generated from these adjoint analyses provided the basis for all absolute exposure calculations and comparison with measurement. These importance functions, when combined with operating cycle specific neutron source distributions, yielded absolute predictions of neutron exposure at the locations of interest for each cycle of irradiation and established the means to perform similar predictions and dosimetry evaluations for all subsequent fuel cycles. It is important to note that the cycle-specific neutron source distributions utilized in these analyses included not only spatial variations of fission rates within the reactor core, but also accounted for the effects of varying neutron yield per fission and fission spectrum introduced by the build-up of plutonium as the burnup of individual fuel assemblies increased.

The absolute cycle specific data from the adjoint evaluations together with the relative neutron energy spectra and radial distribution information from the reference forward calculation provided the means to:

1) Evaluate neutron dosimetry from the surveillance capsule locations.

2) Enable a direct comparison of analytical prediction with measurement.

3) Establish a mechanism for projection of pressure vessel exposure as the design of each new fuel cycle evolves.

The forward transport calculation for the reactor model summarized in Figures 2.1-1 and 2.1-2 was carried out in r,θ geometry using the DORT two-dimensional discrete ordinates code[3] and the BUGLE-93 cross-section library[4]. The BUGLE-93 library is a 47 energy group ENDF/B-VI based data set produced specifically for light water reactor applications. In these analyses anisotropic scattering was treated with a P_3 expansion of the scattering cross-sections and the angular discretization was modeled with an S_8 order of angular quadrature. The core power distribution utilized in the reference forward transport calculation was representative of the burnup weighted average over the first 14 cycles of operation.

All adjoint calculations were also carried out using an S_8 order of angular quadrature and the P_3 cross-section approximation from the BUGLE-93 library. Adjoint source locations were chosen at several azimuthal locations along the pressure vessel inner radius as well as at the geometric center of each surveillance capsule. Again, these calculations were run in r,θ geometry to provide neutron source distribution importance functions for the exposure parameter of interest, in this case $\phi(E \geq 1.0\ MeV)$.

Having the adjoint importance functions and appropriate core source distributions, the response of interest was calculated as:

$$R(r,\theta) = \int_r \int_\theta \int_E I(r,\theta,E)\, S(r,\theta,E)\, r\, dr\, d\theta\, dE$$

where: $R(r,\theta)$ = $\phi(E \geq 1.0\ MeV)$ at radius r and azimuthal angle θ.

$I(r,\theta,E)$ = Adjoint source importance function at radius r, azimuthal angle θ, and neutron source energy E.

$S(r,\theta,E)$ = Neutron source strength at core location r,θ and energy E.

Although the adjoint importance functions used in this analysis were based on a response function defined by the threshold neutron flux $\phi(E \geq 1.0\ MeV)$, prior calculations[5] have shown that, while the implementation of low leakage loading patterns significantly impacts both the magnitude and spatial distribution of the neutron field, changes in the relative neutron energy spectrum are of second order. Thus, for a given location the ratio of [dpa/sec]/[$\phi(E \geq 1.0\ MeV)$] is insensitive to changing core source distributions. In the application of these adjoint importance functions to the Fort Calhoun reactor, therefore, the iron atom displacement rates (dpa/sec) and the neutron flux $\phi(E \geq 0.1\ MeV)$ were computed on a cycle specific basis by using [dpa/sec]/[$\phi(E \geq 1.0\ MeV)$] and [$\phi(E \geq 0.1\ MeV)$]/[$\phi(E \geq 1.0\ MeV)$] ratios from the forward analysis in conjunction with the cycle specific $\phi(E \geq 1.0\ MeV)$ solutions from the individual adjoint evaluations.

In particular, after defining the following exposure rate ratios,

$$R_1 = \frac{[dpa/\sec]}{\phi(E \geq 1.0\ MeV)}$$

$$R_2 = \frac{\phi(E \geq 0.1\,MeV)}{\phi(E \geq 1.0\,MeV)}$$

the corresponding fuel cycle specific exposure rates at the adjoint source locations were computed from the following relations:

$$dpa/\sec = [\,\phi(E \geq 1.0\,MeV)]\,R_1$$
$$\phi(E \geq 0.1\,MeV) = [\,\phi(E \geq 1.0\,MeV)]\,R_2$$

The reactor core power distributions used in the plant specific adjoint calculations were supplied by Omaha Public Power District (OPPD) for the first 14 operating cycles of Fort Calhoun, and for the predicted design distributions for Cycles 15 and 16.

Figure 2.1-1

Fort Calhoun r,θ Reactor Geometry

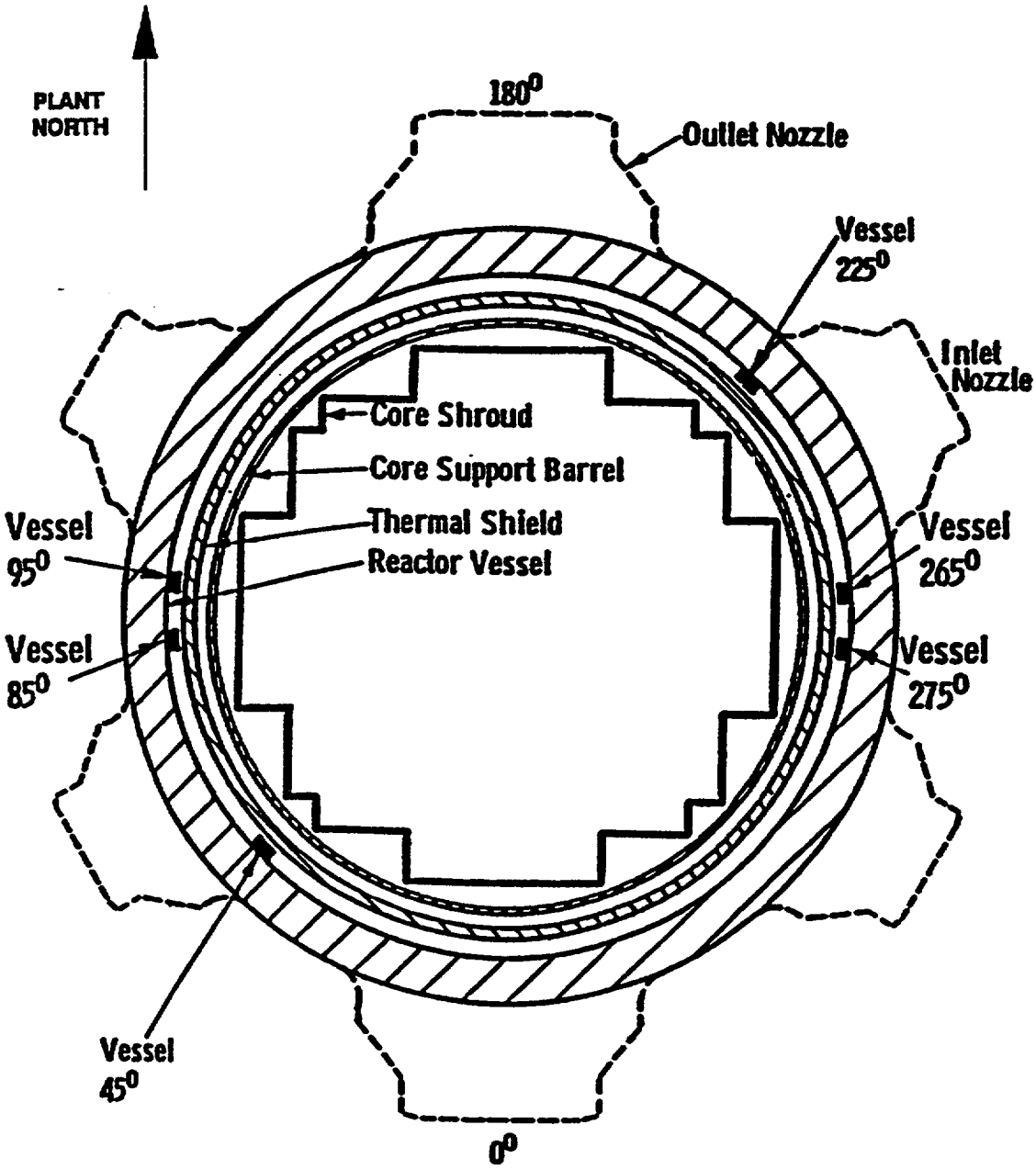

Figure 2.1-2

Surveillance Capsule Geometry

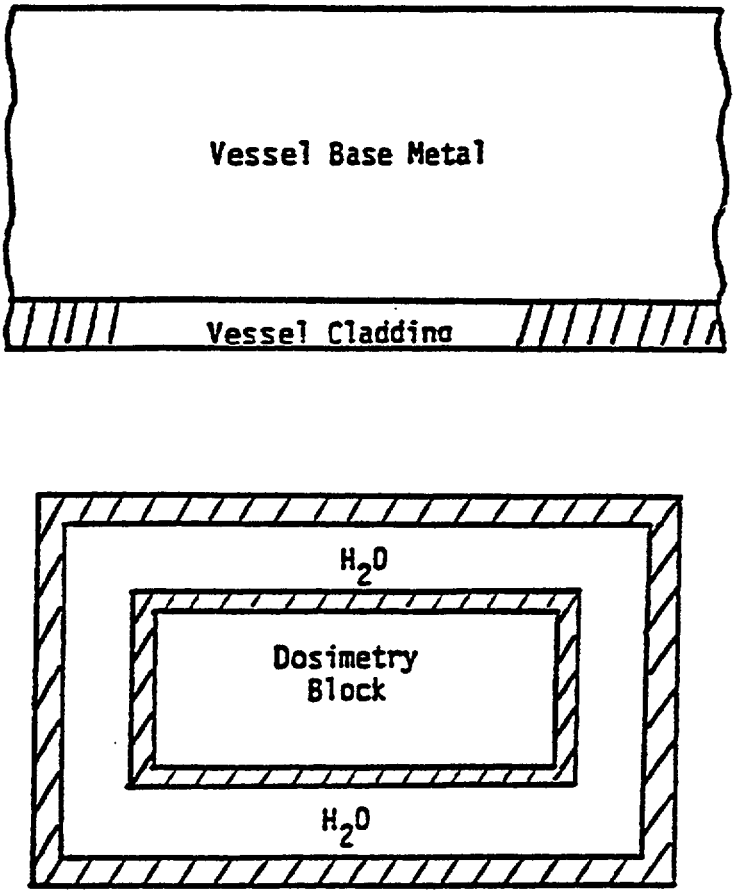

2.2 - Neutron Dosimetry Evaluation Methodology

The use of passive neutron sensors such as those included in the Fort Calhoun surveillance program does not yield a direct measure of the energy dependent neutron flux level at the measurement location. Rather, the activation or fission process is a measure of the integrated effect that the time- and energy-dependent neutron flux has on the target material over the course of the irradiation period. An accurate assessment of the average flux level and, hence, time integrated exposure (fluence) experienced by the sensors may be developed from the measurements only if the sensor characteristics and the parameters of the irradiation are well known. In particular, the following variables are of interest:

1) The measured specific activity of each sensor
2) The physical characteristics of each sensor
3) The operating history of the reactor
4) The energy response of each sensor
5) The neutron energy spectrum at the sensor location

In this section the procedures used to determine sensor specific activities, to develop reaction rates for individual sensors from the measured specific activities and the operating history of the reactor, and to derive key fast neutron exposure parameters from the measured reaction rates are described.

2.2.1 - Determination of Sensor Reaction Rates

The measured specific activity of each of the radiometric sensors contained in the three surveillance capsules withdrawn to date from the Fort Calhoun reactor was reported in Reference 6.

The irradiation history of the reactor over its operating lifetime was obtained from NUREG-0020, "Licensed Operating Reactors Status Summary Report"[7]. In particular, operating data were extracted from that report on a monthly bases from reactor startup to the end of the current evaluation period. For the sensor sets utilized in surveillance capsule irradiations, the half-lives of the product isotopes are long enough that a monthly histogram describing reactor operation has proven to be an adequate representation for use in radioactive decay corrections for the reactions of interest in the exposure evaluations[8].

Having the measured specific activities, the operating history of the reactor, and the physical characteristics of the sensors, reaction rates referenced to full power operation were determined from the following equation:

$$R = \frac{A}{N_0 F Y \sum_j \frac{P_j}{P_{ref}} C_j [1 - e^{-\lambda t_j}] e^{-\lambda t_d}}$$

where:

A	=	measured specific activity (dps/gm)
R	=	reaction rate averaged over the irradiation period and referenced to operation at a core power level of P_{ref} (rps/nucleus)
N_0	=	number of target element atoms per gram of sensor
F	=	weight fraction of the target isotope in the sensor material
Y	=	number of product atoms produced per reaction
P_j	=	average core power level during irradiation period j (MW)
P_{ref}	=	maximum or reference core power level of the reactor (MW)
C_j	=	calculated ratio of $\phi(E \geq 1.0$ MeV) during irradiation period j to the time weighted average $\phi(E \geq 1.0$ MeV) over the entire irradiation period
λ	=	decay constant of the product isotope (sec^{-1})
t_j	=	length of irradiation period j (sec)
t_d	=	decay time following irradiation period j (sec)

and the summation is carried out over the total number of monthly intervals comprising the total irradiation period.

In the above equation, the ratio P_j/P_{ref} accounts for month by month variation of power level within a given fuel cycle. The ratio C_j is calculated for each fuel cycle using the adjoint transport methodology and accounts for the change in sensor reaction rates caused by variations in flux level due to changes in core power spatial distributions from fuel cycle to fuel cycle. For a single cycle irradiation C_j = 1.0. However, for multiple cycle irradiations, particularly those employing low leakage fuel management the additional C_j correction must be utilized.

2.2.2 - Corrections to Reaction Rate Data

Prior to using the measured reaction rates in the least squares adjustment procedure discussed in Section 2.2.3 of this report, additional corrections were made to the U-238 measurements to account for the presence of U-235 impurities in the sensors as well as to adjust for the build-in of plutonium isotopes over the course of the irradiation. In addition to the corrections made for the presence of U-235 in the U-238 fission sensors, corrections were also made to the U-238 sensor reaction rates to account for gamma ray induced fission reactions occuring over the course of the irradiation. These photo-fission corrections were, likewise, location dependent and were based on the reference transport calculations described in Section 2.1.

2.2.3 - Least Squares Adjustment Procedure

Values of key fast neutron exposure parameters were derived from the measured reaction rates using the FERRET least squares adjustment code[9]. The FERRET approach used the measured reaction rate data, sensor reaction cross-sections, and the calculated spectrum as input and proceeded to adjust the group fluxes from the calculated spectrum to produce a best fit (in a least squares sense) to the measured reaction rate data. The resultant best estimate exposure parameters at the measurement locations along with the associated uncertainties were then obtained from the adjusted spectrum.

In the FERRET evaluations, a log-normal least squares algorithm weights both the trial values and the measured data in accordance with the assigned uncertainties and correlations. In general, the measured values *f* are linearly related to the flux ϕ by some response matrix A:

$$f_i^{(s,\alpha)} = \sum_g A_{ig}^{(s)} \phi_g^{(\alpha)}$$

where *i* indexes the measured values belonging to a single data set *s*, *g* designates the energy group, and α delineates spectra that may be simultaneously adjusted. For example,

$$R_i = \sum_g \sigma_{ig} \phi_g$$

relates a set of measured reaction rates R_i to a single spectrum ϕ_g by the multigroup reaction cross-section σ_{ig}. The log-normal approach automatically accounts for the physical constraint of positive fluxes, even with large assigned uncertainties.

In the least squares adjustment, the continuous quantities (i.e., neutron spectra and cross-sections) were approximated in a multi-group format consisting of 53 energy groups. The calculated input spectrum was converted to the FERRET 53 group structure using the SAND-II code[10]. This procedure was carried out by first expanding the 47 group calculated spectrum into the SAND-II 620 group structure using a SPLINE interpolation procedure in regions where group boundaries do not coincide. The 620 point spectrum was then re-collapsed into the group structure used in FERRET.

The sensor set reaction cross-sections, obtained from the ENDF/B-VI dosimetry file[11], were also collapsed into the 53 energy group structure using the SAND-II code. In this instance, the calculated spectrum, as expanded to 620 groups, was employed as a weighting function in the cross-section collapsing procedure. Reaction cross-section uncertainties in the form of a 53 x 53 covariance matrix for each sensor reaction were also constructed from the information contained on the ENDF/B-VI data files. These matrices included energy group to energy group uncertainty correlations for each of the individual reactions. However, correlations between cross-sections for different sensor reactions were not included. The omission of this additional uncertainty information does not significantly impact the results of the adjustment.

As noted above, the neutron spectrum input to the FERRET evaluation was obtained from the plant specific calculation for each capsule location. While the 53 x 53 group covariance matrices applicable to the sensor reaction cross-sections were developed from the cross-section data files, the covariance matrix for the input trial spectrum was constructed from the following relation:

$$M_{g'g} = R_n^2 + R_g R_{g'} P_{g'g}$$

where R_n specifies an overall fractional normalization uncertainty (i.e., complete correlation) for the set of values. The fractional uncertainties R_g specify additional random uncertainties for group g that are correlated with a correlation matrix given by:

$$P_{g'g} = [1 - \theta]\, \delta_{g'g} + \theta\, e^{-H}$$

where:

$$H = \frac{(g - g')^2}{2\gamma^2}$$

The first term in the correlation matrix equation specifies purely random uncertainties, while the second term describes short range correlations over a group range γ (θ specifies the strength of the latter term). The value of δ is 1 when $g = g'$ and 0 otherwise. For the trial spectrum used in the current evaluations, a short range correlation of $\gamma = 6$ groups was used. This choice implies that neighboring groups are strongly correlated when θ is close to 1. Strong long range correlations (or anti-correlations) were justified based on information presented by R. E. Maerker[12]. Maerker's results are closely duplicated when $\gamma = 6$. For the integral reaction rate covariances, simple normalization and random uncertainties were combined as deduced from experimental uncertainties.

In performing the least squares adjustment with the FERRET code, the input spectra from the reference forward transport calculations were normalized to the absolute calculations from the cycle specific adjoint analyses. The specific normalization factors for individual evaluations depended on the location of the sensor set as well as on the neutron flux level at that location.

The specific assignment of uncertainties in the measured reaction rates and the calculated spectra used in the FERRET evaluations was as follows:

REACTION RATE UNCERTAINTY	5%
FLUX NORMALIZATION UNCERTAINTY	30%
FLUX GROUP UNCERTAINTIES	
(E > 0.0055 MeV)	30%
(0.68 ev ≤ E ≤ 0.0055 MeV)	58%
(E < 0.68 ev)	104%

SHORT RANGE CORRELATION	
(E > 0.0055 MeV)	0.9
(0.68 ev $\leq$ E $\leq$ 0.0055 MeV)	0.5
(E < 0.68 ev)	0.5
FLUX GROUP CORRELATION RANGE	
(E > 0.0055 MeV)	6
(0.68 ev $\leq$ E $\leq$ 0.0055 MeV)	3
(E < 0.68 ev)	2

It should be noted that the uncertainties listed for the upper energy ranges extend down to the lower range. Thus, the 58% group uncertainty in the second range is made up of a 30% uncertainty with a 0.9 short range correlation and a range of 6, and a second part of magnitude 50% with a 0.5 correlation and a range of 3.

These input uncertainty assignments were based on prior experience in using the FERRET least squares adjustment approach in the analysis of neutron dosimetry from surveillance capsule, reactor cavity, and benchmark irradiations.

SECTION 3.0

METHODS QUALIFICATION AND UNCERTAINTY EVALUATIONS

As noted in Section 1.0, the qualification of the transport methodology used in the analysis of the fast neutron exposure of the Fort Calhoun pressure vessel consisted of the following three parts:

1 - Comparisons with benchmark measurements from the Pool Critical Assembly (PCA) simulator at the Oak Ridge National Laboratory (ORNL).

2 - Comparisons with a series of power reactor measurements that include data both from internal surveillance capsule dosimetry and reactor cavity dosimetry.

3 - An analytic sensitivity study investigating the dominant sources of uncertainty in the transport model.

The results of these studies, when combined with the Fort Calhoun measurement data base discussed in Section 5.0 of this report, validate the plant specific neutron transport calculations and help to define the uncertainties associated with the projections of the fast neutron neutron exposure of the Fort Calhoun pressure vessel.

3.1 Comparisons with the PCA Pressure Vessel Simulator Benchmark

The pressure vessel simulator benchmark comparisons used in the qualification of the neutron transport methodology are based on the analysis of the PCA 12/13 experimental configuration (see References 13, 14, and 15). A schematic description of this configuration is provided in Figures 3.1-1 and 3.1-2. A plan view of the PCA reactor and pressure vessel simulator showing materials characteristic of the core axial midplane is shown in Figure 3.1-1; whereas, a section view through the center of the mockup is shown in Figure 3.1-2. The description of the 12/13 configuration was derived from information provided in References 13 through 15 and reflects the latest available geometric data for the simulator.

The 12/13 configuration was chosen for the methods evaluation due to the similarity of this particular mockup to the thermal shield - downcomer - pressure vessel designs that are typical of most pressurized water reactors. Of particular note in regard to the areas of similarity are the 12 cm. water gap on the core side of the thermal shield, the 13 cm water gap between the

thermal shield and the pressure vessel simulator, the 6 cm thick thermal shield, the 22.5 cm thick low alloy steel pressure vessel, and the simulated reactor cavity (void box) positioned behind the pressure vessel mockup.

From the viewpoint of fast neutron attenuation, the 12/13 experimental configuration results in a reduction factor for ϕ ($E \geq 1.0$ MeV) of approximately 10^3 between the reactor core and the inner surface of the pressure vessel; and a corresponding reduction factor of about 30 from the inner surface to the outer surface of the pressure vessel wall. These similarities in the geometry and attenuation properties of the PCA mockup and LWR plant configurations provide additional confidence that judgements made regarding measurement/calculation comparisons in the simulator environment can be related to the subsequent analyses performed for operating light water reactors.

During the PCA experiments, measurements were obtained at several locations within the mockup to provide traverse data extending from the reactor core outward through the pressure vessel simulator and on into the void box. The specific measurement locations are illustrated on Figure 3.1-1 and listed in Table 3.1-1. From Figure 3.1-1, note that all of the measurements were obtained on the lateral centerline of the mockup. Furthermore, all of the measurement points were also positioned on the axial midplane of the simulator.

Figure 3.1-1

PCA 12/13 Configuration - X,Y Geometry

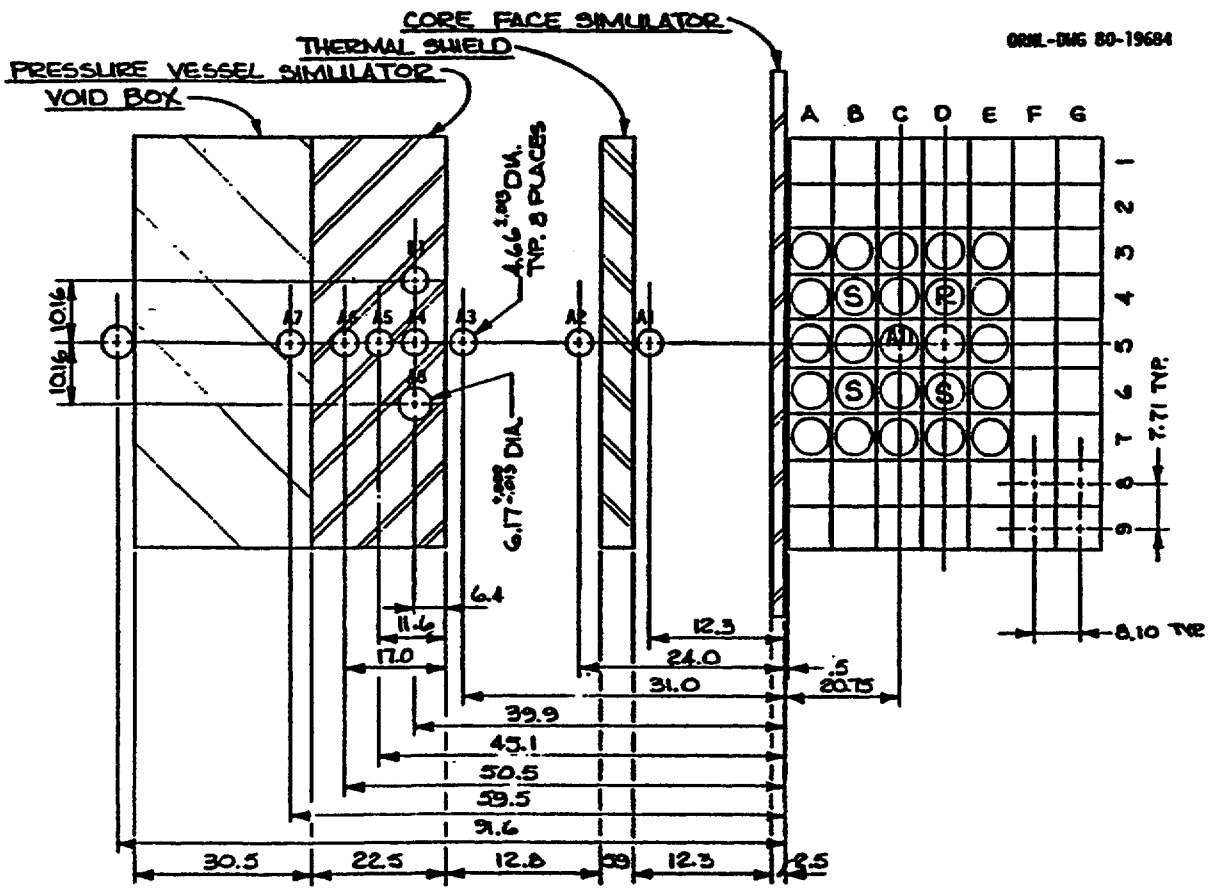

Figure 3.1-2

PCA 12/13 Configuration - Y,Z Geometry

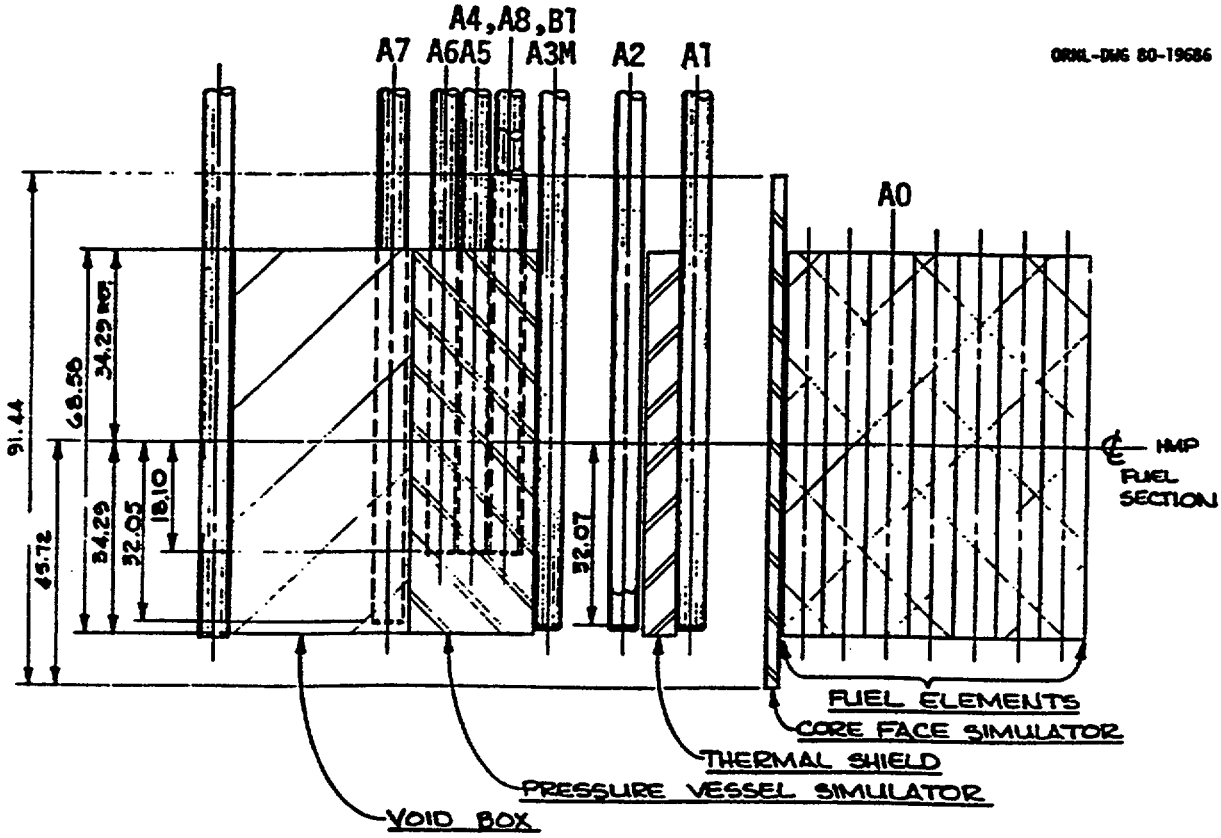

Table 3.1-1

Summary of Measurement Locations Within
The PCA 12/13 Configuration

LOCATION	ID	Y(cm)
CORE CENTER	A0	-20.75
THERMAL SHIELD FRONT	A1	11.98
THERMAL SHIELD BACK	A2	22.80
PRESSURE VESSEL FRONT	A3	29.71
PRESSURE VESSEL 1/4T	A4	39.51
PRESSURE VESSEL 1/2T	A5	44.67
PRESSURE VESSEL 3/4T	A6	50.13
VOID BOX	A7	59.13

Note: Y dimensions are referenced to the core side face of the aluminum window (see Figure 3.1-1).

The measurement locations specified in Table 3.1-1 provide data sufficient to generate measurement/calculation comparisons throughout the entire 12/13 configuration. Data from locations A4, A5, and A6 establish the means for verification of calculated exposure gradients within the pressure vessel wall itself. Since measurements at operating power reactors can, at best, provide data in the downcomer region internal to the vessel wall or in the cavity external to the vessel wall, these PCA data points located interior to the thick walled vessel establish a key set of comparisons to aid in the accurate determination of exposure gradients within the pressure vessel wall.

3.1.1 Method of Analysis

The neutron transport analysis of the PCA 12/13 configuration was carried out using two DORT two-dimensional discrete ordinates transport calculations, one in X,Y geometry and one in Y,Z geometry, as well as a single one-dimensional DORT calculation in planar (Y) geometry to synthesize a three-dimensional solution throughout the PCA simulator. The synthesis was carried out using the following relationship:

$$\phi_g(x,y,z) = \phi_g(x,y) * \frac{\phi_g(y,z)}{\phi_g(y)}$$

where: $\phi_g(x,y,z)$= The group-g neutron flux at position x,y,z within the problem geometry.

$\phi_g(x,y)$ = The group-g neutron flux solution from the x,y DORT computation.

$\phi_g(y,z)$ = The group-g neutron flux solution from the y,z DORT computation.

$\phi_g(y)$ = The group-g neutron flux solution from the y DORT computation.

In this synthesis approach the ratio $[\phi_g(y,z)]/[\phi_g(y)]$ represents an energy dependent axial shape factor that accounts for the finite height of the PCA core as well as for axial leakage effects introduced by the simulator geometry.

In the calculation of the PCA 12/13 configuration, all of the DORT computations were carried out in 67 energy groups (47 neutron, 20 gamma-ray) using a P_3 cross-section expansion from the BUGLE-93 library and an S_8 order of angular quadrature. The geometric models used in the calculations consisted of 71 X 131, 131 X 71, and 131 mesh cell arrays for the x,y, y,z, and y problems, respectively. Material descriptions for each of the regions comprising the simulator geometry were taken as specified in References 13 through 15. Likewise, the spatial distribution of the neutron source within the PCA core was obtained directly from References 13 through 15. In generating the energy dependent source for use in the transport calculations, the specified spatial distribution was coupled with the ENDF/B-VI U-235 fission spectrum supplied with the BUGLE-93 library. Dosimeter reaction rates for comparison with PCA measurements were derived from the synthesized three-dimensional neutron flux distribution using the ENDF/B-VI reaction cross-sections also supplied with the BUGLE-93 library.

3.1.2 Comparison of PCA Calculations with Measurements

Measured data from the PCA experiments using the 12/13 simulator configuration have been documented and discussed extensively in References 13, 14, and 15. In these documents, individual sensor measurements were provided in terms of either equivalent fission flux per source neutron or absolute reaction rates per source neutron for a variety of reactions with responses spanning the fast neutron energy range. For the comparisons presented in this report, all equivalent fission fluxes were converted to absolute reaction rates using fission spectrum averaged reaction cross-sections that were also reported in the PCA documentation. In particular, the following reaction cross-sections were employed to perform the required conversions:

REACTION	σ_f (barns)
Al-27(n,α)	0.000705
Ni-58(n,p)	0.1085
In-115(n,n')	0.189
U-238(n,f)	0.308
Np-237(n,f)	1.334

The appropriate measured reaction rates used for comparison with analytical prediction are summarized in Table 3.1-2.

In regard to the reaction rates listed in Table 3.1-2 it is important to note that, based on discussions contained in Reference 15, the U-238 and Np-237 data for locations within the pressure vessel wall (positions A4, A5, and A6) differ somewhat from the reaction rates given in References 13 and 14. In the earlier reports, a 10% bias was noted between fission chamber measurements and solid state track recorder (SSTR) data. As a result, recommended reaction rates were taken to be the average of the two data sets. Since publication of those earlier documents, the observed bias was determined to be caused by perturbations in the neutron field caused by the presence of the fission chamber structure. Therefore, the SSTR measurements provided a more accurate representation of the U-238(n,f) and Np-237(n,f) reaction rates within the pressure vessel wall. The data listed in Table 3.1-2 incorporate only the SSTR results for positions A4, A5, and A6. Fission rate data for all other locations within the 12/13 configuration remain as reported in References 13 and 14.

In addition to the measured reaction rates for each of the individual neutron sensors, the documentation of the PCA experiments also provides recommended values for important

energy dependent exposure parameters at each of the measurement locations. These derived exposure parameters resulting from the application of least squares adjustment procedures to fit an appropriate calculated neutron energy spectrum to each set of measured reaction rate data include $\phi(E \geq 1.0$ MeV), $\phi(E \geq 0.1$ MeV), and the iron atom displacement rate (dpa/sec). The recommended values of exposure parameters applicable to the 12/13 configuration are also listed in Table 3.1-2. The derived exposure parameters for locations A4, A5, and A6 reflect the use of U-238 and Np-237 fission rates measured by means of the SSTR technique. Thus, the influence of the previously mentioned bias associated with fission chamber perturbations has also been removed from these integral results.

The calculated reaction rates and exposure parameters applicable to the PCA 12/13 configuration are listed in Table 3.1-3. Comparisons of these analytical predictions with the measurements are provided in Table 3.1-4.

TABLE 3.1-2

Measured Sensor Reaction Rates in the PCA 12/13 Configuration

Reaction Rate (rps/nucleus-source neutron)

	Al-27(n,α)	Ni-58(n,p)	In-115(n,n')	U-238(n,f)	Np-237(n,f)
A1	5.48e-33	6.31e-31	1.05e-30		
A2	7.16e-34	6.72e-32	1.14e-31		7.30e-31
A3	3.13e-34	2.50e-32	3.68e-32	5.91e-32	3.05e-31
A4	7.15e-35	5.69e-33	1.11e-32	1.79e-32	1.20e-31
A5	2.92e-35	2.25e-33	5.20e-33	7.88e-33	6.56e-32
A6	1.12e-35	7.99e-34	2.23e-33	3.26e-33	3.47e-32
A7	4.29e-36		6.43e-34	8.65e-34	9.60e-33

	ϕ (E > 1.0 MeV)	ϕ (E > 0.1 MeV)	dpa/sec
A1			
A2	4.01e-07	7.47e-07	5.85e-28
A3			
A4	4.50e-08	1.35e-07	7.41e-29
A5	2.21e-08	9.01e-08	4.20e-29
A6	9.73e-09	5.37e-08	2.22e-29
A7			

Note: Neutron flux values are in units of n/cm^2-sec-source neutron.
Iron displacement rates are in units of dpa/sec-source neutron.

TABLE 3.1-3

Calculated Sensor Reaction Rates in the PCA 12/13 Configuration

Reaction Rate (rps/nucleus-source neutron)

	Al-27(n,α)	Ni-58(n,p)	In-115(n,n')	U-238(n,f)	Np-237(n,f)
A1	5.30e-33	6.05e-31	9.77e-31	1.68e-30	8.19e-30
A2	6.86e-34	6.47e-32	1.06e-31	1.80e-31	9.27e-31
A3	3.10e-34	2.46e-32	3.60e-32	6.28e-32	2.99e-31
A4	6.86e-35	5.48e-33	1.07e-32	1.72e-32	1.16e-31
A5	2.75e-35	2.14e-33	4.82e-33	7.39e-33	6.31e-32
A6	1.04e-35	7.89e-34	2.03e-33	2.95e-33	3.13e-32
A7	3.12e-36	1.96e-34	4.82e-34	6.95e-34	7.38e-33

	ϕ (E > 1.0 MeV)	ϕ (E > 0.1 MeV)	dpa/sec
A1	3.76e-06	6.76e-06	5.66e-27
A2	4.18e-07	8.37e-07	6.37e-28
A3	1.38e-07	2.45e-07	2.12e-28
A4	4.54e-08	1.40e-07	7.48e-29
A5	2.13e-08	9.13e-08	4.11e-29
A6	9.15e-09	5.17e-08	2.07e-29
A7	2.16e-09	1.15e-08	4.69e-30

Note: Neutron flux values are in units of n/cm^2-sec-source neutron.
Iron displacement rates are in units of dpa/sec-source neutron.

TABLE 3.1-4

Ratio of Measurement to Calculation (M/C) in the PCA 12/13 Configuration

	Al-27(n,α)	Ni-58(n,p)	In-115(n,n')	U-238(n,f)	Np-237(n,f)
A1	1.03	1.04	1.08		
A2	1.04	1.04	1.08		0.79
A3	1.01	1.02	1.02	0.94	1.02
A4	1.04	1.04	1.04	1.04	1.04
A5	1.06	1.05	1.08	1.07	1.04
A6	1.08	1.01	1.10	1.11	1.11
A7	1.38		1.33	1.24	1.30

	ϕ (E > 1.0 MeV)	ϕ (E > 0.1 MeV)	dpa/sec
A1			
A2	0.96	0.89	0.92
A3			
A4	0.99	0.96	0.99
A5	1.04	0.99	1.02
A6	1.06	1.04	1.07
A7			

3.2 - Comparisons with Power Reactor Measurements

In this section, comparisons of the measurement results from internal surveillance capsule and reactor cavity dosimetry with corresponding analytical predictions at the measurement locations are presented for two Westinghouse light water reactors that implemented an ex-vessel dosimetry system prior to initial plant startup. As such, the internal and external dosimetry sets have experienced the same reactor operating conditions for extended irradiation periods. The design of these reactors includes a thermal shield and the reactors operate at similar coolant pressure/temperature conditions to Fort Calhoun. The current data base applicable to the first reactor (Plant 1) consists of two sets of internal surveillance capsule dosimetry and four sets of ex-vessel reactor cavity dosimetry. Each set of reactor cavity measurements includes data from four azimuthal angles on the core axial midplane, thus, providing a total of 16 cavity data points for comparison. The data base for the second reactor (Plant 2) consists of three sets of internal surveillance capsule dosimetry and four sets of ex-vessel reactor cavity dosimetry. As was the case with Plant 1, the Plant 2 data base also provides 16 cavity data points on the reactor core midplane.

These comparisons of calculation and measurement are provided on two levels. In the first instance, calculations of fast neutron exposure rates in terms of $\phi(E \geq 1.0$ MeV), $\phi(E \geq 0.1$ MeV), and dpa/sec are compared with the results of the least squares adjustment procedure; while, in the second case, calculations of individual sensor reaction rates are compared directly with the measured data from the counting laboratories. It is shown that these two levels of comparison yield consistent and similar results, indicating that the least squares adjustment methodology is producing accurate exposure results and that the measurement/calculation (M/C) comparisons yield an accurate data set that may be used to validate the calculational procedure.

3.2.1 - Comparison of Least Squares Adjustment Results with Calculation

In Tables 3.2-1 and 3.2-3, comparisons of measured and calculated exposure rates for the internal surveillance capsule dosimetry sets as well as for four cycles of reactor cavity midplane dosimetry sets are given for Plants 1 and 2, respectively. In all cases, the calculated values were based on the methodology described in Section 2.0 using fuel cycle specific exposure calculations averaged over the appropriate irradiation period.

An examination of Table 3.2-1 and 3.2-3 indicates that, considering all of the available core midplane data, the measured exposure rates for Plant 1 were less than calculated values by factors of 0.93, 0.99, and 0.94 for $\phi(E \geq 1.0$ MeV), $\phi(E \geq 0.1$ MeV), and dpa/sec, respectively. The standard deviations associated with each of the 18 sample data sets were 8.4%, 10.2%, and 9.4%, respectively. In the case of Plant 2, the measured exposure rates were also less than the measured values by factors of 0.90, 0.93, and 0.92 for $\phi(E \geq 1.0$ MeV), $\phi(E \geq 0.1$ MeV), and dpa/sec, respectively. The standard deviations associated with each of the 19 sample data sets were 8.1%, 10.4%, and 9.5%, respectively.

3.2.2 - Comparisons of Measured and Calculated Sensor Reaction Rates

In Table 3.2-2 and 3.2-4, measurement/calculation (M/C) ratios for each fast neutron sensor reaction rate from the internal surveillance capsule and external reactor cavity irradiations are listed. These tabulations, provide a direct comparison, on an absolute basis, of calculation and measurement prior to the application of the least squares adjustment procedure.

An examination of Tables 3.2-2 and 3.2-4 shows consistent behavior for all reactions and all measurement points. For Plant 1 the standard deviations observed for the six fast neutron reactions range from 6.4% to 11.7% on an individual reaction basis; whereas, the overall average M/C ratio for the entire data set has an associated 1σ standard deviation of 11.3%. Furthermore, the average M/C ratio of 0.90 observed in the reaction rate comparisons is in excellent agreement with the values of 0.93, 0.99, and 0.94 observed in the exposure rate comparisons shown in Table 3.2-1.

For Plant 2 the standard deviations observed for the six fast neutron reactions range from 4.3% to 18.4% on an individual reaction basis; whereas, the overall average M/C ratio for the entire data set has an associated 1σ standard deviation of 10.2%. Furthermore, the average M/C ratio of 0.92 observed in the reaction rate comparisons is in excellent agreement with the values of 0.90, 0.93, and 0.92 observed in the exposure rate comparisons shown in Table 3.2-3.

Table 3.2-1

Comparison of Calculated and Adjusted Exposure Rates from Surveillance Capsule and Cavity Dosimetry Irradiations - Plant 1

	$\phi(E \geq 1.0$ MeV) $[n/cm^2\text{-}s]$		
	Calculated	Adjusted	A/C
INTERNAL CAPSULE			
Capsule 1	7.37e+10	7.49e+10	1.02
Capsule 2	6.11e+10	5.08e+10	0.83
0 DEGREE CAVITY			
Cycle A	3.14e+08	3.16e+08	1.01
Cycle B	2.79e+08	2.89e+08	1.04
Cycle C	2.50e+08	2.27e+08	0.91
Cycle D	2.44e+08	2.58e+08	1.06
11 DEGREE CAVITY			
Cycle A	4.61e+08	3.86e+08	0.84
Cycle B	3.58e+08	3.34e+08	0.93
Cycle C	3.34e+08	3.06e+08	0.92
Cycle D	3.20e+08	3.16e+08	0.99
35 DEGREE CAVITY			
Cycle A	7.17e+08	6.00e+08	0.84
Cycle B	6.55e+08	6.64e+08	1.01
Cycle C	6.28e+08	5.36e+08	0.85
Cycle D	4.99e+08	4.49e+08	0.90
45 DEGREE CAVITY			
Cycle A	8.07e+08	7.83e+08	0.97
Cycle B	7.13e+08	6.69e+08	0.94
Cycle C	6.89e+08	5.71e+08	0.83
Cycle D	5.25e+08	4.48e+08	0.85
AVERAGE A/C RATIO			0.93
PERCENT STANDARD DEVIATION (1σ)			8.4%

Table 3.2-1 (continued)

Comparison of Calculated and Adjusted Exposure Rates from Surveillance Capsule and Cavity Dosimetry Irradiations - Plant 1

	$\phi(E \geq 0.1$ MeV) [n/cm^2-s]		
	Calculated	Adjusted	A/C
INTERNAL CAPSULE			
Capsule 1	2.42e+11	2.72e+11	1.12
Capsule 2	2.01e+11	1.79e+11	0.89
0 DEGREE CAVITY			
Cycle A	3.59e+09	4.17e+09	1.16
Cycle B	3.19e+09	3.33e+09	1.04
Cycle C	2.86e+09	2.69e+09	0.94
Cycle D	2.79e+09	3.05e+09	1.09
11 DEGREE CAVITY			
Cycle A	5.34e+09	4.96e+09	0.93
Cycle B	4.17e+09	3.87e+09	0.93
Cycle C	3.89e+09	3.90e+09	1.00
Cycle D	3.73e+09	4.20e+09	1.13
35 DEGREE CAVITY			
Cycle A	8.64e+09	7.32e+09	0.85
Cycle B	7.76e+09	8.63e+09	1.11
Cycle C	7.44e+09	6.62e+09	0.89
Cycle D	5.91e+09	5.58e+09	0.94
45 DEGREE CAVITY			
Cycle A	9.08e+09	8.68e+09	0.96
Cycle B	8.35e+09	8.41e+09	1.01
Cycle C	8.06e+09	6.87e+09	0.89
Cycle D	6.14e+09	5.59e+09	0.94
AVERAGE A/C RATIO			0.99
PERCENT STANDARD DEVIATION (1σ)			10.2%

Table 3.2-1 (continued)

Comparison of Calculated and Adjusted Exposure Rates from Surveillance Capsule and Cavity Dosimetry Irradiations - Plant 1

	Iron Displacements [dpa]		
	Calculated	Adjusted	A/C
INTERNAL CAPSULE			
Capsule 1	1.24e-10	1.30e-10	1.05
Capsule 2	1.03e-10	8.71e-11	0.85
0 DEGREE CAVITY			
Cycle A	1.24e-12	1.35e-12	1.09
Cycle B	1.10e-12	1.11e-12	1.01
Cycle C	9.88e-13	8.95e-13	0.91
Cycle D	9.64e-13	1.01e-12	1.05
11 DEGREE CAVITY			
Cycle A	1.84e-12	1.62e-12	0.88
Cycle B	1.44e-12	1.29e-12	0.90
Cycle C	1.34e-12	1.28e-12	0.96
Cycle D	1.28e-12	1.36e-12	1.06
35 DEGREE CAVITY			
Cycle A	2.93e-12	2.41e-12	0.82
Cycle B	2.67e-12	2.79e-12	1.04
Cycle C	2.56e-12	2.18e-12	0.85
Cycle D	2.04e-12	1.83e-12	0.90
45 DEGREE CAVITY			
Cycle A	3.12e-12	2.88e-12	0.92
Cycle B	2.83e-12	2.73e-12	0.96
Cycle C	2.73e-12	2.25e-12	0.82
Cycle D	2.08e-12	1.82e-12	0.88
AVERAGE A/C RATIO			0.94
PERCENT STANDARD DEVIATION (1σ)			9.4%

Table 3.2-2

Comparison of Measured and Calculated Neutron Sensor Reaction Rates
from Surveillance Capsule and Cavity Dosimetry Irradiations - Plant 1

	Cu63(n,α)	Ti46(n,p)	Fe54(n,p)	Ni58(n,p)	U238(n,f)	Np237(n,f)
INTERNAL CAPSULE						
Capsule 1	1.09	0.88	1.01	1.03	1.14	
Capsule 2	0.97		0.78	0.84	0.89	
0 DEGREE CAVITY						
Cycle A	0.92	0.89	0.84	0.85	0.97	1.19
Cycle B	0.98		0.93		1.05	1.04
Cycle C	0.89	0.93	0.85	0.83	0.92	0.93
Cycle D	0.94	1.02	0.88	0.93	1.14	1.09
11 DEGREE CAVITY						
Cycle A	0.78	0.82	0.71	0.72	0.86	0.92
Cycle B	0.87		0.81		0.99	0.89
Cycle C	0.85	0.91	0.79		0.88	1.01
Cycle D	0.87	0.94	0.80	0.83	0.98	1.15
35 DEGREE CAVITY						
Cycle A	0.80	0.86	0.78	0.77	0.87	0.83
Cycle B	0.90		0.83		1.02	1.10
Cycle C	0.88	0.87	0.77		0.90	0.85
Cycle D	0.91	0.96	0.81	0.86	0.94	0.91
45 DEGREE CAVITY						
Cycle A	0.88	0.88	0.81	0.88	1.06	0.92
Cycle B	0.88		0.76		0.96	0.99
Cycle C	0.78	0.83	0.74	0.75	0.87	
Cycle D	0.83	0.88	0.71	0.79	0.90	0.88
AVERAGE	0.89	0.90	0.81	0.84	0.96	0.99
% ST. DEV. (1σ)	8.5	6.4	7.2	9.5	8.2	11.7
OVERALL AVERAGE M/C RATIO						0.90
PERCENT STANDARD DEVIATION (1σ)						11.3%

Table 3.2-3

Comparison of Calculated and Adjusted Exposure Rates from Surveillance Capsule and Cavity Dosimetry Irradiations - Plant 2

	ϕ(E > 1.0 MeV) [n/cm^2-s]		
	Calculated	Adjusted	A/C
INTERNAL CAPSULE			
Capsule 1	9.49e+10	1.14e+11	1.20
Capsule 2	8.55e+10	8.83e+10	1.03
Capsule 3	6.94e+10	5.93e+10	0.86
0 DEGREE CAVITY			
Cycle A	5.33e+08	4.67e+08	0.88
Cycle B	4.15e+08	3.82e+08	0.92
Cycle C	4.42e+08	3.57e+08	0.81
Cycle D	3.90e+08	3.37e+08	0.86
10 DEGREE CAVITY			
Cycle A	7.39e+08	6.00e+08	0.81
Cycle B	5.24e+08	4.18e+08	0.80
Cycle C	5.62e+08	4.25e+08	0.76
Cycle D	4.91e+08	3.91e+08	0.80
35 DEGREE CAVITY			
Cycle A	7.15e+08	6.28e+08	0.88
Cycle B	6.44e+08	6.16e+08	0.96
Cycle C	5.73e+08	4.75e+08	0.83
Cycle D	5.40e+08	5.17e+08	0.96
45 DEGREE CAVITY			
Cycle A	8.10e+08	7.94e+08	0.98
Cycle B	7.11e+08	6.55e+08	0.92
Cycle C	6.13e+08	5.69e+08	0.93
Cycle D	5.92e+08	5.56e+08	0.94
AVERAGE A/C RATIO			0.90
PERCENT STANDARD DEVIATION (1σ)			8.1%

Table 3.2-3 (continued)

Comparison of Calculated and Adjusted Exposure Rates from Surveillance Capsule and Cavity Dosimetry Irradiations - Plant 2

	ϕ(E > 0.1 MeV) [n/cm^2-s]		
	Calculated	Adjusted	A/C
INTERNAL CAPSULE			
Capsule 1	4.25e+11	5.51e+11	1.30
Capsule 2	3.83e+11	4.32e+11	1.13
Capsule 3	3.05e+11	2.66e+11	0.87
0 DEGREE CAVITY			
Cycle A	4.85e+09	4.14e+09	0.86
Cycle B	3.77e+09	3.47e+09	0.92
Cycle C	4.02e+09	3.20e+09	0.80
Cycle D	3.55e+09	3.14e+09	0.89
10 DEGREE CAVITY			
Cycle A	6.90e+09	5.35e+09	0.77
Cycle B	4.92e+09	3.88e+09	0.79
Cycle C	5.28e+09	3.88e+09	0.74
Cycle D	4.61e+09	3.76e+09	0.82
35 DEGREE CAVITY			
Cycle A	8.13e+09	7.32e+09	0.90
Cycle B	7.35e+09	7.56e+09	1.03
Cycle C	6.54e+09	5.66e+09	0.87
Cycle D	6.16e+09	6.35e+09	1.03
45 DEGREE CAVITY			
Cycle A	8.32e+09	8.11e+09	0.97
Cycle B	7.30e+09	6.82e+09	0.93
Cycle C	6.30e+09	6.44e+09	1.02
Cycle D	6.08e+09	5.80e+09	0.95
AVERAGE A/C RATIO			0.93
PERCENT STANDARD DEVIATION (1σ)			10.4%

Table 3.2-3 (continued)

Comparison of Calculated and Adjusted Exposure Rates from Surveillance Capsule and Cavity Dosimetry Irradiations - Plant 2

	Iron Displacements [dpa/s]		
	Calculated	Adjusted	A/C
INTERNAL CAPSULE			
Capsule 1	1.84e-10	2.30e-10	1.26
Capsule 2	1.65e-10	1.80e-10	1.09
Capsule 3	1.33e-10	1.16e-10	0.87
0 DEGREE CAVITY			
Cycle A	1.73e-12	1.48e-12	0.86
Cycle B	1.34e-12	1.23e-12	0.92
Cycle C	1.43e-12	1.15e-12	0.80
Cycle D	1.26e-12	1.11e-12	0.88
10 DEGREE CAVITY			
Cycle A	2.44e-12	1.91e-12	0.78
Cycle B	1.74e-12	1.38e-12	0.79
Cycle C	1.86e-12	1.39e-12	0.74
Cycle D	1.63e-12	1.33e-12	0.81
35 DEGREE CAVITY			
Cycle A	2.74e-12	2.44e-12	0.89
Cycle B	2.47e-12	2.49e-12	1.01
Cycle C	2.19e-12	1.88e-12	0.86
Cycle D	2.07e-12	2.09e-12	1.01
45 DEGREE CAVITY			
Cycle A	2.84e-12	2.75e-12	0.97
Cycle B	2.49e-12	2.30e-12	0.93
Cycle C	2.15e-12	2.13e-12	0.99
Cycle D	2.07e-12	1.96e-12	0.95
AVERAGE A/C RATIO			0.92
PERCENT STANDARD DEVIATION (1σ)			9.5%

Table 3.2-4

Comparison of Measured and Calculated Neutron Sensor Reaction Rates
from Surveillance Capsule and Cavity Dosimetry Irradiations - Plant 2

	Cu63(n,α)	Ti46(n,p)	Fe54(n,p)	Ni58(n,p)	U238(n,f)	Np237(n,f)
SURVEILLANCE CAPSULES						
Capsule 1	1.18		1.09	1.08	1.19	1.33
Capsule 2	1.10		0.94	0.93	1.09	1.12
Capsule 3	1.08		0.89	0.89	0.90	0.84
0 DEGREE CAVITY						
Cycle A	0.94	0.95	0.93	0.89	0.89	0.85
Cycle B	0.93	0.98	0.94	0.89	0.94	0.92
Cycle C	0.87	0.94	0.84	0.86	0.83	0.78
Cycle D	0.93	1.00	0.85	0.89	0.91	
10 DEGREE CAVITY						
Cycle A	0.86	0.89	0.91	0.81	0.83	0.76
Cycle B	0.89	0.94	0.88	0.84	0.79	0.78
Cycle C	0.89	0.94	0.83	0.84	0.78	0.71
Cycle D	0.94	0.99	0.83	0.87	0.81	
35 DEGREE CAVITY						
Cycle A	0.83	0.91	0.88	0.85	0.91	
Cycle B	0.91	0.97	0.92	0.85	0.97	1.05
Cycle C	0.87	0.92	0.81	0.83	0.86	0.85
Cycle D	0.95	0.98	0.86	0.90	1.01	1.02
45 DEGREE CAVITY						
Cycle A	0.94	0.95	0.96	0.93	1.01	
Cycle B	0.92	0.93	0.92	0.86	0.95	0.94
Cycle C	0.96	0.86	0.90	0.90	0.88	1.05
Cycle D	1.02	0.99	0.90	0.94	1.00	
AVERAGE	0.95	0.95	0.90	0.89	0.92	0.93
% ST. DEV. (1σ)	9.4	4.3	7.1	6.5	11.4	18.4
OVERALL AVERAGE M/C RATIO						0.92
PERCENT STANDARD DEVIATION (1σ)						10.2%

3.3 - Analytical Sensitivity Studies

The overall uncertainty associated with calculated exposure rates and integrated exposures can be conveniently subdivided into two broad categories. The first category involves biases or errors that may be present due to inadequacies in the method itself or in the basic nuclear data input to the calculation. These potential biases are addressed via validation of the analytical technique through comparison with measurements from controlled benchmark experiments, from power reactor surveillance capsule and reactor cavity measurement data bases, and, ultimately, from plant specific surveillance capsule and cavity irradiations.

The second category of uncertainty in the analysis of vessel exposure involves variations that may exist in reactor dimensions, coolant temperature, neutron source strength and source distribution, as well as in other parameters that may vary from reactor to reactor or fuel cycle to fuel cycle. This category of uncertainty is most easily addressed via sensitivity studies performed for each of the variables important to the overall evaluation.

For the methodology used in the Fort Calhoun neutron exposure evaluations, several sensitivity studies were carried out to test the effect of variations in reactor geometry and neutron source definition on the calculated vessel exposure based on the analytical approach outlined in Section 2.0. These studies are not all inclusive, but do encompass the major contributors to uncertainties in the analytical approach. Important input parameters addressed in these studies include the following:

Geometry and Material Density
- stainless steel reactor internals
- water annuli
- reactor pressure vessel
- core periphery modeling
- dosimetry positioning (capsule/cavity)

Core Neutron Source
- peripheral assembly source magnitude
- peripheral assembly burnup
- axial power distribution
- relative spatial distribution of the source

As noted earlier in this section, the effects of transport cross-section errors and uncertainties as well as biases introduced by methods approximations were assessed by direct comparisons with measured data rather than via a series of analytical studies.

3.3.1 - Geometric Modeling and Material Density

With the exception of the location of the surveillance capsule geometric center and the pressure vessel inner radius, the calculations performed for the Fort Calhoun reactor made use of nominal design dimensions for all internals components to establish the reactor geometry used in the transport model. In the case of the surveillance capsule and vessel inner radius, as-built data were available and were incorporated into the model. Likewise, nominal average full power coolant temperatures were used to determine water density in the core and downcomer regions. Sensitivity of the calculated fast neutron exposure of the pressure vessel to each of these variables was addressed via a series of parametric studies.

To determine the potential impact of the reactor internals manufacturing and assembly tolerances on the analytical prediction of the fast neutron exposure of the pressure vessel, calculations were performed for cases representing minimum shielding between the reactor core and the pressure vessel (i.e., all components at minimum thickness) and for maximum shielding between the core and the pressure vessel (i.e., all components at maximum thickness). These extreme conditions were then compared to the nominal calculation to establish an upper bound uncertainty in the use of nominal vs as-built internals dimensions. The resultant uncertainty in the calculated exposure of the pressure vessel is $\pm 3\%$.

The sensitivity of the calculated vessel exposure to fluctuations in water temperature was likewise determined via a parametric study in which water temperature and, hence, coolant density was varied over a range of several degrees F relative to nominal conditions. The results of this study indicate that a bounding uncertainty of $\pm 4\%$ results from a temperature variation of ± 10 degrees F. A ± 10 degree fluctuation in water temperature would exceed variations expected during normal operation of the plant over a given fuel cycle. Thus, the projected 4% uncertainty is considered to represent a conservative upper bound estimate.

The modeling of the rectilinear core baffle in r,θ geometry represents another potential source of uncertainty in the geometric modeling of the reactor. The sensitivity of the

solution to the modeling approach was determined by a direct comparison of the results of an r,θ computation with those of an X,Y calculation in which the baffle region and core periphery were modeled explicitly. The comparisons of interest were taken at various locations external to the core baffle. Results of these calculations, in general, agreed within the pointwise flux convergence criterion specified for the transport analyses, thus demonstrating the adequacy of the modeling approach. Therefore, the bounding analytical uncertainty associated with this modeling approximation is taken to be less than ±1%.

It should be noted that the X,Y vs r,θ comparisons described in the preceding paragraph, address not only the adequacy of the geometric modeling of the core periphery, but also demonstrate the adequacy of the transformation of the core neutron source from pin powers to the r,θ DOT model.

The inner radius of the reactor vessel itself and the position of surveillance capsule dosimetry are extremely important in the determination of the exposure of the pressure vessel wall both from an analytical standpoint and from the viewpoint of surveillance capsule dosimetry interpretation. Therefore, sensitivity studies based on the as-built dimensions for both the vessel inner radius and capsule position were also performed.

Parametric evaluations of vessel inner radius indicate that variations in vessel inner radius result in a change in calculated vessel fast neutron exposure of ±5%. Uncertainties associated with the positioning of capsule dosimetry are extremely important in the evaluation of comparisons of calculation with measurement. Parameter studies using the as-built position variations result in positioning uncertainties of ±4% for surveillance capsules.

In developing the above uncertainties, the parametric studies assumed that, in the case of the surveillance dosimetry, displacement of the sensors either introduced or removed water from the area between the reactor core and the sensors.

3.3.2 - Core Neutron Source

In addition to the sensitivity of the transport calculation to tolerances in the geometric model, several studies were also carried out to establish the sensitivity to the strength and spatial distribution of the neutron source within the reactor core. In particular, investigations were carried out to determine the sensitivity of calculated results to the

absolute source strength in fuel assemblies on the core periphery, the pin by pin spatial distribution of neutron source on the core periphery, the burnup of peripheral fuel assemblies, and the axial power distribution used in the flux synthesis procedure. It should be noted that the impacts of changing fission spectra, energy release per fission, and neutron yield per fission were encompassed in the parametric variation of fuel assembly burnup.

For the absolute power level of peripheral fuel assemblies, the self-attenuation afforded by the core materials results in the neutron environment external to the core being dominated by these edge assemblies. An examination of the adjoint transport evaluations performed for the Fort Calhoun reactor demonstrates that 90-95% of the external environment results from neutrons born in these locations. Therefore, the fluence uncertainty associated with the absolute core power level is directly dependent on the uncertainties in the power production of those peripheral assemblies. Based on comparisons of calculated vs measured (derived from in-core flux maps) peripheral power distributions for pressurized water reactors, a bounding uncertainty for peripheral power magnitude has been determined to be $\pm 5\%$.

In a fashion similar to the peripheral assembly power, the uncertainty in the axial power distribution averaged over the irradiation period, translates directly to an uncertainty in the calculated neutron environment external to the core. Over the course of a given fuel cycle, the variation in the axial peaking factor at maximum flux locations is typically 10%. That is, the maximum axial peaking factor may change from a value of approximately 1.15 at beginning of cycle to 1.05 at end of cycle, yielding a cycle average peaking factor of 1.10. This observation was drawn from an examination of numerous axial distributions from a wide variety of pressurized water reactors employing both low leakage and non-low leakage fuel management. In order to bound the uncertainty associated with this cycle average value, a variation of $\pm 5\%$ is taken to be applicable. This uncertainty value is liberal enough to encompass the entire change in axial shape over the course of the fuel cycle.

Sensitivity studies involving source parameters such as fission spectrum, neutron yield per fission and energy release per fission were performed via an evaluation of the sensitivity of the calculated fast neutron flux at the pressure vessel inner radius to the burnup of assemblies on the periphery of the reactor core. These burnup studies encompass significant perturbations in these source parameters due to the build-in of plutonium isotopes as the assembly burnup increases.

For the studies in question, burnup was varied from an assembly average of 3,000 MWD/MTU to 45,000 MWD/MTU. The results of this evaluation indicated that the net change in vessel flux is approximately 0.4%/1,000 MWD/MTU in the burnup range of 3,000-15,000 MWD/MTU and 0.2%/1,000 MWD/MTU in the burnup range of 15,000-45,000 MWD/MTU. The total increase in calculated flux at a burnup of 45,000 MWD/MTU relative to that based on a burnup of 3,000 MWD/MTU is about 10%.

The values quoted in the preceding paragraph are typical of light water reactors. Actual values will vary slightly depending on reactor core configuration, core loadings, and point of interest on the vessel wall. However, these smaller changes are of second order, and therefore the data discussed above provide an adequate evaluation of the sensitivity of the neutron flux at the pressure vessel and at dosimetry locations to these particular parameters.

In the assignment of an overall sensitivity to fuel assembly burnup a liberal approach was utilized. It was first assumed that the sensitivity to burnup effects was 0.4% per 1,000 MWD/MTU, i.e., the largest value obtained from the sensitivity study. It was then further assumed that from the plant specific core design information, a 5,000 MWD/MTU uncertainty exists in the calculated fuel assembly burnup. This is clearly a conservative evaluation, particularly at low to intermediate levels of burnup. Combining these two values yields a bounding sensitivity to fission spectrum, neutron yield per fission, and energy release per fission of $\pm 2\%$.

Core management studies on Westinghouse designed fuel cycles indicate that uncertainties in the relative pin powers in peripheral fuel assemblies can be on the order of 8-10%. Due to the use of similar design methodologies, this uncertainty should apply as well to fuel designs of other manufacturers. Translating this core design uncertainty to vessel exposure results in a $\pm 4\%$ uncertainty in vessel exposure.

3.3.3 - Summary of Analytical Sensitivity Studies

The results of analytically based sensitivity studies of geometric and source distribution input parameters may be summarized as follows:

	Vessel IR	Capsule
r,θ Modeling	1%	1%
Internals Dimensions	3%	3%
Vessel Inner Radius	5%	
Water Temperature	4%	4%
Peripheral Fuel Assembly Source Strength	5%	5%
Axial Power Distribution	5%	5%
Peripheral Assembly Burnup	2%	2%
Spatial Distribution of the Source	4%	4%
Capsule Dosimetry Positioning		4%
TOTAL	11%	10%

When combined these individual sensitivities result in a net impact on the calculated flux levels in the vicinity of the pressure vessel of $\pm$11%. The uncertainty evaluated at the dosimeter locations within internal surveillance capsules is $\pm$10%.

These uncertainties due to potential variations in design and operating parameters for individual reactors must, of course be combined with uncertainties resulting from methods and cross-section errors to determine the total uncertainty in the calculated results. This evaluation of the total uncertainty for the Fort Calhoun fluence evaluations is discussed in Section 6.0.

SECTION 4.0

RESULTS OF NEUTRON TRANSPORT CALCULATIONS

4.1 - Reference Forward Transport Calculation

As noted in Section 2.0 of this report, a reference forward transport calculation based on a core power distribution representative of the burnup weighted average over the first 14 cycles of operation provided data for use in evaluating neutron dosimetry from surveillance capsule evaluations, and in relating the neutron exposure at locations interior to the pressure vessel wall to the calculated fluence at the inner radius. In this section, the key data extracted from this reference forward calculation is presented and its relevance to the dosimetry evaluations and vessel exposure projections is discussed. The reader should recall that the results of the reference forward transport calculation were intended for use on a relative basis and, therefore, should not be used for absolute comparison with the measurements discussed in Section 5.0. All absolute comparisons were based on the results of the fuel cycle-specific adjoint calculations discussed in Section 4.2.

4.1.1 - Surveillance Capsule Locations

Data from the reference forward calculation pertinent to surveillance capsule evaluations are provided in Tables 4.1-1 and 4.1-2.

In Table 4.1-1, the calculated neutron energy spectra at the geometric center of surveillance capsules located at the 225° and 265°/275° azimuthal locations are listed. In Table 4.1-2, the calculated neutron sensor reaction rates and exposure rate ratios associated with the spectra from Table 4.1-1 are provided along with the calculated exposure rates in terms of $\phi(E \geq 1.0$ MeV), $\phi(E \geq 0.1$ MeV), and dpa/sec. Again, these data are applicable to the geometric center of each surveillance capsule.

These reference reaction rates, exposure rates, and exposure rate ratios were used in conjunction with the results of fuel cycle specific adjoint transport calculations from Section 4.2 to provide calculated sensor reaction rates and to project sensor set exposures in terms of $\phi(E \geq 0.1$ MeV) and dpa/sec for each capsule irradiation period.

4.1.2 - Pressure Vessel Wall

Data from the reference forward calculation pertinent to the pressure vessel wall are provided in Tables 4.1-3 through 4.1-6.

In Table 4.1-3, the calculated azimuthal distribution of exposure rates in terms of $\phi(E \geq 1.0$ MeV), $\phi(E \geq 0.1$ MeV), and dpa/sec are listed at approximately 5 degree intervals over the reactor geometry. These data are applicable to the clad/base metal interface. Also given in Table 4.1-3 are the exposure rate ratios $[\phi(E \geq 0.1$ MeV)]/[$\phi(E \geq 1.0$ MeV)] as well as [dpa/sec]/[$\phi(E \geq 1.0$ MeV)] that provide an indication of the variation in neutron energy spectrum as a function of azimuthal angle at the pressure vessel inner radius.

Radial gradient information for $\phi(E \geq 1.0$ MeV), $\phi(E \geq 0.1$ MeV), and dpa/sec is given in Tables 4.1-4, 4.1-5, and 4.1-6, respectively. These data are presented on a relative basis for each exposure parameter at the 0°, 15°, 30°, and 45° azimuthal locations. Exposure rate distributions within the vessel wall were obtained by normalizing the calculated (ϕ_{Calc}) exposure at the vessel inner radius to the gradient data given in Tables 4.1-4 through 4.1-6.

Table 4.1-1

Calculated Reference Neutron Energy Spectra at
Surveillance Capsule Locations

Lower Energy (MeV)	225°	265°/275°	Lower Energy (MeV)	225°	265°/275°
1.42E+01	1.10e+07	9.73e+06	2.97E-01	1.59e+10	1.02e+10
1.22E+01	3.55e+07	3.08e+07	1.83E-01	1.44e+10	9.29e+09
1.00E+01	1.56e+08	1.31e+08	1.11E-01	1.17e+10	7.55e+09
8.61E+00	3.05e+08	2.54e+08	6.74E-02	1.00e+10	6.43e+09
7.41E+00	5.44e+08	4.42e+08	4.09E-02	4.27e+09	2.73e+09
6.07E+00	1.38e+09	1.11e+09	3.18E-02	3.00e+09	1.90e+09
4.97E+00	2.13e+09	1.66e+09	2.61E-02	2.32e+09	1.51e+09
3.68E+00	4.29e+09	3.19e+09	2.42E-02	1.88e+09	1.21e+09
3.01E+00	3.35e+09	2.40e+09	2.19E-02	5.55e+09	3.45e+09
2.73E+00	2.55e+09	1.81e+09	1.50E-02	1.20e+10	7.65e+09
2.47E+00	2.95e+09	2.07e+09	7.10E-03	1.34e+10	8.58e+09
2.37E+00	1.47e+09	1.03e+09	3.36E-03	1.29e+10	8.21e+09
2.35E+00	3.99e+08	2.77e+08	1.59E-03	2.06e+10	1.31e+10
2.23E+00	1.98e+09	1.38e+09	4.54E-04	1.25e+10	7.93e+09
1.92E+00	5.25e+09	3.52e+09	2.14E-04	1.28e+10	8.09e+09
1.65E+00	5.81e+09	3.96e+09	1.01E-04	1.72e+10	1.08e+10
1.35E+00	8.55e+09	5.77e+09	3.73E-05	2.15e+10	1.35e+10
1.00E+00	1.39e+10	9.29e+09	1.07E-05	1.28e+10	8.04e+09
8.21E-01	8.95e+09	5.92e+09	5.04E-06	1.74e+10	1.09e+10
7.43E-01	5.06e+09	3.34e+09	1.86E-06	1.34e+10	8.34e+09
6.08E-01	1.20e+10	7.81e+09	8.76E-07	1.34e+10	8.30e+09
4.98E-01	1.03e+10	6.67e+09	4.14E-07	3.19e+10	1.96e+10
3.69E-01	1.15e+10	7.48e+09	1.00E-07	1.28e+11	7.60e+10
2.97E-01	9.54e+09	6.19e+09	0.00		

NOTE: The upper energy of group 1 is 17.33 Mev.

Table 4.1-2

Reference Neutron Sensor Reaction Rates and Exposure Parameters
at the Center of Surveillance Capsules

	225°	265°/275°
	Reaction Rate (rps/nucleus)	
Cu-63(n,α)	4.80e-17	3.91e-17
Ti-46(n,p)	7.92e-16	6.31e-15
Fe-54(n,p)	5.09e-15	3.84e-15
Ni-58(n,p)	6.68e-15	5.01e-15
U-238(n,f) (Cd)	2.10e-14	1.50e-14
U-238(γ,f)	1.60e-15	1.02e-15
	Neutron Flux (n/cm^2-sec)	
$\phi(E \geq 1.0$ MeV)	5.52e+10	3.85e+10
$\phi(E \geq 0.1$ MeV)	1.45e+11	9.70e+10
	dpa/sec	
Displacement Rate	8.74e-11	6.03e-11
$\phi(E \geq 0.1)/\phi(E \geq 1.0)$	2.63	2.52
[dpa/sec]/$\phi(E \geq 1.0)$	1.58E-21	1.57E-21
U238(γ,f)/U238(n,f)	0.076	0.068

Table 4.1-3

Summary of Exposure Rates at the Pressure Vessel
Clad/Base Metal Interface

Theta	Flux (n/cm^2-sec)			[E > 0.1]	dpa/sec
(deg)	(E > 1.0)	(E > 0.1)	dpa/sec	[E > 1.0]	[E > 1.0]
0.00	2.51e+10	6.58e+10	4.05e-11	2.62	1.61E-21
5.00	2.42e+10	6.81e+10	3.97e-11	2.81	1.64E-21
9.75	2.50e+10	6.56e+10	4.04e-11	2.62	1.62E-21
15.25	2.23e+10	5.92e+10	3.61e-11	2.65	1.62E-21
19.78	1.98e+10	5.07e+10	3.22e-11	2.56	1.63E-21
24.75	1.93e+10	4.86e+10	3.14e-11	2.52	1.63E-21
30.00	2.35e+10	6.21e+10	3.81e-11	2.64	1.62E-21
35.25	3.02e+10	8.66e+10	4.91e-11	2.87	1.63E-21
39.71	3.40e+10	1.01e+11	5.53e-11	2.97	1.63E-21
45.00	3.44e+10	1.00e+11	5.68e-11	2.91	1.65E-21

Table 4.1-4

Relative Radial Distribution of $\phi(E \geq 1.0$ MeV)
Within the Pressure Vessel Wall

Radius (cm)	90.0°	75.0°	60.0°	45.0°	0.0°
179.85[1]	1.000	1.000	1.000	1.000	1.000
180.36	0.973	0.959	0.966	0.966	0.973
182.37	0.785	0.788	0.786	0.787	0.785
184.09	0.637	0.641	0.642	0.640	0.637
184.37[2]	0.617	0.621	0.621	0.620	0.617
186.39	0.470	0.473	0.473	0.472	0.470
188.40	0.357	0.359	0.362	0.359	0.357
190.41	0.270	0.272	0.274	0.271	0.270
192.42	0.202	0.204	0.206	0.202	0.202
193.14	0.183	0.185	0.187	0.183	0.183
193.42[3]	0.176	0.178	0.180	0.176	0.176
194.43	0.150	0.151	0.153	0.149	0.150
196.44	0.108	0.110	0.111	0.106	0.108
197.94[4]	0.089	0.092	0.093	0.088	0.089

NOTES: (1) Indicates Base Metal Inner Radius
(2) Indicates Base Metal 1/4T
(3) Indicates Base Metal 3/4T
(4) Indicates Base Metal Outer Radius

Table 4.1-5

Relative Radial Distribution of $\phi(E \geq 0.1$ MeV)
Within the Pressure Vessel Wall

Radius (cm)	90.0°	75.0°	60.0°	45.0°	0.0°
179.85[1]	1.000	1.000	1.000	1.000	1.000
180.36	1.000	1.000	1.000	1.000	1.000
182.37	0.960	0.957	0.964	0.941	0.960
184.09	0.887	0.884	0.894	0.863	0.887
184.37[2]	0.874	0.871	0.881	0.849	0.874
186.39	0.780	0.777	0.790	0.751	0.780
188.40	0.685	0.682	0.698	0.654	0.685
190.41	0.592	0.591	0.604	0.559	0.592
192.42	0.500	0.503	0.515	0.468	0.500
193.14	0.469	0.472	0.483	0.437	0.469
193.42[3]	0.457	0.460	0.471	0.425	0.457
194.43	0.413	0.417	0.426	0.381	0.413
196.44	0.326	0.332	0.340	0.293	0.326
197.94[4]	0.277	0.285	0.292	0.243	0.277

NOTES: (1) Indicates Base Metal Inner Radius
(2) Indicates Base Metal 1/4T
(3) Indicates Base Metal 3/4T
(4) Indicates Base Metal Outer Radius

Table 4.1-6

Relative Radial Distribution of dpa/sec
Within the Pressure Vessel Wall

Radius (cm)	90.0°	75.0°	60.0°	45.0°	0.0°
179.85[1]	1.000	1.000	1.000	1.000	1.000
180.36	0.974	0.973	0.974	0.974	0.974
182.37	0.832	0.831	0.836	0.834	0.832
184.09	0.714	0.712	0.719	0.717	0.714
184.37[2]	0.697	0.695	0.702	0.700	0.697
186.39	0.575	0.573	0.583	0.576	0.575
188.40	0.474	0.472	0.481	0.473	0.474
190.41	0.388	0.387	0.397	0.387	0.388
192.42	0.315	0.318	0.322	0.311	0.315
193.14	0.292	0.295	0.300	0.287	0.292
193.42[3]	0.283	0.286	0.291	0.278	0.283
194.43	0.250	0.254	0.260	0.245	0.250
196.44	0.194	0.199	0.203	0.186	0.194
197.94[4]	0.165	0.171	0.175	0.154	0.165

NOTES: (1) Indicates Base Metal Inner Radius
(2) Indicates Base Metal 1/4T
(3) Indicates Base Metal 3/4T
(4) Indicates Base Metal Outer Radius

4.2 - Fuel Cycle Specific Adjoint Calculations

Results of the fuel cycle specific adjoint transport calculations for the first 16 cycles of operation at Fort Calhoun are summarized in Tables 4.2-1 through 4.2-6. The data listed in these tables establish the means for absolute comparison of analysis and measurement for the three sets of surveillance capsule dosimetry withdrawn to date. These results also provide the fuel cycle specific relationship among the surveillance capsule measurement locations and key positions at the inner radius of the pressure vessel wall.

The calculated fast neutron flux ($E \geq 1.0$ MeV) at the center of surveillance capsules located at azimuthal positions of 225° and 265°/275° are provided for each of the sixteen operating cycles in Table 4.2-1. The data as tabulated represent the maximum flux location in the axial distribution. Similar data applicable to the pressure vessel inner radius are given in Table 4.2-2.

Exposure parameter ratios necessary to convert the cycle specific data listed in Tables 4.2-1 and 4.2-2 to other key fast neutron exposure units are given in Section 4.1 of this report. Application of these ratios to the data from Tables 4.2-1 and 4.2-2 yielded corresponding exposure in terms of neutron flux ($E \geq 0.1$ MeV) (Tables 4.2-3 and 4.2-4) and iron atom displacement rates (Tables 4.2-5 and 4.2-6).

Table 4.2-1

Calculated Fast Neutron Flux ($E \geq 1.0$ MeV) at
the Surveillance Capsule Center

	Capsule Location	
	225°	265°/275°
Cycle 1	6.85e+10	4.98e+10
Cycle 2	6.72e+10	4.79e+10
Cycle 3	8.03e+10	5.08e+10
Cycle 4	6.91e+10	4.83e+10
Cycle 5	7.14e+10	4.60e+10
Cycle 6	7.36e+10	5.27e+10
Cycle 7	7.40e+10	5.49e+10
Cycle 8	5.15e+10	3.75e+10
Cycle 9	4.90e+10	2.75e+10
Cycle 10	3.35e+10	5.02e+10
Cycle 11	5.80e+10	3.09e+10
Cycle 12	4.87e+10	3.04e+10
Cycle 13	5.10e+10	2.72e+10
Cycle 14	3.53e+10	2.94e+10
Cycle 15	2.73e+10	2.94e+10
Cycle 16	3.04e+10	2.53e+10

Table 4.2-2

Calculated Fast Neutron Flux ($E \geq 1.0$ MeV) at the
Pressure Vessel Clad/Base Metal Interface

	Azimuthal Angle				
	90.0°	75.0°	60.0°	45.0°	0.0°
Cycle 1	3.27e+10	2.80e+10	2.80e+10	4.26e+10	3.27e+10
Cycle 2	3.17e+10	2.65e+10	2.76e+10	4.18e+10	3.17e+10
Cycle 3	3.35e+10	2.84e+10	3.12e+10	4.99e+10	3.35e+10
Cycle 4	3.18e+10	2.72e+10	2.84e+10	4.31e+10	3.18e+10
Cycle 5	3.04e+10	2.58e+10	2.86e+10	4.44e+10	3.04e+10
Cycle 6	3.48e+10	2.93e+10	3.02e+10	4.58e+10	3.04e+10
Cycle 7	3.62e+10	3.04e+10	3.10e+10	4.61e+10	3.62e+10
Cycle 8	2.41e+10	2.40e+10	2.45e+10	3.22e+10	2.41e+10
Cycle 9	1.79e+10	1.68e+10	2.11e+10	3.06e+10	1.79e+10
Cycle 10	3.36e+10	2.57e+10	1.67e+10	2.10e+10	1.05e+10
Cycle 11	1.97e+10	2.14e+10	2.59e+10	3.63e+10	1.80e+10
Cycle 12	1.95e+10	2.04e+10	2.34e+10	3.05e+10	2.11e+10
Cycle 13	1.80e+10	1.70e+10	2.28e+10	3.19e+10	1.66e+10
Cycle 14	1.95e+10	1.63e+10	1.45e+10	2.20e+10	1.08e+10
Cycle 15	1.96e+10	1.61e+10	1.29e+10	1.71e+10	1.32e+10
Cycle 16	1.66e+10	1.50e+10	1.34e+10	1.90e+10	1.12e+10

Table 4.2-3

Calculated Fast Neutron Flux ($E \geq 0.1$ MeV) at
the Surveillance Capsule Center

	Capsule Location	
	225°	265°/275°
Cycle 1	1.80e+11	1.25e+11
Cycle 2	1.77e+11	1.21e+11
Cycle 3	2.11e+11	1.28e+11
Cycle 4	1.82e+11	1.22e+11
Cycle 5	1.88e+11	1.16e+11
Cycle 6	1.93e+11	1.33e+11
Cycle 7	1.94e+11	1.38e+11
Cycle 8	1.35e+11	9.44e+10
Cycle 9	1.29e+11	6.91e+10
Cycle 10	8.82e+10	1.26e+11
Cycle 11	1.52e+11	7.79e+10
Cycle 12	1.28e+11	7.64e+10
Cycle 13	1.34e+11	6.86e+10
Cycle 14	9.27e+10	7.39e+10
Cycle 15	7.16e+10	7.40e+10
Cycle 16	7.99e+10	6.37e+10

Table 4.2-4

Calculated Fast Neutron Flux ($E \geq 0.1$ MeV) at the
Pressure Vessel Clad/Base Metal Interface

	Azimuthal Angle				
	90.0°	75.0°	60.0°	45.0°	0.0°
Cycle 1	8.59e+10	7.39e+10	7.43e+10	1.24e+11	8.59e+10
Cycle 2	8.32e+10	7.01e+10	7.32e+10	1.22e+11	8.32e+10
Cycle 3	8.80e+10	7.51e+10	8.28e+10	1.45e+11	8.80e+10
Cycle 4	8.35e+10	7.19e+10	7.53e+10	1.25e+11	8.35e+10
Cycle 5	7.97e+10	6.81e+10	7.58e+10	1.29e+11	7.97e+10
Cycle 6	9.13e+10	7.74e+10	8.00e+10	1.33e+11	9.13e+10
Cycle 7	9.51e+10	8.03e+10	8.21e+10	1.34e+11	9.51e+10
Cycle 8	6.33e+10	6.34e+10	6.51e+10	9.37e+10	6.33e+10
Cycle 9	4.71e+10	4.42e+10	5.59e+10	8.91e+10	4.71e+10
Cycle 10	8.82e+10	6.80e+10	4.43e+10	6.11e+10	2.76e+10
Cycle 11	5.17e+10	5.66e+10	6.88e+10	1.05e+11	4.73e+10
Cycle 12	5.12e+10	5.39e+10	6.19e+10	8.87e+10	5.54e+10
Cycle 13	4.72e+10	4.49e+10	6.06e+10	9.28e+10	4.36e+10
Cycle 14	5.12e+10	4.30e+10	3.84e+10	6.40e+10	2.84e+10
Cycle 15	5.16e+10	4.24e+10	3.42e+10	4.96e+10	3.47e+10
Cycle 16	4.37e+10	3.96e+10	3.54e+10	5.52e+10	2.94e+10

Table 4.2-5

Calculated Iron Atom Displacement Rate at
the Surveillance Capsule Center

	Capsule Location	
	225°	265°/275°
Cycle 1	1.09e-10	7.80e-11
Cycle 2	1.06e-10	7.50e-11
Cycle 3	1.27e-10	7.96e-11
Cycle 4	1.09e-10	7.56e-11
Cycle 5	1.13e-10	7.20e-11
Cycle 6	1.17e-10	8.26e-11
Cycle 7	1.17e-10	8.59e-11
Cycle 8	8.15e-11	5.87e-11
Cycle 9	7.75e-11	4.30e-11
Cycle 10	5.31e-11	7.87e-11
Cycle 11	9.19e-11	4.85e-11
Cycle 12	7.71e-11	4.76e-11
Cycle 13	8.08e-11	4.27e-11
Cycle 14	5.59e-11	4.60e-11
Cycle 15	4.32e-11	4.60e-11
Cycle 16	4.81e-11	3.96e-11

Table 4.2-6

Calculated Iron Atom Displacement Rate at the
Pressure Vessel Clad/Base Metal Interface

	Azimuthal Angle				
	90.0°	75.0°	60.0°	45.0°	0.0°
Cycle 1	5.29e-11	4.53e-11	4.55e-11	7.04e-11	5.29e-11
Cycle 2	5.12e-11	4.30e-11	4.48e-11	6.91e-11	5.12e-11
Cycle 3	5.41e-11	4.61e-11	5.07e-11	8.24e-11	5.41e-11
Cycle 4	5.14e-11	4.41e-11	4.61e-11	7.11e-11	5.14e-11
Cycle 5	4.91e-11	4.18e-11	4.64e-11	7.34e-11	4.91e-11
Cycle 6	5.62e-11	4.75e-11	4.89e-11	7.56e-11	5.62e-11
Cycle 7	5.85e-11	4.93e-11	5.03e-11	7.61e-11	5.85e-11
Cycle 8	3.90e-11	3.89e-11	3.98e-11	5.32e-11	3.90e-11
Cycle 9	2.90e-11	2.71e-11	3.42e-11	5.06e-11	2.90e-11
Cycle 10	5.43e-11	4.17e-11	2.71e-11	3.47e-11	1.70e-11
Cycle 11	3.18e-11	3.47e-11	4.21e-11	5.99e-11	2.91e-11
Cycle 12	3.15e-11	3.31e-11	3.79e-11	5.04e-11	3.41e-11
Cycle 13	2.90e-11	2.75e-11	3.71e-11	5.27e-11	2.68e-11
Cycle 14	3.15e-11	2.64e-11	2.35e-11	3.63e-11	1.75e-11
Cycle 15	3.17e-11	2.60e-11	2.10e-11	2.82e-11	2.13e-11
Cycle 16	2.69e-11	2.43e-11	2.17e-11	3.13e-11	1.81e-11

SECTION 5.0

EVALUATIONS OF SURVEILLANCE CAPSULE DOSIMETRY

In this section, the results of the evaluations of the three neutron sensor sets withdrawn as a part of the Fort Calhoun Reactor Vessel Materials Surveillance Program are presented. The capsule designation, location within the reactor, and time of withdrawal of each of these dosimetry sets were as follows:

Capsule ID	Azimuthal Location	Withdrawal Time	Irradiation Time (efps)
W225	225°	END OF CYCLE 3	7.72e+07
W265	265°	END OF CYCLE 7	1.87e+08
W275	275°	END OF CYCLE 14	4.28e+08

5.1 - Measured Reaction Rates

The radiometric counting of dosimetry from these three surveillance capsules was carried out by Combustion Engineering Inc. for Capsules W225 and W265 and by B&W Nuclear Technologies Inc. for Capsule W275. The measured specific activities for each of the sensors contained in these dosimetry sets are provided in Reference 6.

The irradiation history of the Fort Calhoun reactor during Cycles 1 through 14 was obtained from NUREG-0020, "Licensed Operating Reactors Status Summary Report"[7] for the applicable operating periods. The data in NUREG-0020 is based on core follow information provided on a monthly basis by OPPD. The fine detail (i.e., monthly intervals) is necessary in performing radioactive decay corrections for each of the neutron sensors. In addition to the reactor power history, for the multiple cycle irradiations of Capsules W225, W265, and W275, the flux level adjustment factors for each cycle were determined from the fuel cycle specific adjoint calculations described in Section 4.2 of this report.

Based on the irradiation history, the individual sensor characteristics, and the measured specific activities, reaction rates averaged over the appropriate irradiation periods were computed for the sensor sets removed from Capsules W225, W265, and W275. The computed reaction rates for the multiple foil sensor sets are provided in Table 5.1-1.

For the data listed in Table 5.1-1, the fission rate measurements from the U-238 sensors include corrections for U-235 impurities, the build-in of plutonium isotopes during the long irradiations, and for the effects of γ,f reactions.

5.2 - Results of the Least Squares Adjustment Procedure

The results of the application of the least squares adjustment procedure to the three sets of surveillance capsule dosimetry are provided in Tables 5.2-1 through 5.2-3. In these tables, the derived exposure experienced by each capsule along with data illustrating the fit of both the trial and adjusted spectra to the measurements are given. Also included in the tabulations are the 1σ uncertainties associated with each of the derived exposure rates.

In regard to the comparisons listed in Tables 5.2-1 through 5.2-3, it should be noted that the columns labeled "calculated" were obtained by normalizing the neutron spectral data from Table 4.1-1 to the absolute calculated $\phi(E \geq 1.0$ MeV) averaged over the applicable irradiation periods (Cycles 1-3 for Capsule W225, Cycles 1-7 for Capsule W265, and Cycles 1-14 for Capsule W275) as discussed in Section 2.0. Thus, the comparisons illustrated in Tables 5.2-1 through 5.2-3 indicate the degree to which the calculated neutron energy spectra matched the measured sensor data before and after adjustment. Absolute comparisons are discussed further in Section 6.0 of this report.

Table 5.1-1

Summary of Reaction Rates Derived From Multiple Foil Sensor Sets
Withdrawn from Internal Surveillance Capsules

Capsule W225

	Reaction Rate (rps/nucleus)		
	Top	Middle	Bottom
Cu-63(n,α) Cd	6.45e-17	6.57e-17	6.15e-17
Ti-46(n,p)	9.77e-16	9.55e-16	9.71e-16
Fe-54(n,p)	6.00e-15	6.39e-15	5.80e-15
Ni-58(n,p) Cd	8.36e-15	8.53e-15	7.74e-15
U-238(n,f) Cd	3.09e-14	3.03e-14	2.55e-14

Capsule W265

	Reaction Rate (rps/nucleus)		
	Top	Middle	Bottom
Cu-63(n,α) Cd	5.94e-17	6.40e-17	5.29e-17
Ti-46(n,p)	7.69e-16	7.23e-16	7.06e-16
Fe-54(n,p)	4.79e-15	4.22e-15	4.32e-15
Ni-58(n,p) Cd	6.05e-15	5.80e-15	5.21e-15
U-238(n,f) Cd	1.71e-14	1.60e-14	1.53e-14

Capsule W275

	Reaction Rate (rps/nucleus)		
	Top	Middle	Bottom
Cu-63(n,α) Cd	6.45e-17	6.57e-17	6.15e-17
Ti-46(n,p)	4.97e-16	6.31e-16	5.78e-16
Fe-54(n,p)	3.67e-15	3.38e-15	3.02e-15
Ni-58(n,p) Cd	4.16e-15	3.90e-15	3.47e-15
U-238(n,f) Cd	1.47e-14	1.36e-14	1.20e-14

Table 5.2-1

Derived Exposure Rates from Surveillance Capsule W225 Dosimetry
Withdrawn at the End of Fuel Cycle 3

	Calculated Value	Adjusted Value	1σ Uncertainty
$\phi(E \geq 1.0$ MeV) [n/cm^2-s]	7.13e+10	7.07e+10	10%
$\phi(E \geq 0.1$ MeV) [n/cm^2-s]	1.80e+11	1.94e+11	19%
dpa/sec	1.12e-10	1.12e-10	12%

Comparison of Measured and Calculated Sensor Reaction Rates
Surveillance Capsule W225

	Reaction Rate (rps/nucleus)				
	Measured	Calculated	Adjusted	M/C	M/A
Cu-63(n,α) Cd	6.39e-17	6.18e-17	6.28e-17	1.03	1.02
Ti-46(n,p)	9.68e-16	1.02e-15	9.74e-16	0.95	0.99
Fe-54(n,p)	6.06e-15	6.55e-15	6.22e-15	0.93	0.97
Ni-58(n,p) Cd	8.21e-15	8.60e-15	8.25e-15	0.95	1.00
U-238(n,f) Cd	2.89e-14	2.71e-14	2.68e-14	1.07	1.08

Table 5.2-2

Derived Exposure Rates from Surveillance Capsule W265 Dosimetry
Withdrawn at the End of Fuel Cycle 7

	Calculated Value	Adjusted Value	1σ Uncertainty
$\phi(E \geq 1.0$ MeV) [n/cm^2-s]	5.00e+10	4.07e+10	9%
$\phi(E \geq 0.1$ MeV) [n/cm^2-s]	1.31e+11	1.05e+11	19%
dpa/sec	1.06e-10	6.52e-11	12%

Comparison of Measured and Calculated Sensor Reaction Rates
Surveillance Capsule W265

	Reaction Rate (rps/nucleus)				
	Measured	Calculated	Adjusted	M/C	M/A
Cu-63(n,α) Cd	5.88e-17	5.05e-17	5.64e-17	1.16	1.04
Ti-46(n,p)	7.33e-16	8.15e-16	7.52e-16	0.90	0.97
Fe-54(n,p)	4.44e-15	4.96e-15	4.46e-15	0.90	1.00
Ni-58(n,p) Cd	5.68e-15	6.47e-15	5.73e-15	0.88	0.99
U-238(n,f) Cd	1.61e-14	1.94e-14	1.63e-14	0.83	0.99

Table 5.2-3

Derived Exposure Rates From Surveillance Capsule W275 Dosimetry
Withdrawn at the End of Fuel Cycle 14

	Calculated Value	Adjusted Value	1σ Uncertainty
$\phi(E \geq 1.0$ MeV) [n/cm^2-s]	4.03e+10	3.29e+10	10%
$\phi(E \geq 0.1$ MeV) [n/cm^2-s]	1.06e+11	8.60e+10	19%
dpa/sec	6.38e-11	5.19e-11	12%

Comparison of Measured and Calculated Sensor Reaction Rates
Surveillance Capsule W275

	Reaction Rate (rps/nucleus)				
	Measured	Calculated	Adjusted	M/C	M/A
Ti-46(n,p)	5.69e-16	6.57e-16	5.62e-16	0.87	1.01
Fe-54(n,p)	3.36E-15	4.00e-15	3.30E-15	0.84	1.02
Ni-58(n,p) Cd	3.84E-15	5.22e-15	4.02E-15	0.74	0.96
U-238(n,f) Cd	1.34E-14	1.56e-14	1.28E-14	0.86	1.05

SECTION 6.0

PROJECTED NEUTRON EXPOSURE FOR FORT CALHOUN PRESSURE VESSEL MATERIALS

In this section the Fort Calhoun specific measurement results provided in Section 5.0 are compared with the results of the neutron transport calculations described in Section 4.0 to provide a further validation of the calculated neutron exposure of the reactor pressure vessel through the completion of Cycle 14. Based on the continued use of the low leakage core power distributions characteristic of the design of Cycles 15 and 16, projections of future vessel exposure are also provided.

6.1 Comparison of Calculations with Measurements

The neutron exposure projections for the Fort Calhoun pressure vessel were based on an absolute plant specific neutron transport calculation using benchmarked analytical techniques. Direct comparisons of the transport calculations with the measurements from Fort Calhoun in-vessel surveillance capsules were used to further validate these computations.

In this section, comparisons of the measurement results from surveillance capsules W225, W265, and W275 with corresponding analytical predictions at the measurement locations are presented. These comparisons are provided on two levels. In the first instance, predictions of fast neutron exposure rates in terms of $\phi(E \geq 1.0$ MeV), $\phi(E \geq 0.1$ MeV), and dpa/sec are compared with the results of the least squares adjustment procedure. In the second case, calculations of individual sensor reaction rates are compared directly with the measured data from the counting laboratories. It is shown that these two levels of comparison yield consistent and similar results

6.1.1 Comparison of Least Squares Adjustment Results with Calculation

In Table 6.1-1, comparisons of adjusted and calculated exposure rates for the three surveillance capsule dosimetry sets withdrawn to date are given. In all cases, the calculated values were based on the fuel cycle specific exposure calculations averaged over the appropriate irradiation period.

An examination of Table 6.1-1 indicates that, considering all of the available core midplane data, the adjusted exposure rates were less than calculated values by factors of 0.874, 0.897,

and 0.880 for $\phi(E \geq 1.0$ MeV), $\phi(E \geq 0.1$ MeV), and dpa/sec, respectively. The 1σ standard deviations associated with each of the 3 sample data sets were 11.7%, 17.7%, and 12.1%, respectively. All of the individual adjusted results are within 20% of the calculated values. It should be noted that these comparisons were intended simply to validate the transport calculation and were not used to modify the analytical results.

6.1.2 Comparisons of Measured and Calculated Sensor Reaction Rates

In Table 6.1-2, measurement/calculation (M/C) ratios for each fast neutron sensor reaction rate from the three surveillance capsule irradiations are listed. This tabulation, provides a direct comparison, on an absolute basis, of calculation and measurement prior to the application of the least squares adjustment procedure.

An examination of Table 6.1-2 shows consistent behavior for all reactions and all measurement points. The standard deviations observed for the six fast neutron reactions range from 6.7% to 13.9% on an individual reaction basis; whereas, the overall average M/C ratio for the entire data set has an associated 1σ standard deviation of 12.8%. Furthermore, the average M/C ratio of 0.918 observed in the reaction rate comparisons is in excellent agreement with the values of 0.874, 0.897, and 0.880 observed in the exposure rate comparisons shown in Table 6.1-1.

Table 6.1-1

Comparison of Adjusted and Calculated Exposure Rates from Surveillance Capsule Dosimetry Irradiations

	ϕ (E > 1.0 MeV) [n/cm^2-s]		
	Calculated	Adjusted	A/C
Capsule W225	7.13e+10	7.07e+10	0.992
Capsule W265	5.00e+10	4.07e+10	0.814
Capsule W275	4.03e+10	3.29e+10	0.816
AVERAGE A/C RATIO			0.874
PERCENT STANDARD DEVIATION (1σ)			11.7%

	ϕ(E > 0.1 MeV) [n/cm^2-s]		
	Calculated	Adjusted	A/C
Capsule W225	1.80e+11	1.94e+11	1.080
Capsule W265	1.31e+11	1.05e+11	0.799
Capsule W275	1.06e+11	8.60e+10	0.812
AVERAGE M/C BIAS FACTOR (K)			0.897
PERCENT STANDARD DEVIATION (1σ)			17.7%

	Iron Displacement Rate [dpa/s]		
	Calculated	Adjusted	A/C
Capsule W225	1.12e-10	1.12e-10	1.003
Capsule W265	7.92e-11	6.52e-11	0.823
Capsule W275	6.38e-11	5.19e-11	0.813
AVERAGE M/C BIAS FACTOR (K)			0.880
PERCENT STANDARD DEVIATION (1σ)			12.1%

Table 6.1-2

Comparison of Measured and Calculated Neutron Sensor Reaction Rates from Surveillance Capsule Irradiations

	Cu63(n,α)	Ti46(n,p)	Fe54(n,p)	Ni58(n,p)	U238(n,f)
CAPSULE W225					
TOP	1.044	0.958	0.916	0.972	1.140
MIDDLE	1.063	0.936	0.976	0.992	1.118
BOTTOM	0.995	0.952	0.885	0.900	0.941
CAPSULE W265					
TOP	1.169	0.938	0.960	0.929	0.877
MIDDLE	1.260	0.882	0.846	0.891	0.821
BOTTOM	1.041	0.861	0.866	0.743	0.785
CAPSULE W275					
TOP		0.753	0.913	0.792	0.936
MIDDLE		0.956	0.841	0.743	0.866
BOTTOM		0.876	0.751	0.661	0.764
AVERAGE	1.095	0.901	0.884	0.853	0.916
% STD DEV (1σ)	8.2	6.7	6.9	12.4	13.9

OVERALL AVERAGE M/C RATIO
PERCENT STANDARD DEVIATION (1σ)

6.2 Calculated Exposure Projections for the Fort Calhoun Reactor Pressure Vessel

To assess the incremental exposure resulting from the Cycles 1 through 14 irradiations, the calculated exposure values from Section 4.2 for the vessel clad/base metal interface were folded with the length of each irradiation cycle to produce fluence levels characteristic of the materials comprising the beltline region of the reactor pressure vessel. The calculated results applicable to the vessel inner surface are incorporated into Table 6.2-1 to establish the exposure accrued by the reactor vessel through the end of Cycle 14. Exposure distributions through the vessel wall, can be developed using these surface exposures and radial distribution functions from Section 4.0.

At the end of Cycle 14, the Fort Calhoun reactor had accrued 13.6 effective full power years (EFPY) of operation. In order to establish a framework for the assessment of future vessel condition, exposure projections through 48 EFPY are also included in Table 6.2-1 in addition to the plant specific exposure assessments through the end of Cycle 14. These exposure projections for the Fort Calhoun pressure vessel are illustrated graphically in Figure 6.2-1.

These temporal extrapolations into the future were based on the assumption that the calculated neutron exposure rates averaged over Cycles 15 and 16 were representative of all future fuel cycles. That is, that future fuel designs would incorporate the low leakage fuel management concept employed during Cycles 15 and 16. Examination of these projected exposure levels establishes the long term effectiveness of the low leakage fuel management incorporated to date and can be used as a guide in assessing strategies for future vessel exposure management. The validity of these projections for future operation will be confirmed via the next scheduled surveillance capsule withdrawal.

Table 6.2-1

Calculated Neutron Exposure Projections at Key Locations
on the Pressure Vessel Clad/Base Metal Interface

	$\Phi(E \geq 1.0$ MeV) [n/cm^2]				
EFPY	90°	75°	60°	45°	0°
EOC 1	8.20e+17	7.03e+17	7.03e+17	1.07e+18	8.20e+17
EOC 2	1.78e+18	1.51e+18	1.54e+18	2.34e+18	1.78e+18
EOC 3	2.51e+18	2.12e+18	2.22e+18	3.42e+18	2.51e+18
EOC 4	3.24e+18	2.75e+18	2.87e+18	4.41e+18	3.24e+18
EOC 5	4.14e+18	3.51e+18	3.71e+18	5.72e+18	4.14e+18
EOC 6	5.19e+18	4.40e+18	4.63e+18	7.11e+18	5.06e+18
EOC 7	6.16e+18	5.21e+18	5.46e+18	8.34e+18	6.03e+18
EOC 8	6.82e+18	5.86e+18	6.12e+18	9.22e+18	6.68e+18
EOC 9	7.45e+18	6.46e+18	6.87e+18	1.03e+19	7.32e+18
EOC 10	8.55e+18	7.30e+18	7.42e+18	1.10e+19	7.66e+18
EOC 11	9.28e+18	8.10e+18	8.38e+18	1.23e+19	8.33e+18
EOC 12	9.86e+18	8.70e+18	9.08e+18	1.33e+19	8.96e+18
EOC 13	1.06e+19	9.41e+18	1.00e+19	1.46e+19	9.65e+18
EOC 14	1.13e+19	1.00e+19	1.06e+19	1.54e+19	1.01e+19
16.0	1.27e+19	1.12e+19	1.16e+19	1.68e+19	1.10e+19
18.0	1.39e+19	1.22e+19	1.24e+19	1.79e+19	1.17e+19
20.0	1.50e+19	1.32e+19	1.32e+19	1.90e+19	1.25e+19
22.0	1.61e+19	1.41e+19	1.41e+19	2.02e+19	1.33e+19
24.0	1.73e+19	1.51e+19	1.49e+19	2.13e+19	1.41e+19
26.0	1.84e+19	1.61e+19	1.57e+19	2.25e+19	1.48e+19
28.0	1.96e+19	1.71e+19	1.65e+19	2.36e+19	1.56e+19
30.0	2.07e+19	1.81e+19	1.74e+19	2.47e+19	1.64e+19
32.0	2.19e+19	1.90e+19	1.82e+19	2.59e+19	1.71e+19
34.0	2.30e+19	2.00e+19	1.90e+19	2.70e+19	1.79e+19
36.0	2.41e+19	2.10e+19	1.99e+19	2.82e+19	1.87e+19
38.0	2.53e+19	2.20e+19	2.07e+19	2.93e+19	1.94e+19
40.0	2.64e+19	2.30e+19	2.15e+19	3.04e+19	2.02e+19
42.0	2.76e+19	2.40e+19	2.24e+19	3.16e+19	2.10e+19
44.0	2.87e+19	2.49e+19	2.32e+19	3.27e+19	2.18e+19
46.0	2.98e+19	2.59e+19	2.40e+19	3.39e+19	2.25e+19
48.0	3.10e+19	2.69e+19	2.48e+19	3.50e+19	2.33e+19

Table 6.2-1 (Continued)

Calculated Neutron Exposure Projections at Key Locations
on the Pressure Vessel Clad/Base Metal Interface

	$\Phi(E \geq 0.1$ MeV) [n/cm^2]				
EFPY	90°	75°	60°	45°	0°
EOC 1	2.15e+18	1.85e+18	1.86e+18	3.11e+18	2.15e+18
EOC 2	4.68e+18	3.98e+18	4.09e+18	6.81e+18	4.68e+18
EOC 3	6.59e+18	5.61e+18	5.88e+18	9.96e+18	6.59e+18
EOC 4	8.51e+18	7.25e+18	7.61e+18	1.28e+19	8.51e+18
EOC 5	1.09e+19	9.26e+18	9.84e+18	1.66e+19	1.09e+19
EOC 6	1.36e+19	1.16e+19	1.23e+19	2.07e+19	1.33e+19
EOC 7	1.62e+19	1.38e+19	1.45e+19	2.43e+19	1.58e+19
EOC 8	1.79e+19	1.55e+19	1.62e+19	2.68e+19	1.75e+19
EOC 9	1.96e+19	1.71e+19	1.82e+19	3.00e+19	1.92e+19
EOC 10	2.24e+19	1.93e+19	1.97e+19	3.20e+19	2.01e+19
EOC 11	2.44e+19	2.14e+19	2.22e+19	3.59e+19	2.19e+19
EOC 12	2.59e+19	2.30e+19	2.41e+19	3.86e+19	2.35e+19
EOC 13	2.79e+19	2.48e+19	2.66e+19	4.24e+19	2.53e+19
EOC 14	2.98e+19	2.65e+19	2.80e+19	4.48e+19	2.64e+19
16.0	3.34e+19	2.96e+19	3.07e+19	4.88e+19	2.88e+19
18.0	3.64e+19	3.22e+19	3.29e+19	5.21e+19	3.08e+19
20.0	3.94e+19	3.47e+19	3.51e+19	5.54e+19	3.29e+19
22.0	4.24e+19	3.73e+19	3.73e+19	5.87e+19	3.49e+19
24.0	4.54e+19	3.99e+19	3.95e+19	6.20e+19	3.69e+19
26.0	4.84e+19	4.25e+19	4.17e+19	6.54e+19	3.89e+19
28.0	5.14e+19	4.51e+19	4.39e+19	6.87e+19	4.09e+19
30.0	5.44e+19	4.77e+19	4.61e+19	7.20e+19	4.30e+19
32.0	5.74e+19	5.03e+19	4.83e+19	7.53e+19	4.50e+19
34.0	6.04e+19	5.29e+19	5.05e+19	7.86e+19	4.70e+19
36.0	6.34e+19	5.55e+19	5.27e+19	8.19e+19	4.90e+19
38.0	6.64e+19	5.81e+19	5.49e+19	8.53e+19	5.10e+19
40.0	6.94e+19	6.07e+19	5.71e+19	8.86e+19	5.31e+19
42.0	7.24e+19	6.32e+19	5.93e+19	9.19e+19	5.51e+19
44.0	7.54e+19	6.58e+19	6.15e+19	9.52e+19	5.71e+19
46.0	7.84e+19	6.84e+19	6.37e+19	9.85e+19	5.91e+19
48.0	8.13e+19	7.10e+19	6.59e+19	1.02e+20	6.12e+19

Table 6.2-1 (Continued)

Calculated Neutron Exposure Projections at Key Locations
on the Pressure Vessel Clad/Base Metal Interface

IRON DISPLACEMENTS [dpa]

EFPY	90°	75°	60°	45°	0°
EOC 1	1.33e-03	1.14e-03	1.14e-03	1.76e-03	1.33e-03
EOC 2	2.88e-03	2.44e-03	2.50e-03	3.86e-03	2.88e-03
EOC 3	4.06e-03	3.44e-03	3.60e-03	5.65e-03	4.06e-03
EOC 4	5.24e-03	4.45e-03	4.66e-03	7.28e-03	5.24e-03
EOC 5	6.68e-03	5.68e-03	6.03e-03	9.44e-03	6.68e-03
EOC 6	8.39e-03	7.12e-03	7.52e-03	1.17e-02	8.17e-03
EOC 7	9.96e-03	8.44e-03	8.87e-03	1.38e-02	9.74e-03
EOC 8	1.10e-02	9.49e-03	9.94e-03	1.52e-02	1.08e-02
EOC 9	1.20e-02	1.05e-02	1.12e-02	1.70e-02	1.18e-02
EOC 10	1.38e-02	1.18e-02	1.21e-02	1.81e-02	1.24e-02
EOC 11	1.50e-02	1.31e-02	1.36e-02	2.04e-02	1.35e-02
EOC 12	1.59e-02	1.41e-02	1.47e-02	2.19e-02	1.45e-02
EOC 13	1.71e-02	1.52e-02	1.63e-02	2.41e-02	1.56e-12
EOC 14	1.83e-02	1.62e-02	1.72e-02	2.54e-02	1.62e-02
16.0	2.05e-02	1.81e-02	1.88e-02	2.77e-02	1.77e-02
18.0	2.24e-02	1.97e-02	2.01e-02	2.96e-02	1.90e-02
20.0	2.42e-02	2.13e-02	2.15e-02	3.14e-02	2.02e-02
22.0	2.61e-02	2.29e-02	2.28e-02	3.33e-02	2.15e-02
24.0	2.79e-02	2.45e-02	2.42e-02	3.52e-02	2.27e-02
26.0	2.98e-02	2.61e-02	2.55e-02	3.71e-02	2.40e-02
28.0	3.16e-02	2.77e-02	2.69e-02	3.90e-02	2.52e-02
30.0	3.35e-02	2.93e-02	2.82e-02	4.08e-02	2.64e-02
32.0	3.53e-02	3.08e-02	2.96e-02	4.27e-02	2.77e-02
34.0	3.72e-02	3.24e-02	3.09e-02	4.46e-02	2.89e-02
36.0	3.90e-02	3.40e-02	3.23e-02	4.65e-02	3.02e-02
38.0	4.08e-02	3.56e-02	3.36e-02	4.84e-02	3.14e-02
40.0	4.27e-02	3.72e-02	3.50e-02	5.03e-02	3.27e-02
42.0	4.45e-02	3.88e-02	3.63e-02	5.21e-02	3.39e-02
44.0	4.64e-02	4.04e-02	3.77e-02	5.40e-02	3.52e-02
46.0	4.82e-02	4.20e-02	3.90e-02	5.59e-02	3.64e-02
48.0	5.01e-02	4.36e-02	4.03e-02	5.78e-02	3.76e-02

Figure 6.2-1

Neutron Exposure Projections at the Pressure Vessel
Clad/Base Metal Interface

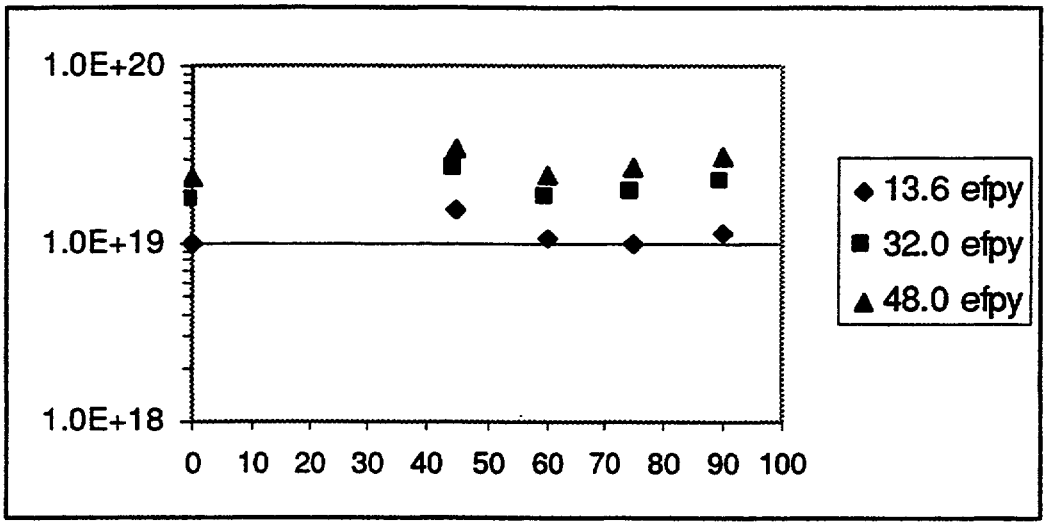

6.3 Uncertainties in Exposure Projections

The uncertainty associated with the calculated exposure of the Fort Calhoun reactor pressure vessel is based on the recommended approach provided in Draft Regulatory Guide DG-1053, "Calculational and osimetry Methods for Determining Pressure Vessel Neutron Fluence". In particular, the qualification of the neutron exposure evaluations was carried out in the following four stages:

1) Comparisons of calculations with benchmark measurements from the Pool Critical Assembly (PCA) simulator at the Oak Ridge National Laboratory.

2) Comparison of calculations with surveillance capsule and reactor cavity measurements from operating power reactors similar to Fort Calhoun.

3) An analytical sensitivity study addressing uncertainty components resulting from important input parameters applicable to the plant specific transport calculations used in the neutron exposure assessments.

   Results of these three phases of the uncertainty assessment are discussed in Section 3.0 of this report.

4) Comparisons of the plant specific transport calculations with all available dosimetry results from the Fort Calhoun reactor vessel surveillance program.

The comparison of the calculated results with the available plant specific dosimetry results was used solely to demonstrate the adequacy of the transport calculations and to confirm the uncertainty estimates associated with the analytical results. This comparison was used only as a check and was not used to modify the final calculated results in any way.

The following summarizes the uncertainties associated with the calculated fluence ($E \geq 1.0$ MeV) for the Fort Calhoun reactor pressure vessel.

PCA Benchmark Comparisons	4.4%
Power Reactor Comparisons	9.2%
Analytic Sensitivity Study	11%
Other Factors	5%

The uncertainty for the PCA comparisons is based on the data provided in Table 3.1-4 for positions A2, A4, A5, and A6 in the pressure vessel simulator. This data shows an average A/C ratio for the neutron flux ($E \geq 1.0$ MeV) of 1.01 with a standard deviation of 4.4%. This comparison was taken to confirm the basic transport calculation within the 4.4% uncertainty. The uncertainty from the power reactor calculations was taken from the data provided in Tables 3.2-1 and 3.2-3. These data comparisons demonstrate a combined average A/C ratio of 0.915 with a standard deviation of 8.7%. This comparison was again taken to confirm the basic power reactor transport calculations within the 8.7% uncertainty. Neither the 1.01 factor from the PCA comparisons or the 0.915 factor from the power reactor calculations was treated as a bias to the calculational methodology. The 11% analytical uncertainty was taken directly from the data provided in Section 3.3 for the vessel IR location. In addition to these uncertainty components, an additional 5% uncertainty was included in the assessment to account for small contributors not specifically addressed in the analytical sensitivity studies.

Combined in quadrature, the overall uncertainty in the Fort Calhoun exposure projections is estimated to be 15.5%. This level of uncertainty is within the guidelines specified in DG-1053.

SECTION 7.0

REFERENCES

1. ASTM Designation E853-87, "Standard Practice for Analysis and Interpretation of Light Water Reactor Surveillance Results," in ASTM Standards, Section 12, American Society for Testing and Materials, Philadelphia, Pa. 1993.

2. Draft Regulatory Guide DG-1053, "Calculational and Dosimetry Methods for Determining Pressure Vessel Neutron Fluence," U.S. Nuclear Regulatory Commission, Office of Nuclear Regulatory Research, September 1999.

3. RSIC Computer Code Collection CCC-543, "TORT-DORT Two- and Three-Dimensional Discrete Ordinates Transport, Version 2.8.14," January 1994.

4. RSIC Data Library Collection DLC-175, "BUGLE-93, Production and Testing of the VITAMIN-B6 Fine Group and the BUGLE-93 Broad Group Neutron/Photon Cross-Section Libraries Derived from ENDF/B-VI Nuclear Data," April 1994.

5. Maerker, R. E., et. al., "Accounting for Changing Source Distributions in Light Water Reactor Surveillance Dosimetry Analysis," Nuclear Science and Engineering, Volume 94, pages 291-308, 1986.

6. DeVan, M. J., et. al., "Evaluation of Irradiated Capsule W-275 OMAHA PUBLIC POWER DISTRICT Fort Calhoun Station Unit Number 1 Reactor Vessel Materials Irradiation Surveillance Program," BAW-2226, November 1994.

7. NUREG-0020, "Licensed Operating Reactors Status Summary Report," Nuclear Regulatory Commission Monthly Publication, September 1973 through October 1993.

8. Norris, E. B., "Effect of Thermal Power Averaging Method on the Determination of Neutron Fluence for LWR-PV Surveillance," Proceedings of the Fifth ASTM/EURATOM Symposium on Reactor Dosimetry, Volume 1, Pages 137-143, GKSS Research Center, Geesthacht, F.R.G., September 1984.

9. Schmittroth, E. A., "FERRET Data Analysis Code," HEDL-TME-79-40, Hanford Engineering Development Laboratory, Richland, Washington, September 1979.

10. McElroy, W. N., et. al., "A Computer-Automated Iterative Method of Neutron Flux Spectra Determined by Foil Activation," AFWL-TR-67-41, Volumes I-IV, Air Force Weapons Laboratory, Kirkland AFB, NM, July 1967.

11. RSIC Data Library Collection DLC-178, "SNLRML Recommended Dosimetry Cross-Section Compendium," July 1994.

12. Maerker, R. E. as reported by Stallman, F. W., "Workshop on Adjustment Codes and Uncertainties," Proceedings of the Fourth ASTM/EURATOM Symposium on Reactor Dosimetry, NUREG/CP-0029, Nuclear Regulatory Commission, Washington, D.C., July 1982.

13. McElroy, W. N., et. al., "LWR Pressure Vessel Surveillance Dosimetry Improvement Program: PCA Experiments and Blind Test," NUREG/CR-1861, Nuclear Regulatory Commission, Washington, D.C., July 1981.

14. McElroy, W. N., et. al., "LWR Pressure Vessel Surveillance Dosimetry Improvement Program: PCA Experiments, Blind Test, and Physics-Dosimetry Support for the PSF Experiments," NUREG/CR-3318, Nuclear Regulatory Commission, Washington, D.C., September 1984.

15. McElroy, W. N., et. al., "LWR Pressure Vessel Surveillance Dosimetry Improvement Program: 1986 HEDL Summary Annual Report," NUREG/CR-4307, Nuclear Regulatory Commission, Washington, D.C., January 1987.

LIC-00-0064
Attachment D

Westinghouse - CE Nuclear Power Report CEN-636, Rev. 2
Evaluation of Reactor Vessel Surveillance Data Pertinent to the Fort Calhoun Reactor Vessel Beltline Materials – Basis for Prediction of RT_{PTS} for the Fort Calhoun RPV,
July 2000

Report Prepared for the
Omaha Public Power District,
Fort Calhoun Station

Final Report dated
July 19, 2000
CEN-636, Revision 02
Verification Status: Complete

Evaluation of Reactor Vessel Surveillance Data Pertinent to the Fort Calhoun Reactor Vessel Beltline Materials

Basis for Prediction of RT_{PTS} for the Fort Calhoun RPV

Westinghouse Electric
CE Nuclear Power
Windsor, Connecticut

Evaluation of Reactor Vessel Surveillance Data Pertinent to the Fort Calhoun Reactor Vessel Beltline Materials

Basis for Prediction of RT_{PTS}

CEN-636, Revision 02

VERIFICATION STATUS: COMPLETE

Prepared by: _____ Date: 7-19-00

C. L. Hoffmann

Reviewed by: _____ Date: 7/19/2000

C. J. Gimbrone

Approved by: _____ Date: 7/19/2000

R. W. Bradshaw

Record of Revision		
No.	Date	Pages Involved
Original Issue	10/22/99	all
1	07/5/00	all
2	07/19/00	34, 35

Table of Contents

List of Tables

List of Tables (cont'd)

List of Figures

1.0 Objective

This report evaluates surveillance data to demonstrate that the Fort Calhoun reactor pressure vessel will not exceed the Pressurized Thermal Shock (PTS) screening criteria (Reference 1) through the end of the current and renewal license terms (August 9, 2013 and August 9, 2033, respectively). This evaluation is based on the use of Position 2.1 of Regulatory Guide 1.99 (Reference 2) to calculate chemistry factors for the limiting weld wire heat combinations and justify reduction of the standard deviation for shift by one-half based on credible surveillance data. The PTS screening criteria projections are based on conservative values of neutron fluence that were calculated using the methods of the U.S. Nuclear Regulatory Commission's Draft Regulatory Guide DG-1053, "Calculational and Dosimetry Methods for Determining Pressure Vessel Neutron Fluence". The approach used for calculating RT_{PTS} complies with 10CFR50.61(b)(3). The objective of this report is to support NRC approval of the report's conclusions.

2.0 Introduction and Background

The Fort Calhoun reactor vessel was fabricated by Combustion Engineering in Chattanooga, Tennessee during the time period 1966 to 1969. The vessel shell was fabricated using steel plates purchased to SA-533 Grade B, Class 1 requirements. The plates were joined together using automatic submerged arc welding using copper-coated electrodes. The primary coolant nozzles and the vessel flange were fabricated using forgings purchased to SA-508 Class 2 requirements. The forgings were joined to the vessel shell using automatic and manual submerged arc welding.

The reactor vessel shell, primary coolant nozzles and the vessel flange were designed to operate at high temperatures and pressures. The reactor vessel beltline materials were also designed for exposure to the fast neutrons generated in the reactor core. The material purchase specifications together with the forming, welding, and post-weld heat treatment processes were intended to provide for a high level of fracture toughness. The pre-service inspection and hydrostatic testing processes were intended to minimize the presence of fabrication-induced defects that could grow during the service lifetime. During the lifetime of the reactor vessel, periodic in-service inspections are conducted to look for defect indications in the vessel welds. In addition, a reactor vessel surveillance program is

maintained throughout the life of the vessel to monitor the effect of neutron irradiation on the beltline materials.

Given the fact that the beltline welds in the Fort Calhoun vessel were fabricated using copper coated electrodes, the copper content in those welds is high (relative to vessel welds fabricated using non-copper coated electrodes). Such high copper welds have been shown to be more sensitive to the hardening effects of fast neutron irradiation than vessels fabricated during the mid- and late-1970s using non-copper coated welding electrodes. Neutron irradiation causes a reduction of the fracture toughness in the reactor vessel beltline materials. This toughness reduction is manifested as a shift in the reference temperature, RT_{NDT}, to a higher value. The shift increases as a function of the fast neutron fluence and chemical content (specifically the copper and nickel content as used in Reference 2). The magnitude of the shift is sensitive to the product form (e.g., plate or weld material).

The methodology for predicting shift that is currently acceptable to the NRC is provided in References 1 and 2. These two documents plus a handout entitled "Evaluation and Use of Surveillance Data" (Reference 3) from a November 12, 1997 NRC-Industry Meeting provide a set of NRC requirements and guidelines for using relevant and credible surveillance data to refine predictions of the shift in RT_{NDT} and calculation of the adjusted reference temperature, ART. (Values of ART, or RT_{PTS} in Reference 1, are obtained using the sum of the initial RT_{NDT}, the shift of RT_{NDT} with irradiation, and a margin term.) In the longer term, work is proceeding on the development of an improved methodology for predicting values of ART. This longer term work entails an ASTM effort to revise ASTM Standard E900 and an NRC effort to revise Regulatory Guide 1.99. A recent report on that program is NUREG/CR-6551 (Reference 4).

The approach being taken in this document is to apply Position 2.1 of Regulatory Guide 1.99 (Reference 2) using surveillance data applicable to the limiting Fort Calhoun beltline welds. (Position 2.1 provides a procedure for adjusting the chemistry factor used to predict shift and for reducing the standard deviation for shift in the margin term.) Several weld wire heats in various combinations were used in the beltline welds for the Fort Calhoun vessel. Therefore, numerous sources of surveillance data are being evaluated to give the broadest possible picture of the irradiation performance for the Fort Calhoun beltline welds. Data

reviewed for applicability to Ft. Calhoun are Mihama Unit 1, Diablo Canyon Unit 1, D.C. Cook Unit 1, Salem Unit 2, and a supplemental surveillance capsule from Palisades. Other welds that used one of the electrode heats in combination with another to produce the surveillance weld were also reviewed. These are labeled in Table 2 as "not fully applicable" to the Fort Calhoun vessel limiting beltline welds. The applicable data were then analyzed in accordance with Position 2.1, chemistry factors were calculated, and data predictability assessed. The results of this Position 2.1 analysis were then used to calculate the adjusted reference temperature, RT_{PTS}, applying the adjusted chemistry factor and the reduced standard deviation for shift from the analysis. The revised values of RT_{PTS} are being reported to the NRC in accordance with the requirements of 10CFR50.61 (b)(3).

3.0 Description of Fort Calhoun Reactor Vessel Beltline Materials

The Fort Calhoun reactor vessel beltline materials and surveillance materials are described in Table 1. The first column gives the plate code or the weld seam identification. The second column gives the heat number for the plate or welding electrode. The third column gives the flux type and lot number for the welds. The fourth column gives the chemistry factor based on the best estimate copper and nickel content. (The material identification and the weld chemistry factor values are from Reference 5.)

The Fort Calhoun beltline consists of the intermediate and lower shell courses of the reactor vessel. Plates D-4802-1, D-4802-2, and D-4802-3 comprise the intermediate shell course. Plates D-4812-1, D-4812-2, and D-4812-3 comprise the lower shell course. The plates and shell courses were joined together using automatic submerged arc welding using Mil B4 copper coated electrodes and Linde 1092 or Linde 124 flux. Weld seams 2-410 A/C (where "A/C" means seams A, B, and C) are the axial welds between the plates to form the intermediate shell. Weld seams 3-410 A/C are the axial welds between the plates to form the lower shell. Weld seam 9-410 is the circumferential weld between the intermediate and lower shell course. Weld seams 2-410 A/C and 9-410 were deposited using the single arc process. Weld seams 3-410 A/C were deposited using the tandem arc process.

Table 1 also provides a description of the Fort Calhoun surveillance program plate and weld material. The surveillance plate was obtained from plate D-4802-2. The surveillance weld

was fabricated using the same welding process as was used for weld seam 9-410 but with a different heat of wire.

The beltline materials are evaluated using Reference 2 to identify the limiting material at end of the license period. The limiting material is the beltline plate or weld with the highest RT_{PTS} value. The limiting materials in the Fort Calhoun vessel beltline are from the lower shell course welds. As stated in the Introduction, the objective of this evaluation is to apply Position 2.1 of Reference 2 to surveillance data that are applicable to the limiting material, the lower shell course welds. The results of this Position 2.1 analysis can then be used to calculate the adjusted reference temperature, RT_{PTS}, at the end of the license period applying the adjusted chemistry factor and the reduced standard deviation for shift from the analysis.

4.0 Description of Surveillance Data Relevant to Fort Calhoun

In Table 1, the weld wires used to fabricate the lower shell course welds (3-410 A/C) in the Fort Calhoun vessel were identified as heat numbers 12008, 13253, and 27204. The approach taken was to match up those heats or combination of heats with those used to fabricate the surveillance welds in other reactor vessels manufactured by Combustion Engineering during a similar period of time.

The surveillance weld matches are identified in Table 2. A match is defined as having the same heat number in the surveillance weld as is in one of the welds in Table 1. In the case of a mixture of heats in the surveillance weld or Fort Calhoun beltline weld, at least one of the two heats in the mixture had to match. The matches are based on CEOG Report CE NPSD-1119 (Reference 6) and similarly developed sources. (In all the matches cited, the traceability of the surveillance weld wire heat was established based on fabrication records as stated in Reference 6.) Data from five PWR surveillance programs (References 7 through 18) were identified as likely sources of information relative to the three heats from the Fort Calhoun weld seam 3-410 A/C. Data determined to be applicable to Fort Calhoun are Mihama Unit 1, Diablo Canyon Unit 1, the weld from the Palisades supplemental surveillance program, the supplemental surveillance capsule for Fort Calhoun, Salem Unit 2, and D.C. Cook Unit 1. Data from three BWR surveillance programs were also identified using Reference 6. Only the Fitzpatrick weld was fully representative of the weld wire heats used in weld seam 3-410 A/C. The remaining two BWR welds were either a mixture or

were representative of another weld (9-410). Analysis of the Fitzpatrick surveillance weld was not done given the limited number of measurements and the uncertainty regarding the effects of differences in irradiation environment between a BWR and the Fort Calhoun PWR vessel.

The data from four of the five PWR surveillance programs and from the Fort Calhoun surveillance program were compiled from the database assembled for the previously cited ASTM E900 effort (Reference 4). That database had been reviewed, updated and augmented by knowledgeable individuals from the Industry and, therefore, provides a credible source of information for each surveillance program. In addition the individual post-irradiation test reports were reviewed to the extent possible to assess the reasonableness of the data updates. The data from the Mihama Unit 1 surveillance program were obtained through a proprietary agreement between Kansai Electric Power Company and the Omaha Public Power District. [Note: Only the non-proprietary data are presented in this report.]

The surveillance program data sets are provided in Tables 3 through 6. The Fort Calhoun surveillance data (References 19 through 21) are provided in Tables 8A, 8B and 8C. Each table contains the surveillance capsule identity, the measured shift, the reported neutron fluence, and the irradiation temperature. [Note: The irradiation temperature for the surveillance specimens was taken as that of the reactor coolant cold leg. The temperatures were obtained from the E900 database and from Kansai for Mihama Unit 1.]

5.0 Regulatory Position 2.1 Analysis of Relevant Surveillance Data

The objective of this section is to analyze the surveillance data in accordance with Position 2.1 of Reference 2. The Position 2.1 analysis will be augmented using the guidance provided by the NRC (Reference 3). The guidance provides a set of NRC review requirements and guidelines for using relevant and credible surveillance data from other reactor vessels to refine predictions of the shift in RT_{NDT} and calculation of the adjusted reference temperature, RT_{PTS}. Position 2.1 of Regulatory Guide 1.99 is applied to available surveillance data that were identified in the preceding section as relevant to the beltline welds in the Fort Calhoun vessel.

5.1 Credibility of Surveillance Data:

Regulatory Guide 1.99 presents five credibility criteria by which surveillance data from a given reactor are judged before the surveillance data can be used in place of Regulatory Position 1. The five criteria are discussed in turn below:

Criterion 1: "Materials in the capsules should be those judged most likely to be controlling with regard to radiation embrittlement according to the recommendations of this guide."

The chemistry factors for each of the three beltline welds (determined using Table 1 of Reference 2) range from 89 °F to 231 °F. [Note: The highest chemistry factor for the beltline plates is less than the lowest beltline weld, 89 °F. Therefore, the beltline plates will not limit vessel operation and are excluded from the subsequent discussion.] The surveillance weld was fabricated using weld wire heat 305414 with Linde 1092 flux lots #3947 and #3951. It was made from different welding consumables than those used for the Fort Calhoun beltline welds. The surveillance weld is representative of but not identical to the beltline welds, so it does not meet Criterion 1. Therefore, it can not be used in a Position 2.1 analysis of the Fort Calhoun beltline welds. The focus of this report is on the use of data from surveillance welds that were fabricated using the same weld wire heats as were used in the Fort Calhoun vessel limiting beltline weld; i.e., surveillance weld data that meet Criterion 1 for the Fort Calhoun beltline welds. The surveillance program welds listed in Table 2 include most of the weld heats listed in Table 1. The one not represented at all, weld wire heat #51989, has a chemistry factor of 89 °F and thus is not a controlling beltline weld. The surveillance welds in Table 2 include the individual heats of controlling beltline weld materials and, therefore, satisfy the first criterion for the most limiting combinations of weld wire heats.

Criterion 2: "Scatter in the plots of Charpy energy versus temperature for the irradiated and unirradiated conditions should be small enough to permit the determination of the 30-foot-pound temperature and the upper-shelf energy unambiguously."

As part of the effort to review the surveillance data for the ASTM E900 effort, all of the data were computer curve fit by Modeling and Computing Services as part of an effort sponsored by the U.S. Nuclear Regulatory Commission (Reference 4). The computer curve fit results (index temperature and transition temperature shift) were used for the E900 effort and reported in that database. Therefore, the individual test results for the materials data applied from Table 2 exhibited behavior consistent with pressure vessel materials, scatter was well within expected ranges, and there were no difficulties experienced in deriving the 30 foot-pound temperature. The second criterion is satisfied.

Criterion 3: "When there are two or more sets of surveillance data from one reactor, the scatter of RT_{NDT} shift values about a best-fit line drawn as described in Regulatory Position 2.1 normally should be less than 28 °F for welds and 17 °F for base metal. Even if the fluence range is large (two or more orders of magnitude), the scatter shall not exceed twice those values. Even if the data fail this criterion for use in shift calculations, they may be credible for determining decrease in upper-shelf energy if the upper shelf can be clearly determined, following the definition given in ASTM E185-82."

The weld metal shift measurements for the materials were evaluated individually against this criterion in Tables 3 through 6 and in Table 8. The results of that evaluation are provided in Section 5.4. In all but one case (Cook Unit 1), the data scatter criterion was satisfied. [The November 1997 Guidelines (Reference 3) expanded on the use of this criterion. Those guidelines were taken into consideration in this report.]

Criterion 4: "The irradiation temperature of the Charpy specimens in the capsule should match the vessel wall temperature at the cladding/base metal interface within $\pm$25°F."

This criterion could not be addressed using temperature monitor data because there was an inconsistent use of monitors among the various surveillance programs. However, both NRC guidance (Reference 3) and the NRC sponsored work (Reference 4) used the reactor coolant inlet temperatures as a best estimate for the

irradiation temperature of the Charpy specimens in the capsule. Implicit in the NRC sponsored approach is the assumption that Criterion 4 will be met. It is based on the premise that the reactor coolant will cool the vessel wall and the adjacent surveillance specimens the same. In the data analysis that follows, the reactor coolant inlet temperatures from the ASTM E900 database (Reference 4) were used to provide an estimate of the temperature of the Charpy specimens, and the differences in irradiation temperature were treated explicitly. Thus Criterion 4 is satisfied.

Criterion 5: "The surveillance data for the correlation monitor material in the capsule should fall within the scatter band of the data base for that material."

There are limited sets of correlation monitor material (termed standard reference material in the Fort Calhoun vessel) data from the various surveillance capsules. For Fort Calhoun, the correlation monitor material measurements were addressed in Reference 20. For the other surveillance data, no such analysis could be performed. Therefore, the Fort Calhoun correlation monitor material measurements satisfy Criterion 5.

In summary, the surveillance data are shown to satisfy the criteria above. The data are assessed individually for Criteria 3 and 4 in Section 5.4, Analysis of Surveillance Data. The plant specific Fort Calhoun surveillance data are assessed for Criterion 5 also in Section 5.4. Therefore, the surveillance data are acceptable for use with Position 2.1 of Regulatory Guide 1.99, Revision 2.

5.2 Traceability of Mihama 1 Surveillance Data

In the specific case of the Mihama Unit 1 surveillance program, foreign data from a Westinghouse designed Pressurized Water Reactor (PWR) are being applied to a domestic Combustion Engineering designed PWR. In order to establish that the weld surveillance data from the Mihama Unit 1 reactor vessel are applicable to the Fort Calhoun vessel, the following information was evaluated: a. Unirradiated and irradiated Charpy data for tandem weld wire heat 12008/27204; b. Irradiation temperature of the capsule based on PWR cold leg; c. Neutron flux of capsules; d.

Gamma heating of capsules; e. Neutron spectrum of capsules; and f. Chemistry of surveillance data.

Each of these items is addressed below:

a. Unirradiated and irradiated Charpy data for tandem weld wire heat 12008/27204
The individual Charpy specimen data for the unirradiated tandem weld wire heat 12008/27204 are provided in Table 2 of Reference 15. Those data were used to establish the unirradiated Charpy curve. The individual Charpy specimen data for the irradiated tandem weld wire heat 12008/27204 were obtained from Kansai (Reference 17) and were used to establish the irradiated Charpy curve. Those data were checked against the Charpy index temperatures cited by Kansai in Reference 16 for the Charpy shift values from each of the three surveillance capsules (V, R and S per Reference 15) and shown to be consistent.

b. Irradiation temperature of the capsule based on PWR cold leg-

Kansai reported a value of 289 °C (552 °F) for the Mihama Unit 1 cold leg temperature (Reference 16). In an evaluation of the capsule configuration (Reference 22), it has been confirmed that that temperature is reasonable for similarly configured reactor vessels designed by Westinghouse.

c. Neutron flux of capsules-

The neutron flux corresponding to each irradiated and tested capsule from Mihama Unit 1 was reported by Kansai in Reference 17 together with their source reference and a description of the methodology used to calculate the neutron flux. In Reference 22, it has been confirmed that the reported flux is reasonable for similarly configured reactor vessels designed by Westinghouse.

d. Gamma heating of capsules-

In Reference 22, Westinghouse has confirmed that the design and construction of the Mihama Unit 1 surveillance capsules are the same as that for other surveillance

capsules that they fabricated during this timeframe. Therefore, it is reasonable to conclude that the gamma heating in the Mihama Unit 1 surveillance capsules is the same as that in similar domestic Westinghouse capsules.

e. Neutron spectrum of capsules-

In a CEOG sponsored program (Reference 23) it was demonstrated that surveillance data applicable to Combustion Engineering fabricated reactor vessel materials were equally predictable using Regulatory Guide 1.99, Revision 2 for plants designed by both Westinghouse and Combustion Engineering. It was concluded from this that the irradiation environment was similar for the surveillance capsules from Westinghouse and Combustion Engineering plants. There was no definitive difference between the spectra such that one needs only to consider differences in the irradiation temperature and the neutron flux. Neutron spectrum was considered to be no more than a second order variable for embrittlement. (For example, embrittlement correlation development work reported in Reference 4 did not identify neutron spectrum as an independent or dependent variable.)

In Reference 24 no discernible differences were found between the neutron spectra for the surveillance capsules from Westinghouse and Combustion Engineering plants. Reference 22 confirmed that the Mihama Unit 1 neutron spectrum is comparable to domestic Westinghouse PWRs. Therefore, the neutron spectra in the Mihama Unit 1 surveillance capsules is not expected to adversely affect the application of those surveillance data to the Fort Calhoun vessel.

f. Chemistry of surveillance data-

Kansai reported copper and nickel contents of 0.19 and 1.08 w/o for the Mihama Unit 1 surveillance weld (Reference 16). Weld analyses by Combustion Engineering and the best estimate for the weld (Reference 6) for heat 12008 and 27204 yielded copper and nickel contents as follows:

WDC-351	(n/a) Cu	0.98 Ni
WDC-1817	0.19 Cu	0.98 Ni
Best estimate	0.219 Cu	0.996 Ni

The Kansai values are fully consistent with a weld deposit made using heats 12008 and 27204. Traceability of the Mihama Unit 1 surveillance weld has been established based on fabrication records from CE-Chattanooga.

5.3 Analysis Approach

The analysis in the following section utilizes the ratio method of Reference 2. The ratio method is based on the relative chemistry factors. Regulatory Guide 1.99 (Reference 2) states that, "if there is clear evidence" of a difference in copper and nickel content, the measured shift should be adjusted by multiplying by the ratio of the chemistry factors for the vessel weld to that of the surveillance weld (i.e., the ratio method). For this evaluation, the ratio method was used to adjust the surveillance data from other programs to the best estimate chemistry for the Fort Calhoun reactor vessel. (This was done whether or not the copper and nickel contents were significantly different.) References 5 and 6 were used to obtain best estimate copper and nickel contents for the weld wire heats so that chemistry factors could be computed for the Fort Calhoun welds.

The effect of differences in the neutron irradiation environment is considered when applying surveillance data from another reactor pressure vessel. These differences have been addressed by the Combustion Engineering Owners Group, BGE, and Duke Power (see References 23, 24, and 25, respectively). The effect of neutron irradiation environment is taken to mean changes in measured transition temperature shift caused by differences in irradiation temperature, neutron flux and neutron energy spectrum. For the BGE and Duke evaluations (References 24 and 25), there was no expected influence of neutron flux or neutron energy spectrum given the use of only PWR surveillance data. The actual values of neutron flux and neutron energy spectrum were compared for the various plants being considered, and the values were within expected ranges for which no difference in irradiation behavior would be

expected. The Duke evaluation entailed the comparison of data from two Westinghouse designed reactor vessels. The BGE evaluation entailed comparisons of data from a Combustion Engineering and a Westinghouse designed reactor vessel. For the CEOG evaluation (Reference 23), a statistical analysis of surveillance data from both Combustion Engineering and Westinghouse designed reactor vessels demonstrated that there was no significant effect of differences in the irradiation environment for vessel materials fabricated by Combustion Engineering. In this report, data from the Combustion Engineering and Westinghouse vessel designs were considered in the analysis. Therefore, prior work suggests that there is no significant effect of neutron flux and neutron energy spectrum expected relative to the results in Table 7.

The effect of irradiation temperature was explicitly considered in the BGE evaluation (Reference 24) using the rationale stated in Reference 3. That rationale assumes there is a 1.0 °F effect on the chemistry factor for each 1.0 °F difference in irradiation temperature. (The higher the irradiation temperature, the lower the chemistry factor would be, and vice versa, per Reference 3. Irradiation temperature is taken as the reactor coolant inlet temperature.) The analysis in the following sections utilizes a modified approach from that given in Reference 3 for adjusting surveillance data for differences in irradiation temperature. A description of the rationale and benefits for the ratio and T_{cold} adjustments for analysis of surveillance data follows.

The rationale and benefits of this approach were described at a March 13, 2000 meeting between the NRC and the Omaha Public Power District in regard to the application of Position 2.1 of Regulatory Guide 1.99, Revision 2 to two heats of surveillance welds applicable to the Fort Calhoun vessel. The chemistry factor calculation has traditionally been done by the NRC as described in Reference 3. However, in order to analyze surveillance data from two separate programs it was necessary to first adjust for both CF differences and T_{cold} differences. Two issues were considered. The first is the viability of the T_{cold} adjustment method. The second is the appropriateness of adjusting the data prior to performing the data scatter analysis.

a) Viability of the T_{cold} Adjustment Method - In November 1997, the NRC presented a set of guidelines (Reference 3) to the industry that supplemented the guidelines

contained in Regulatory Guide 1.99, Revision 02. The activities surrounding Generic Letter 92-01 and its antecedents prompted the need for the supplemental guidelines. That Generic Letter had addressed some of the material variability issues including copper and initial RT_{NDT} and the effect of irradiation temperature on the degree of embrittlement. In the November 1997 NRC-Industry meeting, the NRC presented ways they considered acceptable to treat each aspect:

The "ratio method" was the prescribed way to treat differences in the copper and nickel content between the surveillance program weld being analyzed and the best estimate for the vessel weld.

The use of the σ_i term was the prescribed way to treat variability in initial RT_{NDT}. A value of σ_i = 17 °F was assigned for use with the generic initial RT_{NDT} = -56 °F for welds fabricated by Combustion Engineering. A value of σ_i = 0 °F was assigned for use with a measured initial RT_{NDT} (just as is the case for plates and consistent with the practice for welds).

Position 2.1 of Reference 2 was the prescribed way to analyze surveillance data to derive a chemistry factor (CF) using two or more sets of credible data. The data are to be adjusted for chemistry differences using the ratio method. If the difference between the adjusted measured shift and the predicted shift using the derived CF is less than or equal to σ_Δ = 28 °F, data scatter is deemed acceptable and the derived CF as well as a reduced σ_Δ (28/2 = 14 °F) could be used for predicting future embrittlement of the vessel beltline weld.

The effect of irradiation temperature on the degree of embrittlement was considered initially in the credibility criteria for use of surveillance data (the capsule temperature was to be within 25 °F of the vessel wall) and in November 1997 in a post-CF derivation adjustment to the CF. The initial accounting was done to satisfy the applicability issue; i.e., for irradiation temperatures between 525 °F and 590 °F, the Regulatory Guide 1.99, Revision 02 embrittlement correlation was applicable without adjustment. The adjustment suggested in November 1997 was done to satisfy the NRC

concern that the irradiation temperature of the surveillance capsule in plant "X" was at a higher temperatures than that of vessel "Y" to which the data were to be applied. It was widely believed that higher irradiation temperatures would result in less shift than at lower irradiation temperatures. The "rule-of-thumb" was that the effect was on the order of 1.0 °F increase/decrease in shift for each 1.0 °F difference in irradiation temperature.

At the March 13, 2000 meeting a method was presented for making the T_{cold} adjustment at the same time as was done for the ratio method. The approach followed was to use the recommended equation from NUREG/CR-6551 (Reference 4) to adjust the data for the effect of irradiation temperature differences. The method used was to compute the predicted shift at both temperatures of interest. The temperature effect is then the difference in the two shifts that is added to or subtracted from the measured shift, whichever is appropriate.

The equation in Reference 4 takes into consideration both time and temperature in the computation, thus providing a more rigorous treatment than that afforded by the rule-of-thumb given in Reference 3. It also offers the benefit of the numerical analysis of 609 data points for defining the apparent effect of irradiation temperature differences. (That is, the coefficients for temperature, copper, etc., were developed from the data and refined by statistical analysis.) Finally, use of the recommended equation from Reference 4 to adjust the data before the sum-of-the-squares analysis is mathematically more desirable than making the rule-of-thumb adjustment after the sum-of-the-squares analysis. (The Position 2.1 analysis approach was specifically designed to give more weight to the surveillance data at the higher fluences in recognition of the fact that the higher fluence data were more indicative of the expected behavior than were the low fluence data. Adjusting the data for temperature differences after the sum-of-the-squares analysis would not provide the same significance weighting. The Reference 3 guidelines approach, therefore, diminishes the significance of the effect of temperature on the high fluence data which is in conflict with the intent of the Position 2.1 analysis approach.)

The approach described above fully adjusts the data for both of the Reference 3 issues. Those are the chemistry differences (i.e., using the ratio method) and the T_{cold} differences. The shift measurements are adjusted prior to deriving the chemistry factor and prior to analyzing the scatter in the data.

b) Appropriateness of Data Adjustment Prior to Data Scatter Analysis - The third credibility criterion of Regulatory Guide 1.99, Revision 02 is to ascertain that the scatter of the surveillance measurements about a best-fit line derived using Position 2.1 is no more than 28 °F for welds. If this can be shown, then the derived chemistry factor can be used together with a reduced value for prediction uncertainty ($\sigma_\Delta/2$ = 14 °F). The concept is that the availability of credible measurements from the surveillance program greatly reduces the uncertainty of the prediction, and the lack of significant data scatter demonstrates that the material itself is not anomalous. In other words, the weld material is adequately represented by the embrittlement correlation contained in Regulatory Guide 1.99, Revision 02.

The applicability of the irradiation temperature adjustment depends on the source of the data. In using Position 2.1 to evaluate plant-specific surveillance data, the only data adjustment necessary is for the chemistry difference using the ratio method (if there is a significant difference between the surveillance weld and the vessel weld). There is no need to adjust for irradiation temperature because the capsule temperature and the cold leg temperature are essentially the same (i.e., it is the same vessel).

In using Position 2.1 to evaluate surveillance data from another plant, both the ratio method and irradiation temperature adjustments must be considered. The Reference 3 guidance is to adjust the shift measurements by the ratio method, calculate the CF, and then adjust the derived CF for temperature differences. The analysis of data scatter is done on the ratio adjusted data, so it is not examining the scatter of the original measurements. The Reference 3 approach provides a temperature adjustment but is done without regard to the time dependence of the presumed temperature effect. In using Position 2.1 to evaluate surveillance data from two other plants, both the ratio method and irradiation temperature adjustments must be considered, and they need to be done prior to the sum-of-the-squares

analysis. Doing the analysis on data adjusted for both the ratio method and irradiation temperature accounts for the time dependence of the presumed temperature effect and permits the sum-of-the-squares analysis emphasis on the high fluence data. Doing the analysis without both initial adjustments coupled with the subsequent correction for a temperature effect is inconsistent with the intent of Position 2.1 and places an unrealistic burden on the user to demonstrate the data scatter criterion is met.

c) Illustration of the T_{cold} Adjustment Method - The Position 2.1 analyses were run two ways as shown in Tables 4A, 4B, 6A and 6B. Tables 4A and 6A give the derivation for each surveillance set of CF based on the fully adjusted numbers (i.e., for both CF and T_{cold} differences). Tables 4B and 6B give the derivation for each surveillance set of CF based on the numbers adjusted for CF, followed by the Reference 3 suggested approach to address T_{cold} differences.

For the Mihama 1 surveillance data analysis, Tables 6A and 6B, the derived CFs for weld wire heats 12008 with 27204 were as follows:

> $CF_{TCOLD+CF}$ = 206.6 °F based on shifts adjusted for FCS T_{cold} (543 °F) and best estimate chemistry (Table 6A)
>
> CF= 200.9 °F based on shifts adjusted for best estimate chemistry, and CF_{TCOLD}= 209.9 °F after adjustment for FCS T_{cold} (i.e., 552 °F – 543 °F= 9°F adjustment) (Table 6B)

Therefore, in the case of the Mihama 1 surveillance data, the difference in the derived CFs is small (3.3 °F), but the CF is larger using the rule-of-thumb approach of temperature adjustment. The data scatter is identical for each because the adjustments used were the same in each case.

For the Diablo Canyon 1 surveillance plus the Palisades supplemental capsule data analysis, Tables 4A and 4B, the derived CFs for weld wire heat 27204 (tandem) were as follows:

$CF_{TCOLD+CF}$ = 215.5 °F based on shifts adjusted for FCS T_{cold} (543 °F) and best estimate chemistry (Table 4A)

CF= 220.2 °F based on shifts adjusted for best estimate chemistry, and CF_{TCOLD}= 210.2°F after adjustment for FCS T_{cold} (i.e., 543 °F – 533 °F= 10 °F adjustment) (Table 4B)

The 10°F temperature difference corresponds to the data with the highest fluence exposure because that data has the greatest significance to the CF derivation. For the weld wire heat 27204 surveillance data, the difference in the two derived CFs is small (5.3 °F), but the CF obtained using the rule-of-thumb approach of temperature adjustment is smaller than the CF derived from the fully adjusted data.

The data scatter criterion is met in the case of the CF derived using the fully adjusted data. This is justified because the analysis entails the use of data from two different vessels and three unique T_{cold} values. It would be unreasonable to expect test results that are presumed sensitive to irradiation temperature to be predictable without first removing the bias due to irradiation temperature. As was expected, the data scatter criterion was not met with the data that were corrected only for CF differences.

This method of analyzing surveillance data using both a chemistry factor and irradiation temperature adjustment is seen to result in comparable values to those obtained using the NRC guidelines in Reference 3. Use of the NRC guidelines resulted in a larger adjustment (positive or negative) in the two cases considered because that approach does not take into account time-at-temperature. The approach using the fully adjusted data provides the capability to analyze data irradiated at multiple temperatures.

5.4 Surveillance Data Analysis

D.C. Cook Unit 1- The Cook surveillance weld was fabricated using weld wire heat 13253 (Reference 6). The chemistry factors for the Cook surveillance weld and the Fort Calhoun vessel weld are 206.4 °F and 189.05 °F, respectively. The Cook shift

measurements in Table 3 (References 7 through 9) were adjusted for chemistry factor differences using the ratio 189.1 °F /206.4 °F= 0.916. The shifts were adjusted to the Fort Calhoun irradiation temperature, 543 °F, using the approach outlined in the preceding section. The computed adjustments were –3.2 °F, -5.1 °F, -6.1 °F, and –7.2 °F for capsule T, X, Y and U, respectively. The fully adjusted shift measurements are shown in Table 3.

The chemistry factor derived based on the four capsule results is 116.9 °F. The predicted shifts based on this chemistry factor were compared to the adjusted Charpy shifts. The adjusted minus predicted shifts for capsules Y and U are well in excess of σ_Δ for welds (28 °F). The chemistry factor was re-derived based on three capsule results, where capsule U was excluded because it was the most overpredicted value. The resultant chemistry factor value based on capsules T, X and Y is 137.4 °F, which is higher than the chemistry factor value based on all four capsules. The adjusted minus predicted shifts for those three capsules are within σ_Δ for welds (28 °F). The adjusted minus predicted shift for capsule U is greater than σ_Δ but is negative (i.e., conservative). Therefore, the Cook Unit 1 surveillance data are predictable when the capsule U results are excluded. The derived chemistry factor of 137.4 °F is much lower than the values for the surveillance weld (206.4 °F) from Table 1 and for the Fort Calhoun vessel weld (189.05 °F).

Diablo Canyon Unit 1- The Diablo Canyon surveillance weld was fabricated using weld wire heat 27204 (Reference 6). The chemistry factors for the Diablo Canyon surveillance weld and the Fort Calhoun vessel weld are 221.8 °F and 226.81 °F, respectively. The analysis included the use of data for weld heat 27204 irradiated in the Palisades reactor vessel in a supplemental capsule. The chemistry factor for the Palisades supplemental surveillance weld is 229.04 °F. The Diablo Canyon (References 10 and 11) and Palisades (Reference 18) shift measurements in Table 4 were adjusted for chemistry factor differences using the ratio 226.81°F /221.8°F= 1.022 for the Diablo Canyon data and 226.81 °F/229.04 °F = 0.990 for the Palisades data. The shifts were adjusted to the Fort Calhoun irradiation temperature, 543 °F, using the approach outlined in the preceding section. The computed adjustments were –1.6 °F, -2.0 °F, and –9.0 °F for capsules S and Y from Diablo Canyon and for capsule SA-60-1 for Palisades, respectively. The fully adjusted shift measurements

are shown in Table 4A. A comparative analysis is provided in Table 4B in which the shift measurements were adjusted only for the chemistry factor differences.

The chemistry factor derived in Table 4A based on the three capsule results is 215.5 °F. The predicted shifts based on this chemistry factor were compared to the measured Charpy shifts. The measured minus predicted shifts for the three capsules are all less than σ_Δ. The chemistry factor derived in Table 4B based on the three capsule results is 220.2 °F before adjusting for irradiation temperature differences. The adjusted chemistry factor is 210.2 °F using the guidelines of Reference 3. The predicted shifts based on the Table 4B chemistry factor were compared to the measured Charpy shifts. The measured minus predicted shift for capsule S (fluence of 2.84E18 n/cm^2) is in excess of σ_Δ for welds (28 °F), but the difference is negative (i.e., conservative). The derived chemistry factors of 215.5 and 220.2 °F are slightly lower than the values for the surveillance welds (221.8°F and 229.04 °F) from Table 1 and for the Fort Calhoun vessel weld (226.81 °F). The weld heat 27204 surveillance data are predictable when the data are fully adjusted to account for the differences in both chemical content and irradiation temperature.

Salem Unit 2- The Salem surveillance weld was fabricated using weld wire heat 13253 (Reference 6). The chemistry factors for the Salem surveillance weld and the Fort Calhoun vessel weld are 198.1 °F and 189.05 °F, respectively. The Salem shift measurements in Table 5 (References 12 through 14) were adjusted for chemistry factor differences using the ratio 189.1 °F /198 °F= 0.955. The shifts were adjusted to the Fort Calhoun irradiation temperature, 543 °F, using the approach outlined previously. The computed adjustments were –1.7 °F, -2.2 °F, and –3.0 °F for capsules T, U, and X, respectively. The fully adjusted shift measurements are shown in Table 5.

The chemistry factor derived in Table 5 based on the three capsule results is 190.4°F. The predicted shifts based on this chemistry factor were compared to the measured Charpy shifts. The measured minus predicted shifts for the three capsules are all less than σ_Δ. The derived chemistry factor of 190.4 °F is very similar to the values for the surveillance weld (198.1 °F) from Table 1 and for the Fort

Calhoun vessel weld (189.05 °F). Therefore, the Salem Unit 2 surveillance data are predictable.

Mihama Unit 1- The Mihama Unit 1 surveillance weld was fabricated using weld wire heats 12008 and 27204. The chemistry factors for the Mihama surveillance weld and the Fort Calhoun vessel weld are 227.2 °F and 231.06 °F, respectively. The Mihama shift measurements in Table 6 (Reference 16) were adjusted for chemistry factor differences using the ratio 231.06 °F /227.2 °F= 1.017. The shifts were adjusted to the Fort Calhoun irradiation temperature, 543 °F, using the approach outlined in the preceding section. The computed adjustments were +4.3 °F, +5.3 °F, and +7.4 °F for capsules 1, 2 and 3, respectively. The fully adjusted shift measurements are shown in Table 6A. A comparative analysis is provided in Table 6B in which the shift measurements were adjusted only for the chemistry factor differences.

The chemistry factor derived in Table 6A based on the three capsule results is 206.6 °F. The predicted shifts based on this chemistry factor were compared to the measured Charpy shifts. The measured minus predicted shifts for the three capsules are all less than σ_Δ. The chemistry factor derived in Table 6B based on the three capsule results is 200.9 °F before adjusting for irradiation temperature differences. The adjusted chemistry factor is 209.9 °F using the guidelines of Reference 3. The predicted shifts based on the Table 6B chemistry factor were compared to the measured Charpy shifts. The measured minus predicted shifts for the three capsules are all less than σ_Δ. The derived chemistry factors of 206.6 and 209.9 °F are lower than the values for the surveillance weld (227.2 °F) from Table 1 and for the Fort Calhoun vessel weld (231.06 °F). The Mihama surveillance data are predictable when the data are fully adjusted or partially adjusted to account for the differences in both chemical content and irradiation temperature.

Fort Calhoun - The Fort Calhoun surveillance weld was fabricated using weld wire heat 305414 (Reference 6). The chemistry factor for the Fort Calhoun surveillance weld is 212 °F. The shift measurements in Tables 8A, 8B and 8C are from References 19 through 21). No chemistry factor adjustment was made because the

data are not being related to any vessel weld. The data are being used only to assess predictability of the Fort Calhoun surveillance weld data.

The chemistry factor derived in Table 8A based on the three capsule results is 229.0 °F. The predicted shifts based on this chemistry factor were compared to the measured Charpy shifts. The measured minus predicted shifts for the three capsules are all less than σ_Δ. Therefore, the Fort Calhoun weld surveillance data are predictable. The derived chemistry factor of 229.0 °F is higher than the value for the surveillance weld (212 °F) in Table 1.

The Fort Calhoun surveillance plate was fabricated using heat A1768-1. The chemistry factor for the Fort Calhoun plate is 65 °F based on Table 2 of Reference 2). No chemistry factor adjustment was made because there is no difference between the surveillance plate and the vessel plate chemistry. The data are being used to assess the predictability of the Fort Calhoun surveillance plate data.

The chemistry factor derived in Table 8B for the surveillance plate based on the three capsule results (where the longitudinal and transverse measurements were combined) is 72.0 °F. The predicted shifts based on this chemistry factor were compared to the measured Charpy shifts. The measured minus predicted shifts for the five measurements are all less than σ_Δ. Therefore, the Fort Calhoun plate surveillance data are predictable. The derived chemistry factor of 72.0 °F is similar to the Table 2 value (65 °F).

The standard reference material in the Fort Calhoun surveillance program was from HSST Plate 01. The chemistry factor for the plate is 131.7 °F using the reported chemical content from the E900 database with Table 2 of Reference 2. No chemistry factor adjustment was made because there is no corresponding vessel plate chemistry. The data are being used to assess the predictability of the Fort Calhoun standard reference material data.

The chemistry factor derived in Table 8C for the standard reference material based on the two capsule results is 138.3 °F. The predicted shifts based on this chemistry factor were compared to the measured Charpy shifts. [Note: This exceeds the

requirements of Regulatory Guide 1.99, Revision 2, Criterion 5 in which it is necessary only to show the data are within the scatterband of available measurements.] The measured minus predicted shifts for the two measurements are both less than σ_Δ. The derived chemistry factor of 138.3 °F is similar to the Table 2 value (131.7 °F). Therefore, the Fort Calhoun standard reference material data are predictable.

6.0 Evaluation of Surveillance Data Credibility and Applicability to Fort Calhoun

The results of the preceding analysis are summarized in Tables 7 and 9. The derived chemistry factors are provided in Table 7 for each of the surveillance program welds that are applicable to the Fort Calhoun beltline welds. The derived values correspond to the best estimate chemistry for the weld wire heat(s) used to fabricate the surveillance program welds. The ratio method was applied to adjust the chemistry of the specific surveillance program weld to the best estimate chemistry for the vessel weld. Also shown in Table 7 are the chemistry factors obtained using Table 1 of Reference 2 for the surveillance weld and the best estimate chemistry for the weld wire heat.

All of the surveillance materials analyzed in Tables 3 through 6 are credible with respect to being applicable to the limiting materials in the Fort Calhoun reactor vessel beltline. This applicability is with respect to weld wire heat number, welding flux type, and welding process. Any differences in copper and nickel content between a surveillance weld and the Fort Calhoun reactor vessel beltline weld with the same weld wire heat(s) were addressed through use of the ratio method in accordance with Reference 2. Any difference in irradiation temperature between the surveillance weld and the Fort Calhoun reactor vessel beltline weld was addressed through use of the T_{cold} adjustment method described in Section 5.3. The data were evaluated for scatter using the criterion that the surveillance measurements were to be predictable within one σ_Δ of the predicted shift using the derived chemistry factor in accordance with Reference 2.

In the case of heat 13253 from D.C. Cook Unit 1, Table 3, there are measurements from four surveillance capsules. The high fluence measurement, capsule U, is significantly overpredicted. The derived chemistry factor based on capsules T, X, and Y from D.C. Cook Unit 1 is 137.4 °F. In the case of heat 13253 from Salem Unit 2, Table 6, all three measurements are predictable within one σ_Δ but the derived chemistry factor (190.4 °F) is

higher than obtained from the D.C. Cook Unit 1 data (137.4 °F). Therefore, a conservative chemistry factor adjusted for the Fort Calhoun weld irradiation temperature and chemical content and made with heat 13253 is 190.4 °F. It is based on the fully credible surveillance data from Salem Unit 2. The derived chemistry factor and the vessel weld best-estimate chemistry factor from Table 1 of Regulatory Guide 1.99, Revision 2 are very similar (190.4 °F and 189.1 °F, respectively).

In the case of heat 12008 and 27204 from Mihama Unit 1 (Table 6A), all three surveillance measurements are predictable within one σ_Δ. The derived chemistry factor is 206.6 °F and includes adjustments for differences in irradiation temperature and chemical content between the Mihama Unit 1 surveillance weld and the Fort Calhoun beltline weld. It is based on the fully credible data from Mihama Unit 1. The derived chemistry factor, 206.6 °F is less than the vessel weld best-estimate chemistry factor, 231.06 °F from Table 1 of Reference 2.

In the case of heat 27204 (tandem) from Diablo Canyon Unit 1 and the Palisades supplemental capsule (Table 4A), all three surveillance measurements are predictable within one σ_Δ. The derived chemistry factor is 215.5 °F and includes adjustments to the irradiation temperature and chemical content of the Fort Calhoun beltline welds. It is based on the fully credible data from Diablo Canyon Unit 1 and Palisades. The derived chemistry factor, 215.5 °F is less than the vessel weld best-estimate chemistry factor, 226.8 °F from Table 1 of Reference 2.

In Table 9, the Fort Calhoun surveillance program results are summarized. These data are credible and predictable. The data scatter based on the derived chemistry factors in Tables 8A, 8B, and 8C are within one σ_Δ for all of the Fort Calhoun surveillance materials, and the scatter is especially small for the surveillance plate and the standard reference material (SRM). The Fort Calhoun surveillance program results were further evaluated as follows:

1. One of the criteria of Regulatory Guide 1.99, Revision 2 is to ascertain that the SRM (correlation monitor) data are consistent with the trend of the database for that material. This is addressed in part in Figures 1 and 2 where it can be seen that the two Fort Calhoun results (at 527 °F and 538 °F) are as predictable as the other HSST Plate 01 data. It is further addressed in Table A2. The twelve sets of data from Combustion

Engineering plants were evaluated following Position 2.1 of Reference 2. Those data provide a derived chemistry factor of 130.3 °F. That value is to be compared with the predicted chemistry factor of 131.7 °F based on the best estimate copper and nickel for HSST Plate 01 and the derived chemistry factor of 138.3 °F from the Fort Calhoun measurements alone. The preceding results demonstrate that the Fort Calhoun SRM data are consistent with the trend of the database for that material. The similarity between the derived chemistry factors and the predicted value indicate that the Fort Calhoun vessel irradiation environment is comparable to that of the other Combustion Engineering designed plants.

2. A comparison was made between the Fort Calhoun surveillance weld and the Fort Calhoun beltline welds. The surveillance weld for Fort Calhoun was fabricated using a heat of wire that is not found in any of the beltline welds. It is unique in that it was purchased to a 0.60% nickel specification rather than the 0.0%, 0.75% and 1.00% nickel specifications used to purchase welding electrode heats for the Fort Calhoun beltline welds. The derived chemistry factor for the Fort Calhoun surveillance program weld data is higher than that predicted using Table 1 of Reference 2. That is in contrast to the derived chemistry factors for the surveillance welds from other plants shown in Table 7. The chemistry factors for those welds are consistently equal to or lower than the predicted chemistry factors. In other words, the surveillance weld data that correspond to the weld wire heats used in the Fort Calhoun beltline welds are conservatively predicted. There is no immediate explanation available for the observation that the Fort Calhoun surveillance weld material (i.e., heat #305414) data were underpredicted by Reference 2, whereas the 0.75% and 1.00% nickel specification heats were conservatively predicted. There are no Fort Calhoun beltline welds with a 0.60% nickel content. Therefore, this issue is not applicable.

The data in Table 7 encompass three of the five most limiting weld wire heat combinations used in the Fort Calhoun reactor vessel beltline. The surveillance data coverage by weld seam is as follows:

Welds 3-410 A/C: D.C. Cook 1 heat 13253, Diablo Canyon 1 heat 27204, Palisades supplemental capsule heat 27204, and Salem 1 heat 13253.

Weld 9-410: No applicable data. [Note: The chemistry factor associated with the best estimate copper and nickel content for heat 20291 is 188.41 °F. This weld is unlikely to be limiting because it is a circumferential weld for which the PTS screening criterion is 300 °F.]

Welds 2-410 A/C: No applicable data. [Note: The chemistry factor associated with the best estimate copper and nickel content for heat 51989 is 89.03 °F. These welds will not become limiting for the Fort Calhoun vessel.]

Position 2.1 of Reference 2 allows one to use credible surveillance data to determine the adjusted reference temperature. This is done by deriving a value for the chemistry factor (CF). If the data scatter is within prescribed limits, then the derived CF may be used with half the normal value for σ_Δ to calculate the adjusted reference temperature. Based on the preceding, there are credible surveillance data for three of the limiting heats used in the Fort Calhoun reactor vessel beltline. For each surveillance weld, a chemistry factor was derived using the ratio method together with an adjustment for irradiation temperature. As shown in Table 7, the derived chemistry factors obtained were less than or equal to the value obtainable from Table 1 of Reference 2. Position 2.1 states that "if this procedure gives a higher value of adjusted reference temperature than that given by using the procedures of Regulatory Position 1.1 (i.e., Table 1 of Reference 2), the surveillance data should be used. If this procedure gives a lower value, either may be used." Given the availability of credible surveillance data that show the Regulatory Position 1.1 chemistry factors to be conservative, those chemistry factors may be used. In the calculation of the margin, If the data scatter is within prescribed limits one may use half the normal value for σ_Δ when determining the adjusted reference temperature.

7.0 Calculation of RT_{PTS}

The limiting beltline material for the Fort Calhoun vessel is that from the lower shell axial welds, 3-410 A/C. The preceding analysis has demonstrated that there are credible surveillance data available for three of the four most limiting weld wire heat combinations used to fabricate those axial welds. These three sets of credible data pertain to each of the heats used for the lower shell axial welds, although not for each possible combination of heats. Given the availability of credible and predictable surveillance data for the three weld

wire heat combinations, it is justified to use the derived CF and to use half the normal value for σ_Δ to calculate the margin when determining the adjusted reference temperature. For the one weld wire heat combination for which surveillance data are not yet available, the CF from Table 1 of Reference 2 and the normal value for σ_Δ will be used to calculate the adjusted reference temperature, RT_{PTS}.

Provided below is the determination of the RT_{PTS} for the limiting beltline materials predicted for the end of the current license for Fort Calhoun (August 9, 2013). The neutron fluence was conservatively determined to be 1.728 $x10^{19}$ n/cm^2 (E>1Mev) for that date using an unbiased estimate (see Reference 26). This was projected out to the end of a renewed license period, August 9, 2033, using the same unbiased estimate. (The projected value actually corresponds to the end of that fuel cycle, March 2034 and, therefore, contains an added conservatism.) The projected neutron fluence value is 2.431 $x10^{19}$ n/cm^2 (E>1Mev) (Reference 26). The fluence was calculated in a manner consistent with the methods of the U.S. Nuclear Regulatory Commission's Draft Regulatory Guide DG-1053 (Reference 27). The RT_{PTS} calculation was performed as follows:

$$RT_{PTS} = \text{Initial } RT_{NDT} + \text{Shift} + \text{Margin}$$

Following are the calculations for each of the three heats combinations for which credible and predictable surveillance data are available and for the fourth limiting heat combination for which surveillance data are not yet available.

a. Heat 13253

Initial RT_{NDT} = - 56 °F (generic value for CE welds)

Shift = Chemistry Factor X Fluence Factor

- Chemistry Factor (CF) = 190.4 °F (based on Salem 2 surveillance data)
- Fluence factor (FF) is a function of neutron fluence, f, in units of $1x10^{19}$ n/cm^2
- $FF = f^{(.28 - 0.1 \times \log f)}$

Margin = $2(\sigma_i^2 + \sigma_\Delta^2)^{1/2}$

- σ_Δ = 28 °F/2 = 14 °F (half the value for welds)

- σ_i = 17 °F (for generic CE welds)
- $2(\sigma_i^2 + \sigma_\Delta^2)^{1/2} = 2(17\ °F^2 + 14\ °F^2)^{1/2} = 44.0\ °F$

RT_{PTS} = - 56 °F + 190.4 °F X $f^{(.28 - 0.1 \times \log f)}$ + 44.0 °F

For the end of the current license for Fort Calhoun (August 9, 2013), the RT_{PTS} is:

RT_{PTS} = - 56 °F + 219.0 °F + 44.0 °F = 207 °F

For the end of the renewed license period for Fort Calhoun (August 9, 2033), the RT_{PTS} is:

RT_{PTS} = - 56 °F + 235.9 °F + 44.0 °F = 224 °F

These projected values are less than the PTS screening criterion value of 270 °F for axial welds. Thus the vessel weld will remain below the PTS screening criterion for a period exceeding 20 years beyond the current 40 year license term.

b. Heat 12008 and 27204

Initial RT_{NDT} = - 56 °F (generic value for CE welds) [Note: A measured value of initial RT_{NDT} = -58 °F is available for this weld. For purposes of this calculation the more conservative generic value and its associated margin was used.]

Shift = Chemistry Factor X Fluence Factor

- Chemistry Factor (CF) = 206.6 °F (based on Mihama 1 surveillance data)
- Fluence factor (FF) is a function of neutron fluence, f, in units of $1x10^{19}$ n/cm^2
- FF= $f^{(.28 - 0.1 \times \log f)}$

Margin = $2(\sigma_i^2 + \sigma_\Delta^2)^{1/2}$

- σ_Δ = 28 °F/2 = 14 °F (half the value for welds)
- σ_i = 17 °F (for generic CE welds)

- $2(\sigma_i^2 + \sigma_\Delta^2)^{1/2} = 2(17\ °F^2 + 14\ °F^2)^{1/2} = 44.0\ °F$

$RT_{PTS} = -56\ °F + 206.6\ °F \times f^{(.28 - 0.1 \times \log f)} + 44.0\ °F$

For the end of the current license for Fort Calhoun (August 9, 2013), the RT_{PTS} is:

$RT_{PTS} = -56\ °F + 237.7\ °F + 44.0\ °F = 226\ °F$

For the end of the renewed license period for Fort Calhoun (August 9, 2033), the RT_{PTS} is:

$RT_{PTS} = -56\ °F + 256.0\ °F + 44.0\ °F = 244\ °F$

These projected values are less than the PTS screening criterion value of 270 °F for axial welds. Thus the vessel weld will remain below the PTS screening criterion for a period exceeding 20 years beyond the current 40 year license term.

c. Heat 27204

Initial $RT_{NDT} = -56\ °F$ (generic value for CE welds)

Shift = Chemistry Factor X Fluence Factor

- Chemistry Factor (CF) = 215.5 °F (based on Diablo Canyon 1 and Palisades surveillance data)
- Fluence factor (FF) is a function of neutron fluence, f, in units of 1×10^{19} n/cm^2
- $FF = f^{(.28 - 0.1 \times \log f)}$

Margin = $2(\sigma_i^2 + \sigma_\Delta^2)^{1/2}$

- $\sigma_\Delta = 28\ °F/2 = 14\ °F$ (half the value for welds)
- $\sigma_i = 17\ °F$ (for generic CE welds)
- $2(\sigma_i^2 + \sigma_\Delta^2)^{1/2} = 2(17\ °F^2 + 14\ °F^2)^{1/2} = 44.0\ °F$

$RT_{PTS} = -56\ °F + 215.5\ °F \times f^{(.28 - 0.1 \times \log f)} + 44.0\ °F$

For the end of the current license for Fort Calhoun (August 9, 2013), the RT_{PTS} is:

RT_{PTS} = - 56 °F + 247.9 °F + 44.0 °F = 236 °F

For the end of the renewed license period for Fort Calhoun (August 9, 2033), the RT_{PTS} is:

RT_{PTS} = - 56 °F + 267.0 °F + 44.0 °F = 255 °F

These projected values are less than the PTS screening criterion value of 270 °F for axial welds. Thus the vessel weld will remain below the PTS screening criterion for a period exceeding 20 years beyond the current 40 year license term.

d. Heat 12008 and 13253

Initial RT_{NDT} = - 56 °F (generic value for CE welds)

Shift = Chemistry Factor X Fluence Factor

- Chemistry Factor (CF) = 208.68 °F (from Table 1, Reference 2 for weld heats 12008 and 13253)
- Fluence factor (FF) is a function of neutron fluence, f, in units of $1x10^{19}$ n/cm^2
- $FF= f^{(.28 - 0.1 \times \log f)}$

Margin = $2(\sigma_i^2 + \sigma_\Delta^2)^{1/2}$

- σ_Δ = 28 °F (value for welds)
- σ_i = 17 °F (for generic CE welds)
- $2(\sigma_i^2 + \sigma_\Delta^2)^{1/2} = 2(17\ °F^2 + 28\ °F^2)^{1/2} = 65.5$ °F

RT_{PTS} = - 56 °F + 208.68 °F X $f^{(.28 - 0.1 \times \log f)}$ + 65.5 °F

For the end of the current license for Fort Calhoun (August 9, 2013), the RT_{PTS} is:

RT_{PTS} = - 56 °F + 240.1 °F + 65.5 °F = 250 °F

For the end of the renewed license period for Fort Calhoun (August 9, 2033), the RT_{PTS} is:

RT_{PTS} = - 56 °F + 258.6 °F + 65.5 °F = 268 °F

These projected values are less than the PTS screening criterion value of 270 °F for axial welds. Thus the vessel weld will remain below the PTS screening criterion for a period exceeding 20 years beyond the current 40 year license term.

e. Plate Code D4802-2 (Heat A1768-1)

Initial RT_{NDT} = 18 °F (measured value)

Shift = Chemistry Factor X Fluence Factor

- Chemistry Factor (CF) = 72.0 °F (based on Fort Calhoun surveillance data)
- Fluence factor (FF) is a function of neutron fluence, f, in units of $1x10^{19}$ n/cm^2
- $FF= f^{(.28 - 0.1 \times \log f)}$

Margin = $2(\sigma_i^2 + \sigma_\Delta^2)^{1/2}$

- σ_Δ = 17 °F/2 = 8.5 °F (half the value for plates)
- σ_i = 0 °F (for measured value)
- $2(\sigma_i^2 + \sigma_\Delta^2)^{1/2} = 2(0\ °F^2 + 8.5\ °F^2)^{1/2} = 17.0$ °F

RT_{PTS} = 18 °F + 72.0 °F X $f^{(.28 - 0.1 \times \log f)}$ + 17.0 °F

For the end of the current license for Fort Calhoun (August 9, 2013), the RT_{PTS} is:

RT_{PTS} = 18 °F + 82.8 °F + 17.0 °F = 118 °F

For the end of the renewed license period for Fort Calhoun (August 9, 2033), the RT_{PTS} is:

RT_{PTS} = 18 °F + 89.2 °F + 17.0 °F = 124 °F

These projected values are less than the PTS screening criterion value of 270 °F for plates. Thus the vessel plate will remain below the PTS screening criterion for a period exceeding 20 years beyond the current 40 year license term.

8.0 Conclusions

1) The Fort Calhoun surveillance program data are credible and predictable as summarized in Table 9.

2) There are four sets of credible surveillance weld data available from other plants that are applicable to the Fort Calhoun reactor vessel beltline welds. The derived chemistry factor given in Table 7 for each set was less than or equal to the value obtainable from Table 1 of Regulatory Guide 1.99.

3) Given the availability of credible and predictable surveillance weld data, it is justified to use half the normal value for σ_Δ to calculate the margin when determining the adjusted reference temperature for the Fort Calhoun vessel beltline materials.

4) The highest projected value of RT_{PTS} is 250 °F at the end of the current license. This was determined using the normal value for σ_Δ (28 °F) and the limiting material chemistry factor of 208.68 °F from Table 1 of Regulatory Guide 1.99, Revision 02. It corresponds to weld wire heats 12008 and 13253 for Fort Calhoun weld 3-410 A/C. The highest projected value of RT_{PTS} at the end of the renewed license term is 268 °F for that same weld material as shown in Table 10. These projected values are less than the PTS screening criterion value of 270 °F for plates and axial welds and less than the PTS screening criterion value of 300 °F for circumferential welds. Thus the vessel plates and welds will remain below the PTS screening criterion for a period exceeding 20 years beyond the current 40 year license term.

5) In the analysis of the surveillance data, the data were adjusted for both differences in copper and nickel content and for differences in irradiation temperature. It was necessitated by the fact that the data available for one of the heats was from two different reactor vessel surveillance programs that in turn had to be adjusted for the Fort Calhoun vessel. The irradiation temperature adjustment method was based on the use of NUREG/CR-6551 (Reference 4). In the two cases evaluated, the adjustment method resulted in a derived chemistry factor that was comparable to that obtained using guidelines (Reference 3) developed previously. The proposed method with its dual adjustments was successfully used to reconcile surveillance data from two different plants.

References

1. 10CRF50.61, "Fracture Toughness Requirements for Protection Against Pressurized Thermal Shock Events", Federal Register, Vol. 60, No. 243, December 19, 1995.

2. US Nuclear Regulatory Commission, Regulatory Guide 1.99, Revision 02, "Radiation Embrittlement of Reactor Vessel Materials", May 1988.

3. "Evaluation and Use of Surveillance Data", Handout from NRC-Industry Meeting on Status of Generic Letter 92-01, Supplement 1, Rockville, MD, November 12, 1997.

4. E.D. Eason, et al., "Improved Embrittlement Correlations for Reactor Pressure Vessel Steels", NUREG/CR-6551, dated November 1998.

5. "Response to Request for Additional Information Related to Generic Letter 92-01, Revision 1, Supplement 1", OPPD Letter LIC-98-0124, dated September 28, 1998.

6. "Updated Analysis for Combustion Engineering Fabricated Reactor Vessel Welds Best Estimate Copper and Nickel Content", CEOG Report CE NPSD-1119, Revision 1, dated July 1998.

7. D.C. Cook Unit 1, Capsule T, SWRI-02-4770

8. D.C. Cook Unit 1, Capsule X, SWRI-02-6159

9. D.C. Cook Unit 1, Capsule Y, SWRI-06-7244-001

10. "Analysis of Capsule S from the PGE Diablo Canyon 1 Reactor Vessel Radiation Surveillance Program", December 1987, WCAP-11567.

11. "Analysis of Capsule Y from the PGE Diablo Canyon 1 Reactor Vessel Radiation Surveillance Program", July 1993, WCAP-13750.

12. "Analysis of Capsule T from the Public Service Electric & Gas Company Salem 2 Reactor Vessel Radiation Surveillance Program," March 1984, WCAP-10492.

13. "Analysis of Capsule U from the Public Service Electric & Gas Company Salem 2 Reactor Vessel Radiation Surveillance Program," September 1987, WCAP-11554.

14. "Analysis of Capsule X from the Public Service Electric & Gas Company Salem 2 Reactor Vessel Radiation Surveillance Program," June 1992, WCAP-13366.

15. S.E. Yanichko, "Kansai Electric Power Co., Mihama Unit No. 1 Reactor Vessel Radiation Surveillance Program", Westinghouse Report WCAP-7374, January 1970.

16. Yasunobu Nashida, Kansai Electric Power Co., to J.K. Gasper, Omaha Public Power District, "Mihama Unit No. 1 Reactor Vessel Material Information", dated December 7, 1999.

17. Katsuhiko Shigemune, Kansai Electric Power Co., to J.K. Gasper, Omaha Public Power District, "Reactor Vessel Data of Mihama Unit 1", dated April 17, 2000.

18. Personal telephone communication, J.R. Kneeland, Consumers Energy, January 7, 2000; and T.C. Hardin letter to J.R. Kneeland, "CVGRAPH Analysis of Charpy Energy Data from Capsule SA-60-1", dated August 9, 1999.

19. "OPPD Fort Calhoun Station, Evaluation of Irradiated Capsule W-225", August 1980, TR-O-MCM-001, Revision 1.

20. "OPPD Fort Calhoun Station, Evaluation of Irradiated Capsule W-265", March 1984, TR-O-MCM-002.

21. "OPPD Fort Calhoun Station, Evaluation of Irradiated Capsule W-275", November 1994, BAW-2226.

22. S.L. Anderson, "Mihama Unit 1 Irradiation Environment", Westinghouse Report LTR-REA-00-618, June 22,2000.

23. "Application of Reactor Vessel Surveillance Data for Embrittlement Management", Combustion Engineering Owners Group Report CEN-405-P, Revision 3, September 1996.

24. Robert E. Denton, Baltimore Gas and Electric Company, "Request for Approval of Updated Values of Pressurized Thermal Shock (PTS) Reference Temperatures (RT_{PTS}) Values (10CFR50.61)", letter dated July 21, 1995.

25. "Duke Power Company, Evaluation of McGuire Unit 1, Surveillance Weld Data Credibility", Technical Report No. ATI-98-012-T005, revision 1, November 1998, transmitted by Duke Energy Corporation letter, H.B. Barron to U.S. Nuclear Regulatory Commission, "Reactor Vessel Radiation Surveillance Program", dated January 7, 1999.

26. S.L. Anderson, "Fast Neutron Fluence Evaluations for the Fort Calhoun Unit 1 Reactor Pressure Vessel", Westinghouse Report WCAP-15443, July 2000.

27. U.S. Nuclear Regulatory Commission's Draft Regulatory Guide DG-1053, "Calculational and Dosimetry Methods for Determining Pressure Vessel Neutron Fluence".

Table 1
Identification of Reactor Vessel Plates and Welds
in the Fort Calhoun Reactor Vessel Beltline

Plate or Weld Identification	Plate or Weld Electrode Heat No.	Weld Flux Type and Lot No.	Chemistry Factor (°F)[a]
Plate D4802-1	C2585-3	N/A	82.2
Plate D4802-2	A1768-1	N/A	65
Plate D4802-3	A1768-2	N/A	73.1
Plate D4812-1	C3213-2	N/A	83
Plate D4812-2	C3143-2	N/A	65
Plate D4812-3	C3143-3	N/A	65
Surveillance Plate D4802-2	A1768-1	N/A	72.0[c]
2-410 A/C	51989	Linde 124, #3687	89.03
3-410 A/C	12008 & 13253 (T)[b]	Linde 1092, #3774	208.68
3-410 A/C	13253 (T)[b]	Linde 1092, #3774	189.05
3-410 A/C	12008 & 27204 (T)[b]	Linde 1092, #3774	231.06
3-410 A/C	27204 (T)[b]	Linde 1092, #3774	226.81
9-410	20291	Linde 1092, #3833	188.41
Surveillance Weld	305414	Linde 1092, #3947 and #3951	212

Notes:
a) Chemistry Factor from Table 1 or 2 of Reference 2.
b) "T" denotes a tandem arc weld; other welds are single arc.
c) Chemistry Factor as derived based using surveillance measurements in Table 8B of this report.

Table 2

Identification of Reactor Vessel Surveillance Program
Welds Applicable to the Fort Calhoun Vessel Beltline Welds

Reactor Vessel	Weld Electrode Heat No.	Flux Type and Lot No.	Copper Content (%)	Nickel Content (%)
DC Cook 1	13253	Linde 1092, #3791	.27	.74
Salem 2	13253	Linde 1092, #3774,3833	.254	.726
Diablo Canyon 1	27204	Linde 1092, #3714	.20	1.00
Mihama 1	12008 & 27204	Linde 1092, #3724	.19	1.08
Fort Calhoun Suppl.	27204	Linde 1092, #3714	.19	1.07
Palisades Suppl.	27204	Linde 1092, #3714	.19	1.07
Diablo Canyon 2*	12008 & 21935	Linde 1092, #3869	.219	.871
Fort Calhoun*	305414	Linde 1092, #3947,3951	.35	.60
McGuire 1*	12008 & 20291	Linde 1092, #3854	.198	.874
Fitzpatrick (BWR)	12008 & 13253	Linde 1092, #3774	n/a	n/a
Cooper (BWR)*	20291	Linde 1092, #3833	n/a	n/a
Pilgrim (BWR)*	12008 & 20291	Linde 1092, #3833	.161	.794

* These are not fully applicable to the Fort Calhoun vessel limiting beltline welds.

Table 3

Test Results from the D.C. Cook Unit 1
Reactor Vessel Surveillance Program
(Surveillance Weld Wire Heat No. 13253)

Capsule Identity	Charpy Shift, °F	Adjusted[(a)] Charpy Shift, °F	Neutron Fluence, n/cm^2	Irradiation Temperature, °F
T	70	60.9	2.69E18	537
X	146	128.7	8.13E18	537*
Y	184	162.5	1.23E19	537
U	109	92.6	1.77E19	537

* not reported; assumed to be same as other reported values

Capsule Identity	Adjusted[(a)] Charpy Shift, °F	(FF) x Adjusted Shift	Fluence Factor (FF)	$(FF)^2$	Adjusted – Predicted[b] Shift, °F
T	60.9	39.1	.6424	.4127	60.9-88.3=-27.4
X	128.7	121.2	.9419	.8872	128.7-129.4=-0.7
Y	162.5	171.9	1.0577	1.1187	162.5-145.3=17.2
U	92.6	107.1	1.1569	1.3383	92.6-159=-66.4

$CF_{(ALL)}$=439.3/3.7569= 116.9 °F Σ=439.3 Σ =3.7569

$CF_{(W/O\ U)}$=332.2/2.4186= 137.4 °F Σ =332.2 Σ =2.4186

(a) Shift adjusted for FCS T_{cold} (543 °F) and best estimate chemistry
(b) Predicted using $CF_{(W/O\ U)}$= 137.4 °F

Table 4A
Test Results from Diablo Canyon Unit 1 and Supplemental Capsule with T_{cold} and CF Pre-Adjustment for Weld Heat 27204

Capsule Identity	Charpy Shift, °F	Adjusted[(a)] Charpy Shift, °F	Neutron Fluence, n/cm^2	Irradiation Temperature, °F
DC1-S	113	114	2.84E18	539
DC1-Y	233	236	9.41E18	540
SA-60-1	250	239	1.62E19	533

Capsule Identity	Adjusted[(a)] Charpy Shift, °F	(FF) x Adjusted Shift	Fluence Factor (FF)	(FF)^2	Adjusted – Predicted** Shift, °F
DC1-S	114	74.8	.6562	.4306	114-141=-27
DC1-Y	236	232.0	.9830	.9662	236-212= 24
SA-60-1	239	270.8	1.1331	1.2840	239-244= -5
		Σ =577.6		Σ =2.6808	

CF=577.6/2.6808= 215.5 °F

(a) Shift adjusted for FCS T_{cold} (543 °F) and best estimate chemistry

Table 4B
Test Results from Diablo Canyon Unit 1 and Supplemental Capsule with Separate Adjustment for T_{cold} and CF for Weld Heat 27204

Capsule Identity	Charpy Shift, °F	Adjusted[(a)] Charpy Shift, °F	Neutron Fluence, n/cm^2	Irradiation Temperature, °F
DC1-S	113	115.5	2.84E18	539
DC1-Y	233	238.1	9.41E18	540
SA-60-1	250	247.5	1.62E19	533

Capsule Identity	Adjusted[(a)] Charpy Shift, °F	(FF) x Adjusted Shift	Fluence Factor (FF)	$(FF)^2$	Adjusted – Predicted** Shift, °F
DC1-S	115.5	75.8	.6562	.4306	115-144=-29
DC1-Y	238.1	234.0	.9830	.9662	238-216= 22
SA-60-1	247.5	280.4	1.1331	1.2840	247-249= -2
		Σ =590.2		Σ =2.6808	

CF=590.2/2.6808= 220.2 °F
CF_{Tcold}= 220.2 °F + (533 °F – 543 °F) = 210.2 °F

(a) Shift adjusted for best estimate chemistry

Table 5

Test Results from the Salem Unit 2
Reactor Vessel Surveillance Program
(Surveillance Weld Wire Heat No. 13253)

Capsule Identity	Charpy Shift, °F	Adjusted[(a)] Charpy Shift, °F	Neutron Fluence, n/cm^2	Irradiation Temperature, °F
T	145	136.8	2.75E18	539
U	180	169.7	5.50E18	539
X	188	176.6	1.07E19	539

Capsule Identity	Adjusted[(a)] Charpy Shift, °F	(FF) x Shift	Fluence Factor (FF)	(Fluence Factor)^2	Measured minus Predicted Shift, °F
T	136.8	88.6	.6480	.4199	136.8-123.4=13.4
U	169.7	141.3	.8328	.6936	169.7-158.6= 11.1
X	176.6	179.9	1.0189	1.0382	176.6-194= -17.4
		Σ = 409.8		Σ = 2.1517	

CF=409.8 /2.1517= 190.4 °F

(a) Shift adjusted for FCS T_{cold} (543 °F) and best estimate chemistry

Table 6A
Test Results from Mihama Unit 1 Surveillance Capsules with T_{cold} and CF Pre-Adjustment for Weld Heats 12008 and 27204

Capsule Identity	Charpy Shift, °F	Adjusted[(a)] Charpy Shift, °F	Neutron Fluence, n/cm^2	Irradiation Temperature, °F
1	187.2	194.8	6.0 E18	552
2	205.2	214.1	1.2 E19	552
3	226.8	238.2	2.1 E19	552

Capsule Identity	Adjusted[(a)] Charpy Shift, °F	(FF) x Adjusted Shift	Fluence Factor (FF)	$(FF)^2$	Adjusted – Predicted** Shift, °F
1	194.8	166.9	.85696	.7344	195-177= 18
2	214.1	225.0	1.05086	1.1043	214-217= -3
3	238.2	286.3	1.20182	1.4444	238-248= -10
		Σ =678.2		Σ =3.2831	

CF=678.2/3.2831= 206.6 °F

(a) Shift adjusted for FCS T_{cold} (543 °F) and best estimate chemistry

Table 6B
Test Results from Mihama Unit 1 Surveillance Capsules with Separate Adjustment for T_{cold} and CF for Weld Heat 12008 and 27204

Capsule Identity	Charpy Shift, °F	Adjusted[(a)] Charpy Shift, °F	Neutron Fluence, n/cm^2	Irradiation Temperature, °F
1	187.2	190.4	6.0 E18	552
2	205.2	208.6	1.2 E19	552
3	226.8	230.7	2.1 E19	552

Capsule Identity	Adjusted[(a)] Charpy Shift, °F	(FF) x Adjusted Shift	Fluence Factor (FF)	$(FF)^2$	Adjusted – Predicted** Shift, °F
1	190.4	163.2	.85696	.7344	190-172= 18
2	208.6	219.2	1.05086	1.1043	209-211= -2
3	230.7	277.3	1.20182	1.4444	231-241= -10
		Σ =659.7		Σ =3.2831	

CF=659.7/3.2831= 200.9 °F
CF_{Tcold}= 200.9 °F + (552 °F – 543 °F) = 209.9 °F

(a) Shift adjusted for best estimate chemistry

Table 7
Derived Chemistry Factors for Reactor Vessel Surveillance Program Welds Applicable to Fort Calhoun Vessel Weld 3-410

Reactor Vessel	Weld Electrode Heat No.	Flux Type and Lot No.	Derived Chemistry Factor[a], CF (°F)	RG 1.99 CF (°F) for Surveillance Weld Chemistry[b]	RG 1.99 CF (°F) for Best Estimate Weld Chemistry[c]
DC Cook 1	13253	Linde 1092 #3791	137.4	206.4	189.1
Diablo Canyon 1 and Supp. Capsule	27204	Linde 1092 #3714	215.5 (210.2)	221.8	226.8
Salem 2	13253	Linde 1092 #3774,3833	190.4	198	189.1
Mihama 1	12008 & 27204	Linde 1092 #3724	206.6 (209.9)	227.2	231.06

a) Adjusted to Best Estimate CF and T_{cold} for Fort Calhoun (543 °F); value in parentheses was determined by adjusting for T_{cold} after deriving chemistry factor.
b) Chemistry Factor (CF) from Table 1 of Reference 2 based on the copper and nickel content for the surveillance weld.
c) Chemistry Factor (CF) from Table 1 of Reference 2 based on the best estimate copper and nickel content for the weld wire heat or combination of heats.

Table 8A

Test Results from the Fort Calhoun Reactor Vessel Surveillance Program (Surveillance Weld Wire Heat No. 305414)

Capsule Identity	Charpy Shift, °F	Neutron Fluence, n/cm^2	Irradiation Temperature, °F
W225	210	5.53E18	527
W265	225	7.71E18	534
W275	219	1.28E19	538

Capsule Identity	Charpy Shift, °F	(FF) x Shift	Fluence Factor (FF)	$(FF)^2$	Measured - Predicted Shift, °F
W225	210	175.2	.8343	.6961	210-191.1=18.9
W265	225	208.6	.9270	.8593	225-212.3=12.7
W275	219	234.0	1.0687	1.1421	219-244.7=-25.7
	CF=617.8/2.6975= 229.0 °F	Σ =617.8		Σ =2.6975	

Table 8B

Test Results from the Fort Calhoun Reactor Vessel Surveillance Program (Surveillance Plate Heat No. A1768-1)

Capsule Identity	Charpy Shift, °F (Lg,Tr)[a]	Neutron Fluence, n/cm^2	Irradiation Temperature, °F
W225	60, N/A	5.53E18	527
W265	74,70	7.71E18	534
W275	73,72	1.28E19	538

a) "Lg" is longitudinal and "Tr" is for transverse orientation Charpy data

Capsule Identity	Charpy Shift, °F (Lg,Tr)	(FF) x Shift	Fluence Factor (FF)	$(FF)^2$	Measured - Predicted Shift, °F
W225	60	50.1	.8343	.6961	60-60.1=-0.1
W265	74,70	68.6,64.9	.9270	.8593	74-66.7=7.3 70-66.7=3.3
W275	73,72	78.0,76.9	1.0687	1.1421	73-76.9=-3.9 72-76.9=-4.9
		CF=338.5/4.6989= 72.0 °F	Σ =338.5	Σ =4.6989	

Table 8C

Test Results from the Fort Calhoun Reactor Vessel Surveillance Program (Standard Reference Material)

Capsule Identity	Charpy Shift, °F	Neutron Fluence, n/cm^2	Irradiation Temperature, °F
W225	124*	5.53E18	527
W265	N/A	7.71E18	534
W275	141*	1.28E19	538

* shift per Surveillance Program test report

Capsule Identity	Charpy Shift, °F	(FF) x Shift	Fluence Factor (FF)	$(FF)^2$	Measured - Predicted Shift, °F
W225	124	103.5	.8343	.6961	124-115.4=8.6
W275	141	150.7	1.0687	1.1421	141-147.8=-6.8
	CF=254.2/1.8382= 138.3 °F		Σ =254.2	Σ =1.8382	

Table 9

Derived Chemistry Factors for Fort Calhoun Reactor Vessel Surveillance Materials

Material Identity	Material Description	Derived Chemistry Factor (°F)	RG 1.99 Table 1 or 2 Chemistry Factor (°F)
Weld	Heat 305414, Linde 1092	229.0	212
Plate D4802-2	SA 533B Class 1	72.0	65
SRM	HSST Plate 01	138.3	131.7

Table 10
Predicted RT_{PTS} for the Fort Calhoun Reactor Vessel Beltline Plates and Welds

Plate or Weld Identification	Plate or Weld Electrode Heat No.	Chemistry Factor (°F)	Predicted RT_{PTS} through 2033 (°F)
Plate D4802-1	C2585-3	82.2[a]	136
Plate D4802-2	A1768-1	72.0[b]	124
Plate D4802-3	A1768-2	73.1[a]	125
Plate D4812-1	C3213-2	83[a]	137
Plate D4812-2	C3143-2	65[a]	115
Plate D4812-3	C3143-3	65[a]	115
2-410 A/C	51989	89.03[a]	120
3-410 A/C	12008 & 13253 (T)	208.68[a]	268
3-410 A/C	13253 (T)	190.4[b]	224
3-410 A/C	12008 & 27204 (T)	206.6[b]	244
3-410 A/C	27204 (T)	215.5[b]	255
9-410	20291	188.41[a]	243

Notes:
a) Chemistry Factor from Table 1 or 2 of Reference 2 or derived using surveillance measurements in this report.
b) Chemistry Factor derived using surveillance measurements in this report.

Figure 1
Effect of Tcold on SRM Data
HSST Plate 01 Results
Normalized to 1E19 n/cm2

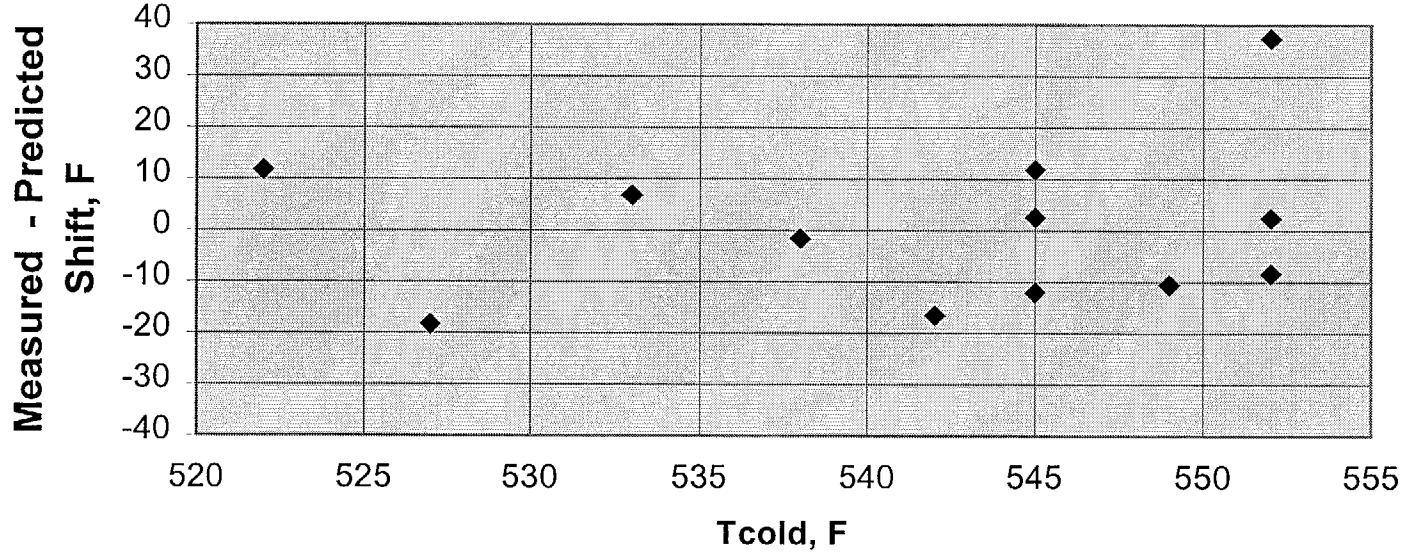

Figure 2
Effect of Tcold on SRM Data
HSST Plate 01 Results (CF=130.3 F)

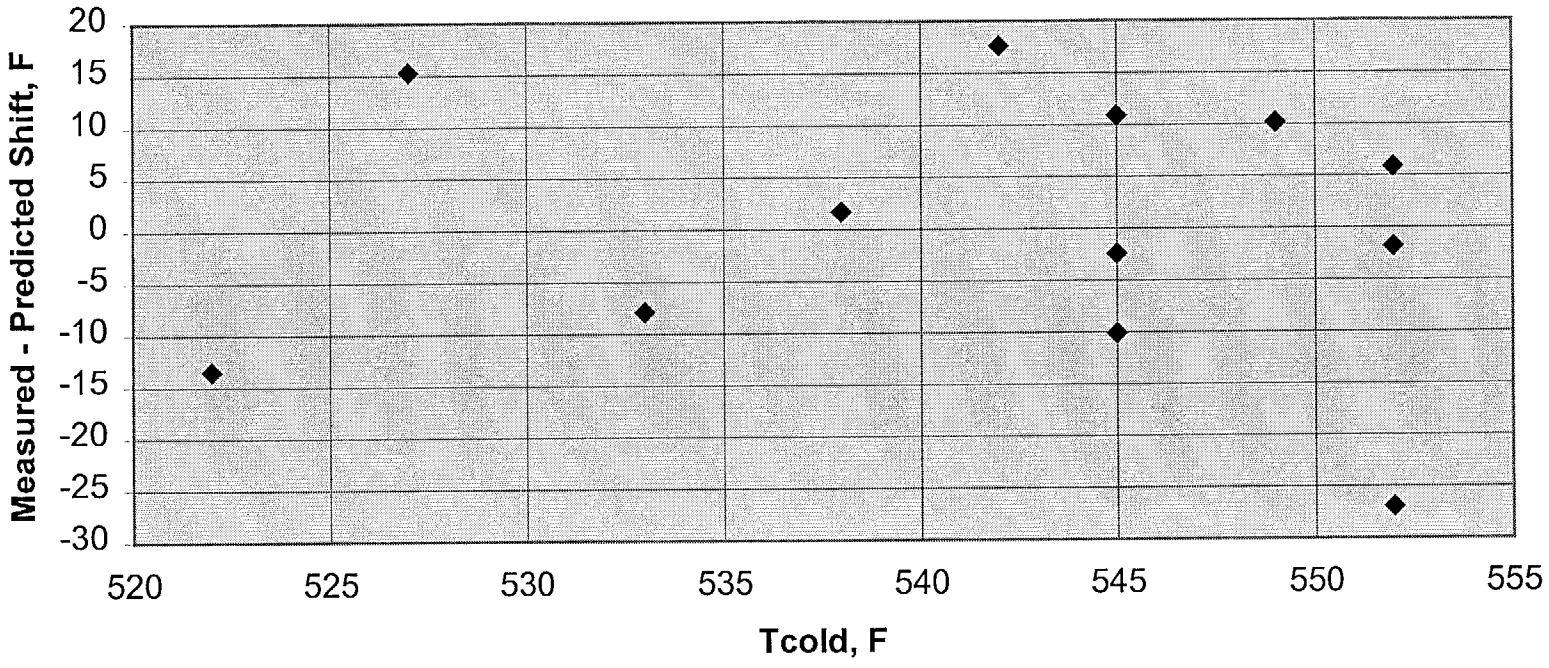

Table A1
Standard Reference Material Data from
Combustion Engineering Designed Surveillance Capsules

Reactor Vessel	Surveillance Capsule	SRM Material Identification	Charpy Shift (°F)	Neutron Fluence (10^{19} n/cm^2)	Irradiation Temperature (°F)
Calvert Cliffs 1	W263	HSST 01	101	0.59	545
Calvert Cliffs 2	W263	HSST 01	120	0.806	545
Fort Calhoun	W225	HSST 01	124* (116)	0.553	527
Fort Calhoun	W275	HSST 01	141* (162)	1.28	538
Millstone 2	W104	HSST 01	136	0.884	549
Maine Yankee	A25	HSST 01	137	1.76	522
Maine Yankee	W253	HSST 01	156	1.25	542
Palisades	W110	HSST 01	143	1.78	533
Palo Verde 1	W137	HSST 01	98	0.345	552
Palo Verde 2	W137	HSST 01	96	0.407	552
Palo Verde 3	W137	HSST 01	67*	0.364	552
St. Lucie 1	W104	HSST 01	129	0.716	545

*Shift per surveillance report

Table A2
Analysis of Standard Reference Materials

Irradiation Temperature, (°F)	Shift (°F)	(FF) x Shift	$(FF)^2$	Fluence (10^{19} n/cm^2)	Fluence Factor (FF)	Measured-Predicted Shift, (°F)
545	101	86.08	0.7264	0.59	0.85229	101 - 111.1 = -10.1
545	120	112.74	0.8827	0.806	0.93950	120 – 122.4 = -2.4
527	124*	103.46	0.6961	0.553	0.83434	124 – 108.7 = 15.3
538	141*	150.69	1.1422	1.28	1.06873	141 – 139.3 = 1.7
549	136	131.30	0.9321	0.884	0.9654	136 – 125.8 = 10.2
522	137	157.28	1.3348	1.76	1.1554	137 – 150.5 = -13.5
542	156	165.70	1.1282	1.25	1.0622	156 – 138.4 = 17.6
533	143	165.65	1.3418	1.78	1.1584	143 – 150.9 = -7.9
552	98	69.26	0.4994	0.345	0.70669	98 – 92.1 = 5.9
552	96	72.06	0.5635	0.407	0.75066	96 – 97.8 = -1.8
552	67*	48.30	0.5196	0.364	0.72085	67 – 93.9 = -26.9
545	129	116.91	0.8214	0.716	0.90630	129 – 118.1 = 10.9

*Shift per surveillance report

$\underline{\text{(FF) x Shift}}$ $\underline{(FF)^2}$

Σ=1379.43 Σ=10.5882 CF=(1379.43)/ (10.5882)=130.3 °F